# PEAK VERTICAL FLOOR ACCELERATIONS OF TALL STEEL STRUCTURES

BY

GEORGIAN ADRIAN TUTUIANU
B.S., University of New Hampshire, 2011

THESIS

Submitted to the University of New Hampshire
in Partial Fulfillment of
the Requirements for the Degree of

Master of Science
in
Civil Engineering

September, 2019

This thesis/dissertation was examined and approved in partial fulfillment of the requirements for the degree of

Master of Science in Civil Engineering by:

Thesis/Dissertation Director, Dr. Erin S. Bell, Associate Professor of Civil Engineering

Dr. Raymond A. Cook, Associate Professor of Civil Engineering

Dr. Kyle P. Kwiatkowski, Assistant Professor of Civil Engineering

On May 29th 2019

Approval signatures are on file with the University of New Hampshire Graduate School.

## ACKNOWLEDGEMENTS

This work was supported by my adviser Dr. Ricardo Medina of the University of New Hampshire as well as the UNH Civil Engineering Department. Over the years the teaching and research assistantships I received were instrumental in allowing me to complete this work. I would like to specifically thank my advisor Dr. Ricardo Medina for his dedication, patience and valuable guidance as well as the rest of my defense committee consisting of Dr. Erin Bell, Dr. Raymond Cook and Dr. Kyle Kwiatkowski. My fellow graduate students also deserve recognition for their well-placed criticism, perspective and ideas. In particular, Miguel Negrete-Padilla, Shokoufeh Zargar, Annika Mathiasson, Antonio Garcia Palencia, and Sam White. I would also like to thank Dr. Farzin Zareian whom I've never personally met but whose work has been essential in helping me to quickly evaluate and successfully iterate the seismic design of my building. Finally, I would like to thank my friends and family who've been supporting me along the way in every non-technical way possible.

TABLE OF CONTENTS

LIST OF TABLES

LIST OF FIGURES

# ABSTRACT

PEAK VERTICAL FLOOR ACCELERATIONS OF TALL STEEL STRUCTURES

By

Georgian Tutuianu

University of New Hampshire, September 2019

To meet modern day challenges structural engineers must properly design not only the primary structural elements of buildings but increasingly the secondary elements too. Damage or failure of nonstructural components (NSCs) and their attachments can present large economic losses, impaired building services and functionality, as well as life safety and emergency egress concerns. To properly design these components, it is important to accurately estimate their maximum acceleration demands including horizontal and vertical components of acceleration. In an effort to better understand vertical acceleration demands of rigid NSCs in multistory buildings and assess the building code provisions a 20-story office building, that is representative of a typical structure, is designed. Vertical acceleration demands are characterized through the use of floor acceleration spectra which are obtained for various points on the plan floor by running elastic modal time histories using 106 recorded ground motions. The main findings of this study are that peak vertical floor acceleration (PVFA) demands vary in plan due to the out of plane flexibility of the floor. Points in the mid portions of the floor slab experience much higher accelerations than points at column locations. The vertical seismic force design provisions of ASCE 7-10 underestimates the PVFA in a majority of the points found in the floor plan at least 50% of the time. A comparison and discussion between these results and the findings of a recent study out of the University of Reno is provided.

LIST OF ACRONYMS

| | |
|---|---|
| $\Delta t$ | Dynamic time step |
| $\rho$ | Seismic redundancy factor |
| $\Omega_0$ | Overstrength factor |
| C1 | Corner column |
| $C_d$ | Deflection amplification factor |
| CQC | Complete quadratic combination |
| ELF | Equivalent lateral force |
| E-W | East-West direction |
| f | Fundamental frequency |
| $F_a$ | Short period site coefficient |
| FEMA | Federal Emergency Management Agency |
| FFE | Furniture, Fixtures, Equipment, |
| $F_p$ | ASCE 7 vertical seismic design force |
| FRS | Floor Response Spectra |
| $F_v$ | Long period site coefficient |
| G1 | Largest gravity column |
| G2 | Smallest gravity column |
| h | Vertical thickness of shell |
| H | Mean roof height of the structure |
| $h_r$ | Steel metal deck rib height |
| $H_s$ | The total height of the steel metal deck |
| HVAC | Heating Ventilation Air Conditioning |
| LA | Los Angeles |
| LFRS | Lateral Force Resisting Systems |
| LRFD | Load Resistance Factor Design |

| | |
|---|---|
| $MCE_R$ | Risk Targeted Maximum Considered Earthquake |
| MDOF | Multiple Degree of Freedom |
| MEP | Mechanical, Electrical, and Plumbing |
| NBCC | National Building Code of Canada |
| NEES | Network for Earthquake Engineering Simulation |
| NEHRP | National Earthquake Hazards Reduction Program |
| N-S | North-South direction |
| NSCs | Nonstructural Component(s) |
| PEER NGA | Pacific Earthquake Engineering Research Next Generation Attenuation |
| PFA | Peak Floor Acceleration |
| PGA | Peak Ground Acceleration |
| PHFA | Peak Horizontal Floor Acceleration |
| PSA | pseudo spectral acceleration |
| PVFA | Peak Vertical Floor Acceleration |
| R | Response modification coefficient |
| RBS | Reduced beam section |
| RSA | Response Spectrum Analysis |
| $S_1$ | One second period acceleration at site |
| Sa | Spectral Acceleration |
| SAC | Joint venture partners between the Structural Engineers Association of California, the Applied Technology Council, and Consortium of Universities for Research in Earthquake Engineering |
| SCWB | Strong Column Weak Beam |
| $S_{D1}$ | One second period design acceleration |
| SDOF | Single Degree of Freedom |
| $S_{DS}$ | Short period design acceleration |
| SMRF | Steel Moment Resisting Frame |

| | |
|---|---|
| $S_r$ | Steel metal deck rib spacing |
| $S_s$ | Short period acceleration at site |
| T | Fundamental period |
| $T_0$ | Constant acceleration transition period |
| $T_L$ | Long period |
| $t_s$ | Slab height beyond the rib height in the steel metal deck |
| $T_s$ | Constant velocity transition period |
| UZ | Modal Mass participation, % in vertical |
| $W_p$ | Weight of nonstructural component |
| $W_r$ | Steel metal deck rib width |
| X | Cartesian coordinate in the plan East-West direction, positive to the right |
| Y | Cartesian coordinate in the plan North-South direction, positive up |
| Z | Cartesian coordinate in the vertical direction, positive up |
| z | Story height |
| z/H | Story height relative to the total building height |

CHAPTER 1

INTRODUCTION

## 1.1 Background

Modern buildings are comprised of structural and nonstructural components (NSCs). The structural components are primarily elements such as floor slabs, decking or sheathing, floor beams, girders, joists, trusses, columns, posts, pillars, bracing, shear walls, and any other elements which directly resist gravity and lateral forces. These elements are referred to as primary structural systems. In contrast, NSCs are defined as all the rest of the portions and contents of a building not explicitly designated as belonging to the primary structural system and they are broadly referred to as secondary systems. These secondary systems while not directly part of the gravity or lateral force resisting system may still be subject to strong seismic forces which must be resisted through their anchorage or attachments to the primary system or through their own structural characteristics [1]. The distinction between primary structural and secondary systems can be observed from the following figure where the same structure is detailed with (*a*) only the primary structural system and (*b*) the secondary system on top of the primary structural system.

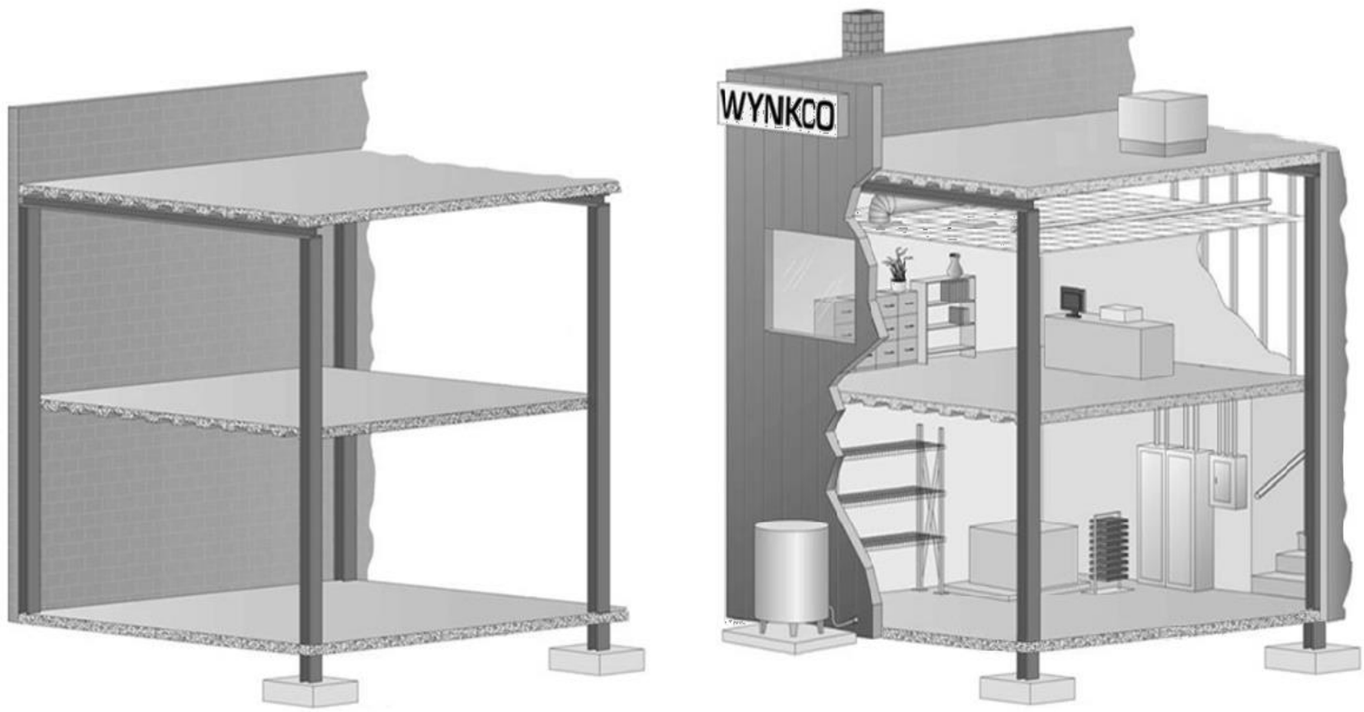


*(a)* *(b)*

Figure 1: (a) Primary structural system (b) Secondary and primary structural systems [2]

This definition of secondary systems results in a wide variety of components covered under the nonstructural designation. Broadly, NSCs fall into three major categories including [2]:

1.) Architectural Components

2.) Mechanical, Electrical, and Plumbing (MEP) Components

3.) Furniture, Fixtures, Equipment, (FFE) and Contents

See Table 1 for a non-exhaustive list of examples from each of the categories.

Table 1: Three Major Categories of NSCs [1] [2] [3].

| **Architectural Components** | **Mechanical, Electrical, and Plumbing Components** | **Furniture, Fixtures, Equipment, and Contents** |
|---|---|---|
| Storefronts | Pumps, Turbines, Generators, Engines and Motors | Desks |
| Glazing | Motor Control Centers | Books, Book Cases and Shelving |
| Cladding Systems | Control Panels | Industrial Storage Racks |
| Veneers | Transformers | File Cabinets |
| Partitions | Emergency Power Systems | Wall Mounted TV's and Monitors |
| Suspended Ceilings | Distribution Panels | Medical Records |
| Chimneys | Piping, Ductwork, Conduits | Retail Merchandise |
| Elevator Penthouses | Storage Tanks and Pressure Vessels | Specialty Equipment: Kitchen and Machine Shop |
| Heliports | Antennas | Industrial Chemicals and Hazardous Materials |
| Lighting Systems | Smoke Stacks | Museum Artifacts |
| Parapets | Cranes | Collectables |
| Fences | Cooling Towers | |
| Stairways | Fans | |
| Signboards | Chillers | |
| Architectural Ornamentation | Air Handling Units | |
| | Computers and Data Acquisition Systems | |
| | Radar and Object Tracking Devices | |
| | Escalators | |

Within these three categories NSCs can be further classified based on the type of seismic response they exhibit: whether or not the component is sensitive to excessive acceleration, deformation, or both. Deformation-sensitive components are items that are susceptible to being damaged by racking or excessive story drift deformation. This category typically includes components that run vertically through the building such as glass or curtain walls. Acceleration-sensitive components are items that are susceptible to being damaged by shifting, overturning or toppling over. This category includes items such as suspended ceilings or HVAC equipment. It should be noted that from a dynamics point of view the acceleration that a component experiences in reality is the result of the component-floor system-structure interaction. Generally, this interaction produces component acceleration demands that may be greatly amplified compared to the earthquake-induced peak ground acceleration (PGA) at the site. This is especially true if the component period in any of the three orthogonal directions (x,y,z) is close to the modal period of the floor system or structure in the corresponding direction [4]. Examples of components that are primarily characterized as being either acceleration-or deformation-sensitive are shown in Table 2 below, which is obtained from ASCE 41-06 Seismic Rehabilitation of Existing Buildings [3]. The remainder of this study will focus on acceleration-sensitive components.

Table 2: Acceleration or Deformation-Sensitive Components [3].

| Component | Acceleration | Deformation |
|---|---|---|
| EXTERIOR SKIN | | X |
| Veneer (Including Stone & Marble) | | X |
| Glass Blocks | | X |
| Prefabricated Panels | | X |
| PARTITIONS | | X |
| CEILINGS | | |
| Directly Applied to Structure | X | |
| Dropped Furred Gypsum Board | X | |
| Suspended Lath and Plaster | | X |
| Suspended Integrated Ceilings | | X |
| PARAPETS & APPENDAGES | X | |
| CANOPIES & MARQUEES | X | |
| CHIMNEYS & STACKS | X | |
| STAIRS | X | |
| MECHANICAL EQUIPMENT | X | |
| Boilers, Heaters and Furnaces | X | |
| Manufacturing and Processing Equipment | X | |
| HVAC | X | |
| STORAGE VESSELS | X | |
| PRESSURE PIPING | X | |
| FIRE SUPPRESSION PIPING | X | |
| DUCTWORK | X | |

## 1.2 Importance

A small sample of what damage to nonstructural components may look like is presented in the figures shown below. Figure 2 and Figure 3 show the damage a library sustained by the magnitude 7.1 earthquake off the coast of New Zealand in 2010. Figure 4 shows collapsed precast concrete staircases in a multistory precast concrete building damaged in the same New Zealand earthquake.

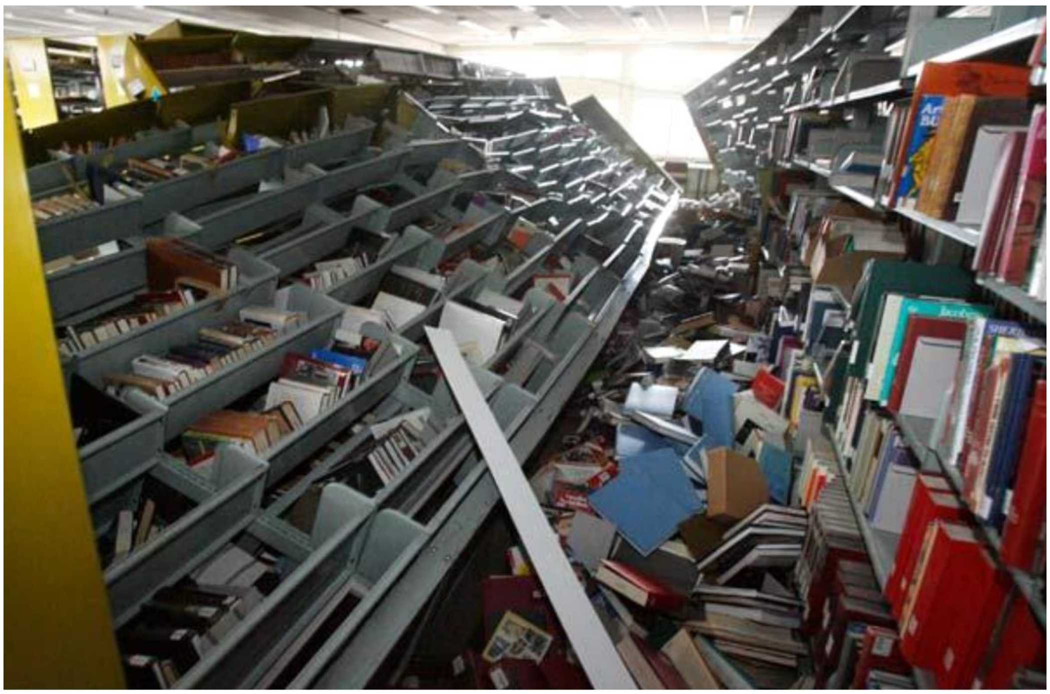

Figure 2: Bookshelf damage from the New Zealand 2010 earthquake [5].

Figure 3: Ceiling damage from the New Zealand 2010 earthquake [5].

Figure 4: Staircase damage from the New Zealand 2011 earthquake [6].

Nonstructural components are important to civil and structural engineers because during a strong seismic event damage to these components may result in any or all of the following:

1.) *Significant Financial Losses*

The number and type of NSCs is ever expanding due to technological advancements. In fact these secondary systems are so numerous and so essential to everyday modern living that they can comprise between 75-85% of the total construction cost of commercial buildings. As shown in Figure 5, from Whittaker and Soong 2003 [7], the nonstructural components of a building represent the largest cost in terms of total construction cost for typical office, hotel and hospital type buildings.

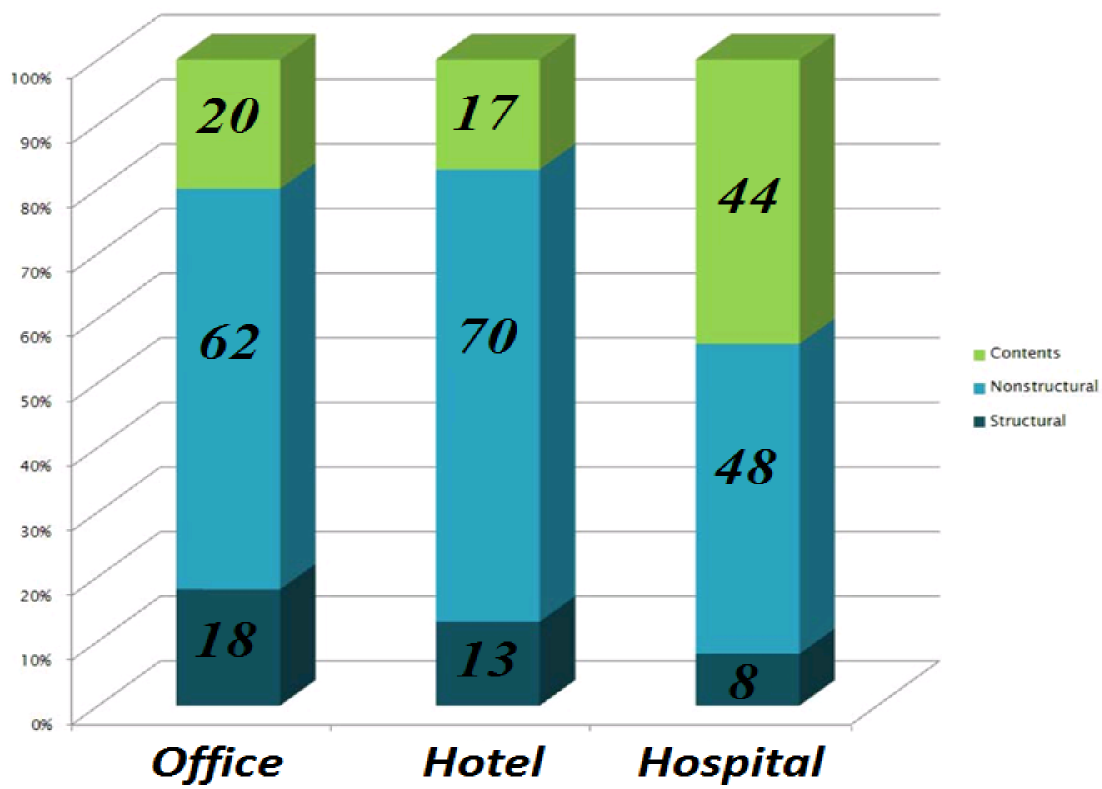


Figure 5: Typical cost breakdown of NSCs, building contents, and structural components [2].

Since NSCs contribute such a large portion of the total construction cost of buildings; building operators and owners have a very large financial incentive to protect their assets especially considering that in some cases damage to these components from earthquakes have resulted in repair and replacement costs exceeding the total cost of the building itself [1]. While it is generally difficult to put a precise monetary value on the cost of nonstructural damage from earthquakes due to the way structural and nonstructural costs are lumped together by building owners and tenants when making insurance claims, a reasonable estimate puts nonstructural losses from recent earthquake events in developed countries at approximately 50% or more of total earthquake losses [8]. For example, of the approximate $6.3 billion of direct economic loss to non-residential buildings that occurred due to the 1994 Northridge earthquake in California, about $5.2 billion was due to nonstructural damage [9].

*2.) Disruption of Essential Services and Business Operations*

After a strong seismic event, essential equipment may be damaged or entirely destroyed and debris caused by falling objects and overturned furniture may critically impair or hinder the performance of essential facilities such as fire and police stations, hospitals, emergency command centers, communication facilities, power stations, and water treatment and supply plants [1]. Furthermore, in the aftermath of a significant seismic event, these obstructions may prevent or greatly diminish the ability of emergency services including firefighters, paramedics and other first responders to adequately target and administer aid to disaster victims in an efficient manner [1].

Businesses may also incur large indirect financial losses from having to close down operations while clean up and repair efforts are undertaken. For example, as a result of the 2004 Niigata earthquake in Japan, the semiconductor plant belonging to Sanyo Electric Company had to be closed down for several months due to damage to its machinery. This resulted in over $690 million in repairs and lost income for the Sanyo Electric Company [8].

*3.) Life Safety and Injury Concerns*

Aside from emergency responders not being able to quickly get into or through a building because of fallen debris or overturned furniture and other building contents; the uninjured building occupants may not be able to quickly get out because of those same obstructions. For example it could be very difficult to impossible to escape a multiple story building if the staircase damage is extensive like it was from the February 2011 earthquake which struck New Zealand see Figure 4. Furthermore, the risk of personal injury or death resulting from heavy falling debris should not be underestimated. For example, a student was struck and killed by a falling precast panel while walking out of a parking garage during the 1987 Whittier Narrows earthquake in California [1].To further illustrate the hazards of falling debris on February 22, 2011 as a bus passed along Colombo Street in central Christchurch, New Zealand a magnitude 6.3 earthquake struck, sending masonry crashing down from buildings and killing 12 people in the street. Eight of the dead were the driver and passengers on the bus, and the other four were pedestrians [10]. Fortunately, by better understanding the seismic behavior of nonstructural components and building contents, structural engineers can reduce these economic and life safety risks the public faces through properly designing supports and anchorage systems for nonstructural components.

## 1.3 Objective, Scope and Contribution of This Work

Recent earthquake events underscore the need to avoid or reduce the potential hazards to human life, safety and property that damaged NSCs pose. To meet this challenge the seismic demands on acceleration-sensitive components must be better understood and quantified. Since earthquakes produce accelerations in all three orthogonal directions, NSCs must be analyzed and properly anchored or constrained in both horizontal and vertical directions. Unfortunately, there have been very few studies that evaluate the vertical component of ground motion with respect to NSC performance, and even fewer studies incorporating three dimensional analytical building models. These 3-D models are important because in order to assess vertical component acceleration demands that affect NSCs attached to floors or ceilings, the out-of-plane flexibility of the floor diaphragm needs to be accurately captured. The most recent and noteworthy study that explicitly takes into account the out-of-plane floor flexibility is the 2012 work conducted by Pekcan et al. [4] That study focuses on conducting ground motion simulations on 3-D nonlinear steel moment frame buildings ranging from 3, 9 and 20 stories in height. However, based on the author's current knowledge there is no study that explicitly models the composite beam and floor slab connection. For instance, Pekcan et al. [4] uses an "equivalent shell" formulation where the secondary beam and the concrete slab section stiffnesses are lumped into an equivalent shell thickness. Furthermore, even when the vertical component of ground motion has been incorporated in a 3-D building analysis either experimentally or analytically, only a few number of ground motions have been used. For example, Pekcan et al. [4] uses only 21 ground motion recordings.

Therefore, the main objective of this thesis is to evaluate the vertical acceleration demands of elastic NSCs, supports, and attachments attached to a building exposed to a set of 106 recorded ground motions with various frequency contents, intensities, and durations. The quantification of vertical component acceleration demands includes:

a) Floor acceleration amplification with respect to the PGA
b) Vertical component acceleration amplification with respect to maximum vertical floor acceleration
c) The variation of vertical component acceleration demands along the height of the structure
d) The spatial variation of vertical component acceleration demands at a given floor level

*Contribution of This Work*

Vertical component acceleration demands are obtained via response history analysis on a 20-story office building using SAP2000 [11]. This building is designed to current building code standards including ASCE7-10 and the 2010 AISC Seismic Provisions and it is located in Los Angeles, California. This typical 20-story office building not only allows for an evaluation of results with respect to those obtained by Pekcan et al. [4] but also provides insight into the vertical seismic response of NSC attached to tall special moment resisting frame structures. In an effort to provide a reasonable model of the floor system the composite behavior of the steel beam and concrete floor is modeled separately as opposed to using an equivalent shell thickness. The floor system in this study is relatively more flexible than most conventional floor systems in order to provide a conservative (upper bound) estimate of the influence of higher mode effects on vertical component acceleration demands. The NSC acceleration demands are evaluated statistically using central values (i.e., medians) and a measure of dispersion (i.e., standard deviation of the natural logarithm of the values). Statistically representative NSC vertical acceleration demands are evaluated with respect to estimated design values from ASCE 7-10.

The remainder of this chapter further presents recent work in the field of acceleration-sensitive NSCs and provides an overview of the ASCE 7-10 NSC design provisions. Chapter 2 addresses the design of the 20-story office building. Chapter 3 discusses the analytical computational model and analysis procedures. Chapters 4 and 5 present the major results and conclusions of this study.

## 1.4 Literature Survey and Previous Work Related to Quantifying Seismic Behavior of NSC

There has been considerable effort towards understanding, and quantifying NSC behavior in the last couple of decades. This section highlights some of the most relevant work conducted during the past decade. Villaverde [1] describes this research being focused in three primary areas:

1.) Conducting and refining various methods of seismic analysis by using linear or nonlinear models; producing the acceleration response for a point on the primary structure where the NSC is attached by running either earthquake time histories or by directly using the ground acceleration spectrum (e.g., response spectrum analysis methods),
2.) NSC dynamic characterization through the use of component instrumentation and shake table tests or in-situ forced vibration loading,
3.) Proposing simplified design methods to be incorporated in building codes.

The next sections will give an overview of recent studies in these research areas and describe some of their merits and limitations.

### 1.4.1 Response Spectrum Analysis Methods

Villaverde [1] states that standard methods of analyzing NSCs in tandem with their supporting structures generally result in a system with an excessive number of degrees of freedom and large differences in the values of its various masses, stiffnesses and damping constants. As a result, the conventional methods of analysis become computationally expensive, potentially inaccurate, and inefficient. For example, a modal analysis exhibits difficulties in the computation of natural frequencies and mode shapes, and a step-by-step integration method may become sensitive to the selected integration time step.

Furthermore, a computational model combining both the structural system and each individual NSC may be too impractical since during preliminary design, the supporting structure would have to be reanalyzed every time a change is introduced to each nonstructural element. From a logistical point of view this approach has further problems since normally structures and nonstructural elements are designed by different teams at different times, which is not necessarily best practice. Therefore, problems of scheduling and efficiency become nontrivial issues.

In an effort to avoid the analysis of a combined system and overcome the aforementioned difficulties researchers have proposed simpler analysis approaches [1] for horizontal component acceleration demands. One such approach comes from Miranda and Taghavi [12]. They develop an approximate method to estimate floor acceleration demands in multistory buildings responding elastically to earthquake ground motions. This simplified method approximates the dynamic characteristics of buildings by modeling them as equivalent continuum structures consisting of a combination of a flexural beam and a shear beam. This approach allows the development of closed-form solutions for mode shapes, period ratios, and modal participation factors.  Using modal analysis the acceleration demands in the building are computed from these approximate dynamic properties. In Miranda and Reinoso [13] this simplified approach is evaluated by comparing peak floor acceleration demands and acceleration time histories to those recorded during earthquakes in six instrumented high-rise buildings. The method is also used to develop approximate floor spectra and these are compared to spectra computed with recorded motions. They conclude that this simplified method produces relatively good results compared to the instrumented records.

Miranda and Taghavi [14] also conducted a parametric study of the interaction between the primary structure and the secondary components on floor response acceleration spectra. This is important because the standard methods for computing acceleration response curves do not explicitly take into account the dynamic interaction between the primary and secondary system masses. The researchers varied the height of the primary structure, the component mass and damping ratio and as well as its location over the height of the building. They conclude that neglecting the interaction in general leads to an overestimation of the seismic demand on secondary systems and therefore to an overly conservative design. Furthermore, a component to primary mass ratio less than 1% will yield reasonably accurate floor spectra results compared to taking into account the interaction between masses.

A number of other researchers have studied the effects of nonlinear primary systems including shear walls [15] and moment resisting frames [16] attached to linear secondary systems on horizontal acceleration response spectra. Villaverde and Chaudhuri [17] performed a parametric study to investigate the impact of building nonlinearity on the seismic response of NSCs. They conducted their investigation by using response history analysis with earthquake ground motion time histories on steel moment resisting frames attached to linear and nonlinear single-degree-of-freedom nonstructural components. Their main conclusions are in line with previous nonlinear studies [15] [16] namely that in general, the nonlinear behavior of the supporting structures reduces the seismic response of the nonstructural components in comparison with the linear counterparts. However, they find that in a few cases, the NSC response is actually amplified however, in most cases NSCs may be designed based on a linear response analysis.

Historically researchers have focused on the horizontal component of floor acceleration and the research efforts previously described are no exception. This is because generally (except in the near field and at short natural periods) horizontal spectral acceleration dominates the vertical component [18] [19], and there is an implicit (yet unproven) assumption that designing components supports and attachments for gravity loading will provide a sufficient margin of safety against damage caused by vertical accelerations. Very recently though in order to better understand NSC behavior some researchers have investigated the effects of three dimensional earthquake loading. Pekcan et al. [20] generated both horizontal and vertical acceleration spectra in linearly elastic concrete buildings and concluded that the vertical component accelerations were significant and in some cases even exceeded the horizontal component accelerations. That work partly motivated Pekcan et al. [4] [21] to perform nonlinear finite element analyses on four steel moment frame buildings ranging from 3, 9 and 20 stories in height to study vertical component acceleration demands. Three of the four buildings in their study came from a SAC Joint Venture steel project investigation lead by Krawinkler and Gupta [22]. These SAC structures were designed with the 1994 Uniform Building Code [23] and the 1995 FEMA 267 Guidelines [24]. As described previously, Pekcan et al. [4] used an equivalent shell method which combined the thicknesses of the steel beam and concrete floor slab in order to model the composite behavior of the floor system. These structures were simultaneously exposed to the three components of earthquake ground motion (two orthogonal and one vertical) from 21 recorded earthquake motions. The main findings of the 2012 study are in line with other previous works on the effect of nonlinear behavior of the primary structure on the horizontal component of acceleration-sensitive NSC response. Namely, the acceleration response of NSCs is reduced by the nonlinear behavior of the primary system by changes in period, and increased ductility. It was also shown that the acceleration varies nonlinearly along the height of the building. In contrast to this finding the researchers discovered that in the vertical direction the acceleration response is independent of structural period, level of ductility, and relative height of the component location in the building. However, vertical component acceleration demands showed a strong dependence on the out-of-plane flexibility of the floor system. Variation and amplification of vertical floor acceleration demands were observed away from the columns and towards the middle of the open bay sections of the floor system. These results were used to evaluate the current code provisions for estimating peak vertical floor accelerations.

### 1.4.2 NSC Dynamic Characterization through Experimentation and Instrumentation

Other approaches, aside from theoretical methods to better understanding and quantifying NSC behavior involve shake table and forced vibration tests. While there have been numerous tests conducted in order to seismically qualify equipment and other NSCs there have not been very many experiments whose direct aim is to further investigate the seismic behavior of NSCs or to verify the analytical findings of previous studies [1]. Despite this observation the last decade has seen a shift in this trend. For example, Christoph Adam [23] conducted a small scale shake table test of a three story nonlinear shear frame with an attached NSC and compared the results to what a numerical analysis would produce for the same set up. Again, the acceleration demands of the NSC were in agreement with what more recent analytical studies predicted namely that these demands are smaller than in the linear case.

Reinhorn et al. [24] also employed shake table tests but their work focused specifically on the testing and qualification of suspended ceilings and their accessories. They verify their experimental setup and procedures and conclude by proposing new formulations for quantifying required response spectrum in the vertical direction. Furthermore, they propose an alternative testing protocol for seismic qualification NSCs with multi-point attachments for future consideration. This study is unique in that it experimentally quantifies NSC behavior explicitly in the vertical direction while the majority of research involving shake tables typically focus on the horizontal component of acceleration for NSCs.

Other prominent shake table tests implement the use of very large shake tables which are used to study both the structural behavior of full scale building and as well as the attached nonstructural components. For example Panagiotou et al. [25] use the Large High Performance Outdoor Shake Table at the University of California San Diego to investigate the forces on and performance of suspended pipes and their anchorages in a full scale seven story building exposed to several strong earthquake ground motions. The results of this experiment were the quantification of anchor forces and horizontal floor accelerations. The authors also provide evidence for reconsidering the current seismic anchor loading protocol. While strong vertical floor accelerations were observed and vertical accelerometers were in place during this study, this data was not recorded. A full scale shake table investigation which did record vertical acceleration data can be found in the work of Soroushian et al [26]. That study employed the large E-Defense shake table to test a full scale five story steel moment frame building under 2- and 3-D ground motions. Ceiling and piping system NSC were attached to the building and outfitted with accelerometers.  The tests were conducted while the structure was equipped with base isolators and while the base was fixed. The preliminary results include the following: vertical floor accelerations caused damage to the ceiling attachments and drop panels and that lateral bracing including compression may not improve the seismic response and damage of the ceilings. For another example of the use of large shake table tests the reader is referred to Matsuoka et al. [27], who used the E-Defense shake table to test a full scale four story building outfitted with NSCs until collapse and observe seismic performance and damage.

Hutchinson et al [28] subjected a full-scale building to forced vibration loading through the use of roof mounted linear and eccentric mass shakers. This building was also instrumented with an interior monitoring system which recorded the dynamic response of a variety of NSCs including a bench and shelf furnishing system, furnishing mounted equipment, and piping systems. The main test result findings highlight the importance of considering the transmissibility characteristics of building furnishings when estimating building NCS dynamic response.

In an effort to specifically measure the performance of NSCs and/or qualify them for use in buildings the University of Buffalo in association with the Network for Earthquake Engineering Simulation (NEES) have constructed a nonstructural component simulator with the ability to replicate, under controlled laboratory conditions, the effects of strong seismic shaking on distributed nonstructural systems located at the upper levels of multistory buildings. Furthermore, this testing equipment allows for assessing the seismic interactions between displacement and acceleration-sensitive nonstructural subsystems, providing a more realistic procedure for the seismic fragility assessment of combined nonstructural systems. The simulator can subject full-scale nonstructural specimens to accelerations of up to 3g, peak velocities of 100 in/s and displacements in the range of ±40 in, enveloping the peak seismic responses recorded at the upper levels of multistory buildings during historical earthquakes. It has been successfully used in assessing the performance of partition wall subsystems Filiatrault et al. [29] as well as a typical emergency room setup Filiatrault et al [30].

### 1.4.3 Simplified Design Methods Proposed for Building Codes

Significant research effort from structural engineers and researchers from around the world has been put forward in evaluating, verifying, and making proposals to improve the nonstructural component design sections of various building codes. Specifically, a number of studies have targeted the distribution of peak horizontal floor acceleration (PHFA) in nonlinear moment frames [31] [32] [33] [34] [16] [35] [21].These studies use the same general procedure by running time histories on nonlinear primary steel frame structures and they only really differ in their proposed design simplifications. For example Hutchinson et al. [32] proposes an equation to estimate the vertical distribution of PHFA amplification with respect to the ground peak acceleration value. That equation is primarily based on the height of the building and empirical constants whereas other researchers [21] proposes a modification based on the period of the primary supporting structure.

Another noteworthy study comes from Canada. Shooshtari et al. [36] propose a method for generating floor response spectra from uniform hazard spectra for western and eastern Canadian cities. The focus of their investigation was to bring design floor response spectra up to date with the National Building Code of Canada 2005 which evaluates seismic hazard data on the basis of uniform hazard spectra.

### 1.4.4 Previous Work Overview

While research into new analytical methods for NSC analysis was initially motivated by the shortcomings of standards approaches including modal analysis and explicit time integration techniques, modern analytical methods have relieved many of these problems. It has been demonstrated that dynamic analyses based on a special set of load- dependent Ritz vectors yield more accurate results than the use of the same number of natural mode shapes. Ritz vectors provide a better modal mass participation factor, which enables the analysis to run faster, with the same level of accuracy [37]. Currently available commercial packages such as SAP2000 and ETABS and open source packages such as OpenSees [40] employ fast nonlinear analysis methods to efficiently and accurately produce reliable seismic analyses of structures [38].

The reliability of these modern analysis packages has led to numerous studies by researchers into the seismic behavior of NSC both in terms of linear and nonlinear primary structure behavior. This effort has enhanced and strengthened the state of the art when it comes to the design and analysis of these components. However, the majority of these studies have been conducted on two dimensional buildings and concentrated on the in-plane behavior of components namely the horizontal direction of acceleration as a function of building height. However, it is important to remember that buildings experience all three components of earthquake ground motions. Pekcan et al. [20] and Panagiotou et al. [25] express a need to better understand all three directions of NSC behavior, but only very recently has there been any substantial analytical work undertaken including the vertical direction and considering three dimensional effects [4] [21].

On the experimental side, despite the nonstructural component simulator at the University of Buffalo's impressive capabilities it is both financially and logistically limiting since it is not practical to run a series of simulations consisting of a multitude of different earthquake ground motions. This latter criticism is valid for not only the simulator but also the shake table and forced vibration tests of both small-and full-scale buildings.

Despite the many simplified design formulations of the amplification of horizontal acceleration demands building codes have been slow to adopt changes. For example, ASCE 7-10 [42] uses a linear amplification factor based on the height of the building to calculate the floor acceleration at a particular story when many of the previous studies also integrate the building period for this calculation in order to get a more realistic PHFA distribution along the building height. When it comes to the estimation of vertical component accelerations, a more rudimentary approach is used, as described in the next section.

## 1.5 Vertical Design of NSCs Seismic Provisions per ASCE 7-10

Chapter 13 of ASCE 7-10 details the seismic requirements for nonstructural components. NSCs must resist concurrent horizontal and vertical seismic forces. In the vertical direction the code requires that components must resist the following design force formula:

$$F_p = \pm 0.2 S_{DS} W_p \tag{1.1}$$

Where:

$F_p$ : Vertical Seismic Design Force, kip.

$S_{DS}$ : Short Period Design Earthquake Spectral Response Acceleration, gravity (g).

$W_p$ : Weight of Component, kip.

In design practice this force is applied to the center mass of the component. This formula assumes that there is no component amplification with respect to the PGA, and no variation of vertical component acceleration demands with period of the component or the building, and that there is no floor to ground amplification in plan or relative to the height of the building. The building code assumes that because buildings are typically very stiff in the vertical direction, their dynamic vertical response will be equivalent to that of a rigid body. Furthermore, building codes assume that the component frequencies are such that they do not resonate with the vertical frequencies of the floor or roof system.

CHAPTER 2

# 20-STORY STRUCTURE DESIGN

## 2.1 Introduction

In order to evaluate whether or not the vertical design formula from ASCE 7-10 (equation 1.1) accurately captures the magnitude and variation of vertical NSC acceleration demands throughout the building both in plan and elevation requires the use of a multi-story building. For this purpose a typical 20-story office building assumed to be located in Los Angeles, California is considered. This particular building choice allows this work to be evaluated with respect to the results of Pekcan et al. [4], which also simulated vertical ground motions in a 20-story office building. This particular choice of building height is also close to the practical design limits of what is possible for steel moment resisting frame (SMRF) sections since column W shapes tend to get very deep and heavy towards the bottom of the building in the first couple of stories when the building is at or exceeds 20 stories in height [39].

This 20-story office building is equipped with steel moment resisting frame lateral force resisting systems (LFRS) in both the East-West (E-W) and North-South (N-S) directions. The SMRF systems are designed with reduced beam sections (RBS). The floor system consists of a steel metal deck made composite with a concrete slab through shear studs. This office building is designed according to load resistance factor design (LRFD) specifications, ASCE/SEI 7–2010 [40], ANSI/AISC 341-2010 [41], and AISC 2010 [42]. The building geometry including the number of stories, story height, column layout and floor plan, as well as the soil site properties are all based on an archetype model used in FEMA P695 [39]. As seen from Figure 7 the building footprint in plan view is 140 by 100 feet in the E-W and N-S directions, respectively. Figure 6 shows the full profile view of the building including the height which is 262 feet from the base to the roof. The first story of the building is 15 feet tall while all other stories are at a height of 13 feet.

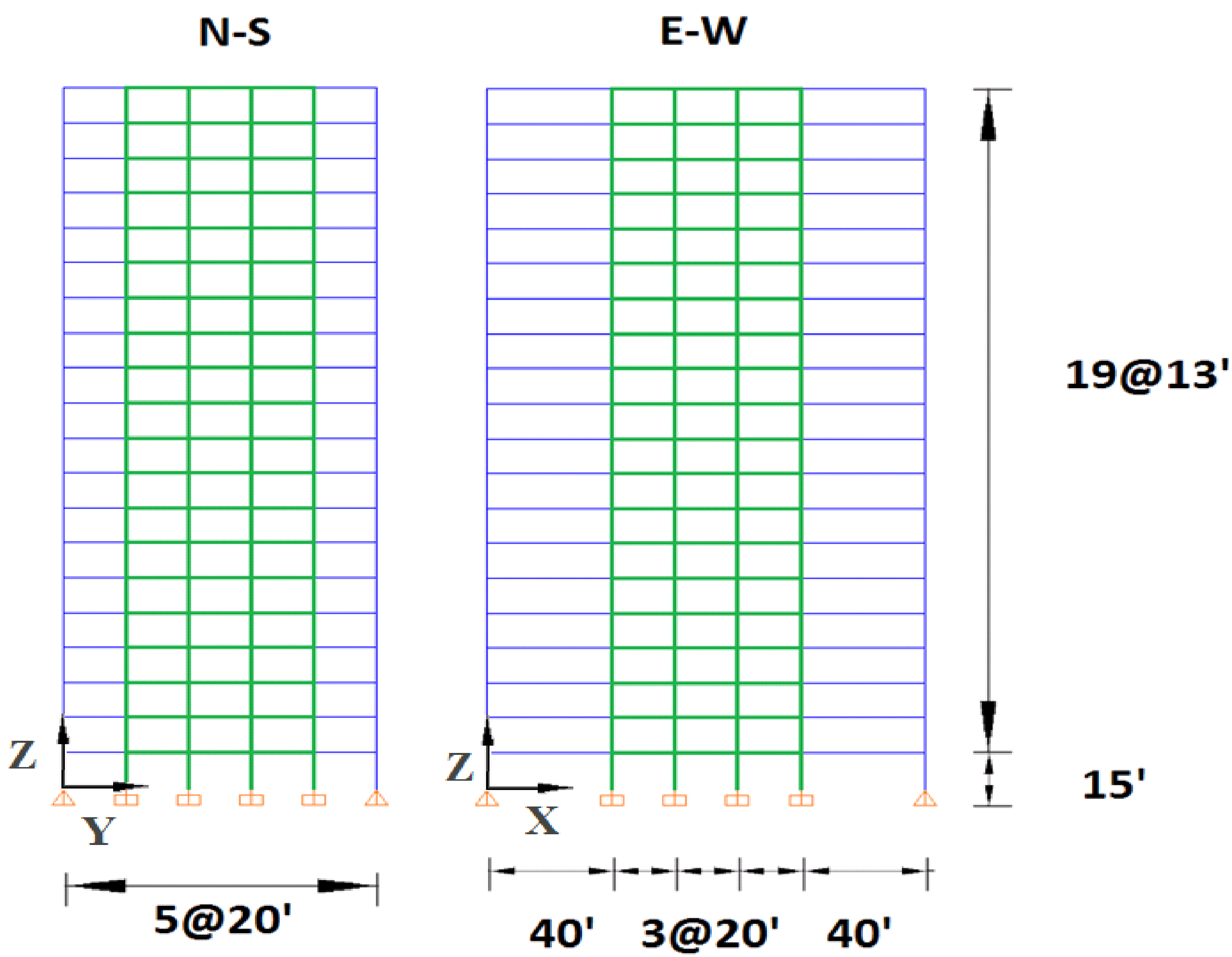


Figure 6: E-W and N-S elevation views of the 20-story office building. The special steel moment frames are highlighted in green.

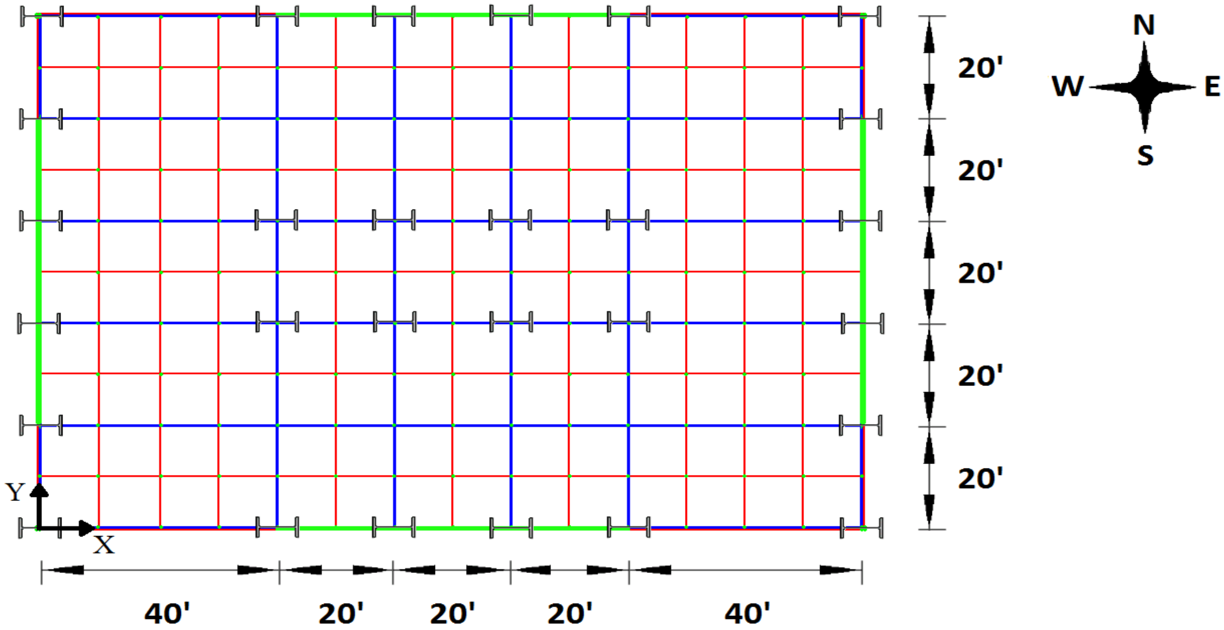


Figure 7: Plan view of the 20-story office building. The special steel moment frames are highlighted in green.

## 2.2 Materials

The structural steel material properties and specifications are obtained from the AISC Steel Construction Manual Tables 2-3 and 2-5 [43]. The material specifications for the rest of the building are outlined in the following table:

Table 3: Building Material Specification and Properties.

| Material | Specification | Grade, $F_y$ (ksi) | Fracture Stress, $F_u$ (ksi) | Ratio of Expected to Min Yield Stress, $R_y$ | Modulus of Elasticity, $E$ (ksi) | Elements |
|---|---|---|---|---|---|---|
| Steel | A992 | 50 | 65 | 1.1 | 29,000 | Beams Columns |
| Steel | A108 | 36 | 65 | | 29,000 | Shear Studs |
| Steel | A653 [44] | 37 | 52 | | 29,000 | Metal Deck |
| Concrete | Normal Weight | 3 | | | 3,122 | Slab |

## 2.3 Design Loads

The design loading for dead, live and seismic load cases is obtained from ASCE 7-10 [40], ASC Steel Deck Technical Floor Deck Specifications [45], and engineering judgment.

### 2.3.1 Design Dead Loads

Dead loads are primarily calculated based on material volumes and material unit weights as well as obtained from technical documents and engineering judgment. Unit weights used for concrete and steel are 150 pcf and 490 pcf respectively. See Table 4 for a summary of typical floor dead loads.

Table 4: Estimated Dead Loads for a Typical Floor.

| Typical Floor Loading | Load | Units | Tributary Area | Units | Weight, (kip) |
|---|---|---|---|---|---|
| 4" Normal Weight Concrete Slab [45] | 38 | psf | 14,000 | $ft^2$ | 527 |
| 18 ga. Steel Metal Deck [45] | 5 | psf | 14,000 | $ft^2$ | 71 |
| Interior Partitions | 10* | psf | 14,000 | $ft^2$ | 140 |
| Floor Beams | 75 | plf | 960 | ft | 72 |
| Girders (Average) | 100 | plf | 480 | ft | 48 |
| Columns (Average) | 200 | plf | 364 | ft | 73 |
| Miscellaneous (Flooring & Ceiling, MEP, Fireproofing etc.) | 12 | psf | 14,000 | $ft^2$ | 168 |
| Exterior Cladding | 25 | psf | 6,240 | $ft^2$ | 156 |

* Note that interior partitions are 20 psf for design dead load but 10 for seismic dead load as per ASCE 7-10 12.7.2 [40].

Typical floor seismic dead load totals to approximately 1,255 kips which distributes uniformly in plan to 90 psf. For design dead load the uniformly distributed weight comes to 100 psf. See the following table for final design dead loads.

Table 5: Final Design Dead Loads.

| Typical Loading | Load (psf) |
|---|---|
| Gravity Dead Load | 70 |
| Interior Partitions (Seismic/Gravity) | 10/20 |
| Cladding | 25 |
| Seismic Dead Load | 90 |

### 2.3.2 Design Live Loads

Occupancy and roof live loads are based on Table 4-1 Minimum Uniformly Distributed Live Loads from ASCE 7-10 [40]. The occupancy live load for the office building is 50 psf and the roof live load is 20 psf.

### 2.3.3 Live Load Reduction

Occupancy live loads are reduced for $K_{LL}A_T \geq 400 \text{ ft}^2$ according to the following ASCE 7 formula:

$$L = L_0\left[0.25 + \frac{15}{\sqrt{K_{LL}A_T}}\right] \tag{2.1}$$

Where:

$L$ : Reduced Distributed Live Load, psf.

$L_0$ : Unreduced Distributed Live Load, psf.

$K_{LL}$ : Live Load Element Factor, unitless.

$A_T$ : Tributary Area, $\text{ft}^2$.

### 2.3.4 Lateral Loads

Earthquake loads acting on the structure are obtained through the use of design spectra and by performing modal response spectrum analysis (RSA) per section 12.9 of ASCE 7-10 [40].

Wind loads acting on the structure are obtained by following the direction procedure outline in Table 27.2-1 in ASCE 7-10 [40].

## 2.4 Load Combinations

The load case combinations governing the design of this structure are from Chapter 2.3.2 and Chapter 12.4.3.2 ASCE 7-10 [40]. The governing lateral load case is seismic. The base shear due to seismic loads in the North-South direction is 1243 kips which is slightly larger than the 1233 kips due to wind loading. The overturning moment due to seismic is approximately 249,000 kip-ft vs. 173,000 kip-ft for wind. See Appendix A for additional information about wind loading. For the seismic load cases a redundancy factor $\rho$ equal to 1 is used in accordance with section 12.3.4.2. When required, the overstrength factor $\Omega_0$ is considered in the governing load combinations. From the load combinations available the relevant combinations are the following:

1. $$1.4D \tag{2.2}$$
2. $$1.2D + 1.6L + 0.5L_r \tag{2.3}$$
3. $$1.2D + 0.5L + 1.6L_r \tag{2.4}$$
4. $$1.2D + 0.5L + 0.5L_r \tag{2.5}$$
5. $$(1.2 + 0.2S_{DS})D + 0.5L \pm \rho E \tag{2.6}$$
6. $$(0.9 - 0.2S_{DS})D + 0.5L \pm \rho E \tag{2.7}$$

## 2.5 Seismic SMRF E-W Frame Design

### 2.5.1 SMRF, Site Properties, Importance Factor & Risk Category

This section summarizes the design of the E-W frame. The corresponding calculations and results for the N-S frame can be found in Appendix C. The design properties of the SMRF frame are obtained from Table 12.2-1 Design Coefficients and Factors for Seismic Force Resisting Systems. The response modification coefficient, *R*, is taken as 8 and is used to set the minimum acceptable strength at which the structure will develop its first significant yielding [46]. The overstrength factor $\Omega_0$ is 3 and it is a quantification of the additional strength over the design strength a structure has due to full plastic hinge formation, actual material yield strength instead of nominal yield strength, and other redundancies built into design codes and common engineering practice. The deflection amplification factor $C_d$ is 5.5 and it multiplies the calculated elastic deformations in order to estimate the deformations likely to result from the design ground motion [47]. Figure 8 from NEHRP Seismic Provisions provides a visual interpretation of the aforementioned factors.

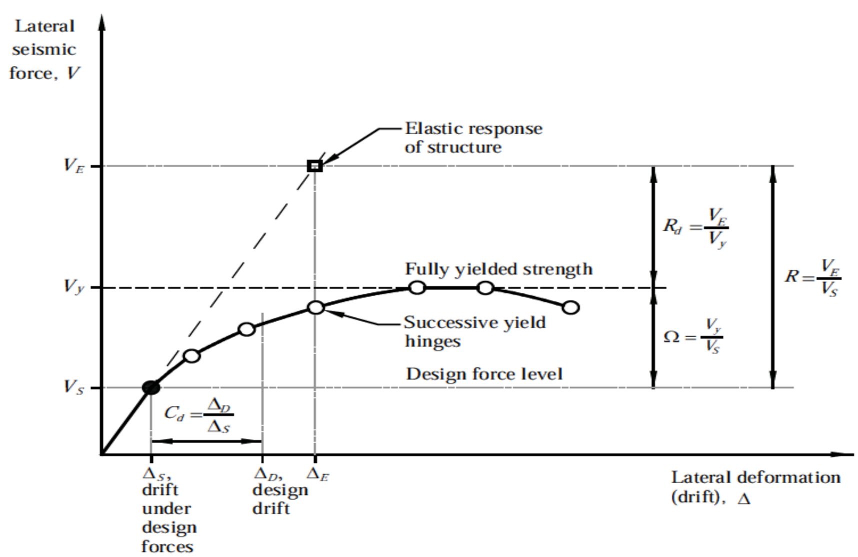


Figure 8: Seismic force vs. lateral deformation [47].

Based on Table 1.5-1 Risk Category of Buildings and Other Structures from ASCE 7-10 [40] the office building falls within risk category II with a corresponding seismic importance factor, *I*, of 1.0. In lieu of a detailed geotechnical investigation into the site soil properties, and in the absence of soil information which would require a higher class designation section 11.4.2 of ASCE 7 [40] allows the site classification to be conservatively designated as Site Class D.

### 2.5.2 Design Spectral Acceleration and Design Response Spectrum

For this building the risk-targeted maximum considered earthquake ($MCE_R$) spectral response acceleration at short periods, $S_s$, and at 1 second period, $S_1$, is taken to be 1.5g and 0.6g respectively. The design earthquake spectral response acceleration parameter at short period, $S_{DS}$, and at 1 second period, $S_{D1}$ are obtained from the following equations:

$$S_{DS} = {}^{2}/_{3}\, F_a S_s \qquad (2.8)$$

$$S_{D1} = {}^{2}/_{3}\, F_v S_1 \qquad (2.9)$$

Where $F_a$ and $F_v$ are the short and long period site coefficients obtained as 1.0 and 1.5 from tables 11.4-1 and 11.4-2 out of ASCE 7 [40]. Thus, $S_{DS}$ and $S_{D1}$ are calculated to be 1.0g and 0.6g. These spectral accelerations are used to define the design response spectrum according to the following figure:

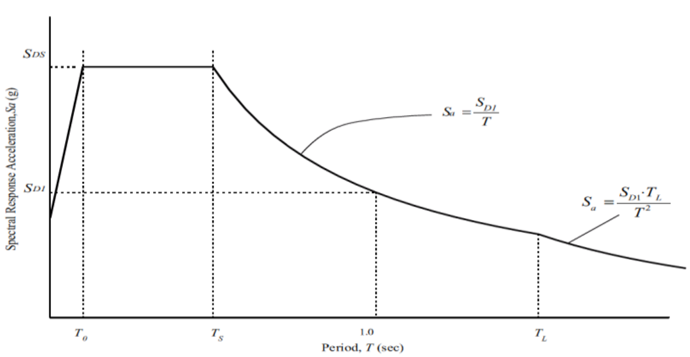


Figure 9: ASCE 7 design response spectrum [40].

Where:

$S_a$ : Spectral Response Acceleration, g.

$T$ : Fundamental Period of the Structure, s.

$T_0 = 0.2\frac{S_{D1}}{S_{DS}}$ : Constant Acceleration Transition Period, s.

$T_S = \frac{S_{D1}}{S_{DS}}$ : Constant Velocity Transition Period, s.

$T_L$ : Constant Displacement Transition Period also Long Period, s.

Table 6: Design Response Spectrum as a Function of Fundamental Period.

| Spectral Acceleration, $S_a$ (g) | Fundamental Period, $T$ (s) |
|---|---|
| $\left[0.4 + 0.6\frac{T}{T_0}\right] S_{DS}$ | $T \leq T_0$ |
| $S_{DS}$ | $T_0 \leq T \leq T_s$ |
| $\left[\frac{1}{T}\right] S_{D1}$ | $T_s \leq T \leq T_L$ |
| $\left[\frac{T_L}{T^2}\right] S_{D1}$ | $T \geq T_L$ |

Adhering to the aforementioned process yields the following design response spectrum for this 20-story building and is shown in Figure 10.

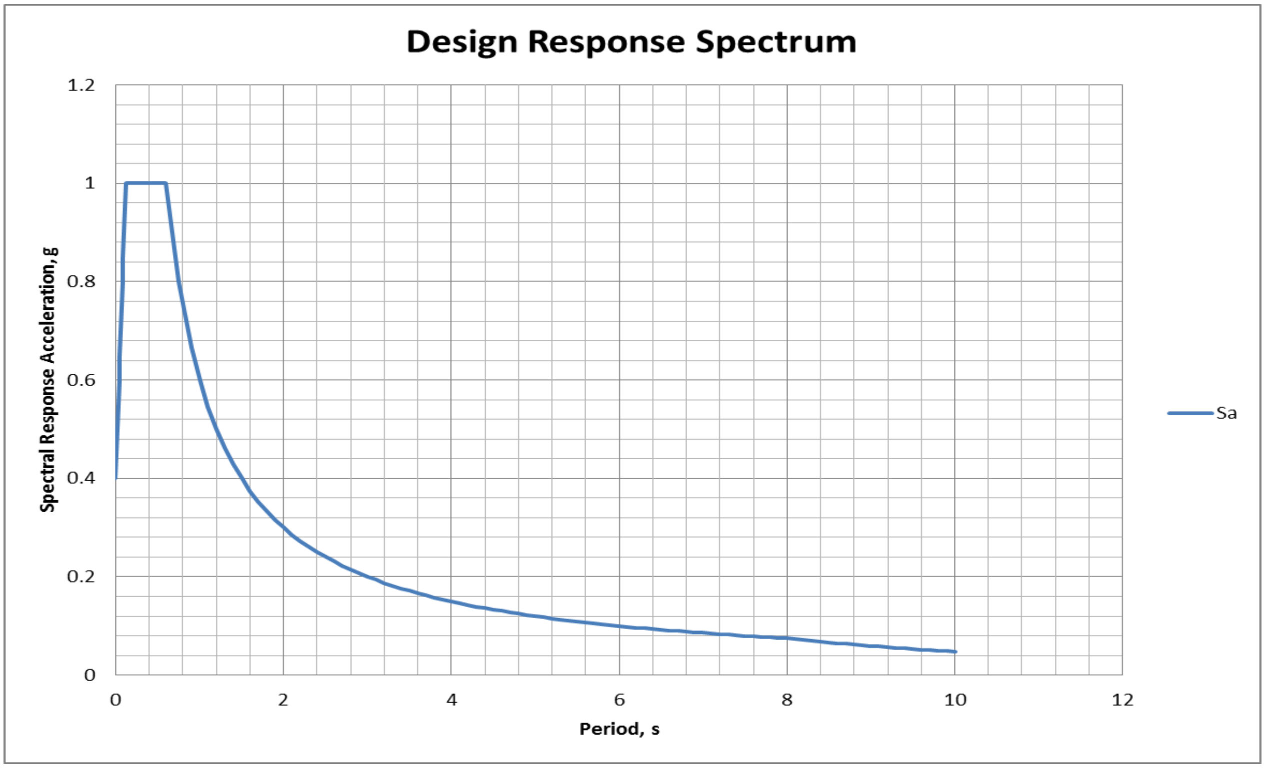


Figure 10: Design response spectrum for the office building.

### 2.5.3 Modal Response Spectrum Analysis

The availability of a design response spectrum permits the building to be analyzed using a dynamic analysis approach such as the modal response spectrum method (RSA). RSA requires the design response spectrum to be scaled by the factor (*I/R*). ASCE 7-10 requires that the member forces determined through response spectrum analysis be scaled so that the total applied lateral force in any direction is not less than 80% of the base shear calculated using the equivalent-lateral force (ELF) method for regular structures nor 100% for irregular structures. This scaling requirement was introduced to ensure that assumptions used in building the analytical model do not result in excessively flexible representations of the structure and, consequently, an underestimate of the required strength [46]. In this method, an MDOF structure is decomposed into N number of single-degree-of-freedom systems, each having its own mode shape and natural period of vibration. The number of modes available is equal to the number of dynamic degrees of freedom of the structure. However, the analysis must include a minimum number of modes of vibration in order to capture the participation of at least 90% of the structural effective mass in each of the three orthogonal directions. As can be seen from the following tables produced by the analysis software package ETABS [48] more than 90% of the effective mass is captured in the analysis model.

Table 7: Effective Modal Mass in the E-W Direction.

| Mode | Period (s) | Frequency (Hz) | UX | ΣUX | RY | ΣRY | RZ | ΣRZ |
|---|---|---|---|---|---|---|---|---|
| 1 | 5.494 | 0.18 | 75.687 | 75.7 | 99.8173 | 99.817 | 80.399 | 80.4 |
| 2 | 1.781 | 0.56 | 12.141 | 87.8 | 0.0091 | 99.826 | 9.857 | 90.3 |
| 3 | 1.001 | 1.00 | 4.204 | 92.0 | 0.1467 | 99.973 | 1.846 | 92.1 |
| 4 | 0.659 | 1.52 | 2.321 | 94.4 | 0.0092 | 99.982 | 0.378 | 92.5 |
| 5 | 0.470 | 2.13 | 1.481 | 95.8 | 0.0088 | 99.991 | 0.073 | 92.6 |
| 6 | 0.355 | 2.82 | 1.020 | 96.9 | 0.0012 | 99.992 | 0.045 | 92.6 |
| 7 | 0.279 | 3.58 | 0.732 | 97.6 | 0.0043 | 99.997 | 0.107 | 92.7 |
| 8 | 0.224 | 4.46 | 0.561 | 98.1 | 0.0004 | 99.997 | 0.314 | 93.0 |
| 9 | 0.182 | 5.48 | 0.459 | 98.6 | 0.0015 | 99.998 | 0.690 | 93.7 |
| 10 | 0.146 | 6.86 | 0.518 | 99.1 | 0.0006 | 99.999 | 1.778 | 95.5 |
| 11 | 0.108 | 9.28 | 0.513 | 99.6 | 0.0008 | 100 | 2.354 | 97.8 |
| 12 | 0.069 | 14.40 | 0.361 | **100** | 0.0002 | **100** | 1.838 | **99.7** |

Table 8: Effective Modal Mass in the N-S Direction.

| Mode | Period (s) | Frequency (Hz) | UY | ΣUY | RX | ΣRX | RZ | ΣRZ |
|---|---|---|---|---|---|---|---|---|
| 1 | 4.578 | 0.22 | 72.775 | 72.8 | 99.6035 | 99.604 | 64.448 | 64.4 |
| 2 | 1.468 | 0.68 | 12.529 | 85.3 | 0.0394 | 99.643 | 12.208 | 76.7 |
| 3 | 0.866 | 1.15 | 5.687 | 91.0 | 0.2859 | 99.929 | 6.585 | 83.2 |
| 4 | 0.579 | 1.73 | 2.765 | 93.8 | 0.0520 | 99.981 | 4.073 | 87.3 |
| 5 | 0.422 | 2.37 | 1.515 | 95.3 | 0.0103 | 99.991 | 2.881 | 90.2 |
| 6 | 0.323 | 3.10 | 1.026 | 96.3 | 0.0007 | 99.992 | 2.447 | 92.6 |
| 7 | 0.261 | 3.84 | 0.859 | 97.2 | 0.0040 | 99.996 | 2.387 | 95.0 |
| 8 | 0.213 | 4.69 | 0.663 | 97.8 | 0.0003 | 99.996 | 1.968 | 97.0 |
| 9 | 0.176 | 5.67 | 0.506 | 98.3 | 0.0014 | 99.997 | 1.382 | 98.4 |
| 10 | 0.141 | 7.10 | 0.594 | 98.9 | 0.0008 | 99.998 | 1.217 | 99.6 |
| 11 | 0.105 | 9.51 | 0.664 | 99.6 | 0.0014 | 100 | 0.126 | 99.7 |
| 12 | 0.069 | 14.45 | 0.415 | **100** | 0.0002 | **100** | 0 | **99.7** |

For a given direction of earthquake ground motion loading, any dynamic response quantity *r(t)* such as internal member forces, base shear, overturning moment etc. can be computed by summing the contributions of all modes in the following manner [49] [50]:

$$r(t) = \sum_{j=1}^{N} r_j^{st} A_j(t) \tag{2.10}$$

Where:

$r(t)$ : Specific Dynamic Response Quantity of Interest, variable units.

$r_j^{st}$ : Static Response of Mode *j* due to External Static Load Pattern $S_j$, variable units.

$S_j$ : Equivalent Spatial Load Vector, mass.

$A_j(t)$ : Pseudo-acceleration Response of the *j*th Mode Linearly Independent SDOF System, ft/s$^2$.

However, for design purposes the peak modal dynamic response is of particular interest therefore, equation 2.10 becomes [49] [50]:

$$r_{j,max} = r_j^{st} S_a \tag{2.11}$$

Where:

$r_{j,max}$ : Maximum Specific Dynamic Response Quantity of Interest for Mode $j$, variable units.

$S_a$ : Pseudo-acceleration Response Obtained from a Response Spectra, ft/s$^2$.

Since the peak response quantity for each mode is determined based on the corresponding spectral acceleration and because the direction and time of occurrence of the maximum acceleration are not evident while creating a response spectrum, there is no way to recombine modal responses exactly such that the maximum response would be identical to that of a response history analysis. However, statistical combination of modal responses produces sufficiently accurate estimates of displacements and component forces for design purposes [47]. The modal combination rule used in this work is the complete quadratic combination (CQC) which comes from random vibration theory and is briefly described below [50].

$$r_{o,CQC} = \left(\sum_{i=1}^{N} \sum_{k=1}^{N} \rho_{ik} r_{io} r_{ko}\right)^{1/2} \tag{2.12}$$

Where:

$r_{o,CQC}$ : Maximum Dynamic Response Quantity of Interest Based on CQC Rule, variable units.

$\rho_{ik}$ : Modal Correlation Coefficient between Modes $i$ and $k$, unitless.

$r_{io}$ : Maximum Dynamic Response Quantity of Interest for Mode $i$, variable units.

$r_{ko}$ : Maximum Dynamic Response Quantity of Interest for Mode $k$, variable units.

The modal correlation coefficients can be calculated from the following formula produced by Der Kiureghian:

$$\rho_{ik} = \frac{8\varsigma^2(1+\beta_{ik})\beta_{ik}^{3/2}}{\left(1-\beta_{ik}^2\right)^2+4\varsigma^2\beta_{ik}(1+\beta_{ik})^2} \tag{2.13}$$

Where:

$\rho_{ik}$ : Modal Correlation Coefficient between Modes *i* and *k*, unitless.

$\varsigma$ : Percent Damping Ratio, unitless.

$\beta_{ik}$ : Frequency Ratio of Mode *i* and Mode *k*, $\omega_i/\omega_k$, unitless.

### 2.5.4 Perimeter Beam Design

Once the building has been analyzed and the maximum earthquake loads are obtained from the RSA method and combined with the other design loads through load combinations, the individual members can be iteratively designed. The frame columns and girders are designed simultaneously and both are designed to meet the AISC Steel Construction Manual Standards [43], and the AISC Seismic Provisions for Structural Steel Buildings [41]. The girders are designed in the following process: the initial design is based on assuming W36 column shapes and then computing the required beam moment of inertia to resist estimated story shears, and code drift limits. From here the ETABS® analytical model is analyzed under design loads and checked for strength capacity and drift limits until satisfactory member sizes are achieved. Final beam sizes, compactness, strength and inter-story drift checks for the E-W frame are shown in Table 9-Table 14.

Table 9: Interior Left Girders of E-W Frame Final Design and Checks.

| Floor | Section | $M_{u,max}$ (kip-in) | $V_{u,max}$ (kip) | Flexure | Shear | Flexure ≤ 1 Shear ≤ 1 |
|---|---|---|---|---|---|---|
| 20 | W24X94 | 1,831 | 14.16 | 0.160 | 0.041 | OK |
| 19 | W24X62 | 1,950 | 15.73 | 0.283 | 0.054 | OK |
| 18 | W24X62 | 2,324 | 19.19 | 0.337 | 0.066 | OK |
| 17 | W24X62 | 2,494 | 21.23 | 0.362 | 0.073 | OK |
| 16 | W24X146 | 4,477 | 38.78 | 0.238 | 0.088 | OK |
| 15 | W24X146 | 4,480 | 38.29 | 0.238 | 0.087 | OK |
| 14 | W24X146 | 4,598 | 39.22 | 0.244 | 0.089 | OK |
| 13 | W24X146 | 4,778 | 40.77 | 0.254 | 0.093 | OK |
| 12 | W24X146 | 4,992 | 42.61 | 0.265 | 0.097 | OK |
| 11 | W24X131 | 4,874 | 41.90 | 0.293 | 0.102 | OK |
| 10 | W24X131 | 5,024 | 44.15 | 0.302 | 0.108 | OK |
| 9 | W24X131 | 5,170 | 45.68 | 0.311 | 0.111 | OK |
| 8 | W24X131 | 5,411 | 49.04 | 0.325 | 0.120 | OK |
| 7 | W24X131 | 5,539 | 50.30 | 0.333 | 0.123 | OK |
| 6 | W24X131 | 5,610 | 51.01 | 0.337 | 0.124 | OK |
| 5 | W24X146 | 6,452 | 57.55 | 0.343 | 0.131 | OK |
| 4 | W24X146 | 6,723 | 60.57 | 0.357 | 0.138 | OK |
| 3 | W24X146 | 6,727 | 59.76 | 0.358 | 0.136 | OK |
| 2 | W24X146 | 6,404 | 56.98 | 0.340 | 0.130 | OK |
| 1 | W24X146 | 5,132 | 44.12 | 0.273 | 0.100 | OK |

Table 10: Interior Right Girders of E-W Frame Final Design and Checks.

| Floor | Section | $M_{u,max}$ (kip-in) | $V_{u,max}$ (kip) | Flexure | Shear | Flexure ≤ 1 Shear ≤ 1 |
|---|---|---|---|---|---|---|
| 20 | W24X94 | 616 | 21.90 | 0.054 | 0.063 | OK |
| 19 | W24X62 | 974 | 23.46 | 0.141 | 0.081 | OK |
| 18 | W24X62 | 1,340 | 26.92 | 0.195 | 0.093 | OK |
| 17 | W24X62 | 1,559 | 28.95 | 0.226 | 0.100 | OK |
| 16 | W24X146 | 2,407 | 46.50 | 0.128 | 0.106 | OK |
| 15 | W24X146 | 2,491 | 46.00 | 0.132 | 0.105 | OK |
| 14 | W24X146 | 2,730 | 46.93 | 0.145 | 0.107 | OK |
| 13 | W24X146 | 3,063 | 48.49 | 0.163 | 0.110 | OK |
| 12 | W24X146 | 3,451 | 50.32 | 0.183 | 0.115 | OK |
| 11 | W24X131 | 3,706 | 49.50 | 0.223 | 0.121 | OK |
| 10 | W24X131 | 4,091 | 50.78 | 0.246 | 0.124 | OK |
| 9 | W24X131 | 4,431 | 51.22 | 0.266 | 0.125 | OK |
| 8 | W24X131 | 4,977 | 54.10 | 0.299 | 0.132 | OK |
| 7 | W24X131 | 5,263 | 54.80 | 0.316 | 0.134 | OK |
| 6 | W24X131 | 5,527 | 54.86 | 0.332 | 0.134 | OK |
| 5 | W24X146 | 6,289 | 61.40 | 0.334 | 0.140 | OK |
| 4 | W24X146 | 6,285 | 62.49 | 0.334 | 0.142 | OK |
| 3 | W24X146 | 5,939 | 64.30 | 0.316 | 0.146 | OK |
| 2 | W24X146 | 5,581 | 61.94 | 0.297 | 0.141 | OK |
| 1 | W24X146 | 4,173 | 49.95 | 0.222 | 0.114 | OK |

Table 11: Exterior Left Girders of E-W Frame Final Design and Checks.

| Floor | Section | $M_{u,max}$ (kip-in) | $V_{u,max}$ (kip) | Flexure | Shear | Flexure ≤ 1 Shear ≤ 1 |
|---|---|---|---|---|---|---|
| 20 | W24X94 | 1,348 | 12.5 | 0.118 | 0.036 | OK |
| 19 | W24X62 | 1,584 | 14.5 | 0.230 | 0.050 | OK |
| 18 | W24X62 | 1,931 | 17.9 | 0.280 | 0.062 | OK |
| 17 | W24X62 | 2,265 | 21.2 | 0.329 | 0.073 | OK |
| 16 | W24X146 | 3,933 | 38.4 | 0.209 | 0.087 | OK |
| 15 | W24X146 | 3,931 | 38.2 | 0.209 | 0.087 | OK |
| 14 | W24X146 | 4,115 | 39.9 | 0.219 | 0.091 | OK |
| 13 | W24X146 | 4,374 | 42.3 | 0.233 | 0.096 | OK |
| 12 | W24X146 | 4,658 | 45.0 | 0.248 | 0.102 | OK |
| 11 | W24X131 | 4,687 | 45.1 | 0.282 | 0.110 | OK |
| 10 | W24X131 | 4,925 | 47.3 | 0.296 | 0.115 | OK |
| 9 | W24X131 | 5,090 | 48.7 | 0.306 | 0.119 | OK |
| 8 | W24X131 | 5,713 | 54.8 | 0.343 | 0.134 | OK |
| 7 | W24X131 | 5,821 | 55.8 | 0.350 | 0.136 | OK |
| 6 | W24X131 | 5,863 | 56.1 | 0.352 | 0.137 | OK |
| 5 | W24X146 | 6,044 | 57.7 | 0.321 | 0.131 | OK |
| 4 | W24X146 | 6,040 | 58.4 | 0.321 | 0.133 | OK |
| 3 | W24X146 | 5,713 | 54.7 | 0.304 | 0.125 | OK |
| 2 | W24X146 | 5,266 | 50.3 | 0.280 | 0.115 | OK |
| 1 | W24X146 | 3,574 | 33.7 | 0.190 | 0.077 | OK |

Table 12: Exterior Right Girders of E-W Frame Final Design and Checks.

| Floor | Section | $M_{u,max}$ (kip-in) | $V_{u,max}$ (kip) | Flexure | Shear | Flexure ≤ 1 Shear ≤ 1 |
|---|---|---|---|---|---|---|
| 20 | W24X94 | 1,348 | 18.3 | 0.118 | 0.053 | OK |
| 19 | W24X62 | 1,584 | 20.3 | 0.230 | 0.070 | OK |
| 18 | W24X62 | 1,931 | 23.7 | 0.280 | 0.082 | OK |
| 17 | W24X62 | 2,265 | 27.0 | 0.329 | 0.093 | OK |
| 16 | W24X146 | 3,933 | 44.1 | 0.209 | 0.100 | OK |
| 15 | W24X146 | 3,931 | 44.0 | 0.209 | 0.100 | OK |
| 14 | W24X146 | 4,115 | 45.7 | 0.219 | 0.104 | OK |
| 13 | W24X146 | 4,374 | 48.1 | 0.233 | 0.110 | OK |
| 12 | W24X146 | 4,658 | 50.8 | 0.248 | 0.116 | OK |
| 11 | W24X131 | 4,687 | 50.9 | 0.282 | 0.124 | OK |
| 10 | W24X131 | 4,925 | 53.1 | 0.296 | 0.129 | OK |
| 9 | W24X131 | 5,090 | 54.5 | 0.306 | 0.133 | OK |
| 8 | W24X131 | 5,713 | 60.6 | 0.343 | 0.148 | OK |
| 7 | W24X131 | 5,821 | 61.6 | 0.350 | 0.150 | OK |
| 6 | W24X131 | 5,863 | 61.9 | 0.352 | 0.151 | OK |
| 5 | W24X146 | 6,044 | 63.5 | 0.321 | 0.145 | OK |
| 4 | W24X146 | 6,040 | 61.3 | 0.321 | 0.140 | OK |
| 3 | W24X146 | 5,713 | 60.5 | 0.304 | 0.138 | OK |
| 2 | W24X146 | 5,266 | 56.1 | 0.280 | 0.128 | OK |
| 1 | W24X146 | 3,574 | 39.9 | 0.190 | 0.091 | OK |

Table 13: Girders of E-W Frame Seismic Compactness Checks.

| Floor | Section | $\frac{1}{2}\frac{b_f}{t_f}$ | Flange Thickness Ratio Flexure $\leq 7.22$ | $\frac{h}{t_w}$ | Web Thickness Ratio $\leq 59$ | $\frac{h}{t_w}$ | Web Thickness Ratio Shear $\leq 53.95$ |
|---|---|---|---|---|---|---|---|
| 20 | W24X94 | 5.18 | OK | 20.95 | OK | 20.95 | OK |
| 19 | W24X62 | 5.97 | OK | 25.05 | OK | 25.05 | OK |
| 18 | W24X62 | 5.97 | OK | 25.05 | OK | 25.05 | OK |
| 17 | W24X62 | 5.97 | OK | 25.05 | OK | 25.05 | OK |
| 16 | W24X146 | 5.92 | OK | 16.6 | OK | 16.6 | OK |
| 15 | W24X146 | 5.92 | OK | 16.6 | OK | 16.6 | OK |
| 14 | W24X146 | 5.92 | OK | 16.6 | OK | 16.6 | OK |
| 13 | W24X146 | 5.92 | OK | 16.6 | OK | 16.6 | OK |
| 12 | W24X146 | 5.92 | OK | 16.6 | OK | 16.6 | OK |
| 11 | W24X131 | 6.7 | OK | 17.8 | OK | 17.8 | OK |
| 10 | W24X131 | 6.7 | OK | 17.8 | OK | 17.8 | OK |
| 9 | W24X131 | 6.7 | OK | 17.8 | OK | 17.8 | OK |
| 8 | W24X131 | 6.7 | OK | 17.8 | OK | 17.8 | OK |
| 7 | W24X131 | 6.7 | OK | 17.8 | OK | 17.8 | OK |
| 6 | W24X131 | 6.7 | OK | 17.8 | OK | 17.8 | OK |
| 5 | W24X146 | 5.92 | OK | 16.6 | OK | 16.6 | OK |
| 4 | W24X146 | 5.92 | OK | 16.6 | OK | 16.6 | OK |
| 3 | W24X146 | 5.92 | OK | 16.6 | OK | 16.6 | OK |
| 2 | W24X146 | 5.92 | OK | 16.6 | OK | 16.6 | OK |
| 1 | W24X146 | 5.92 | OK | 16.6 | OK | 16.6 | OK |

Table 14: E-W Frame Drift Limit Check.

| Story | Story Drift | Drift Limit | Drift Check ≤ 0.02 |
|---|---|---|---|
| 20 | 0.011 | 0.020 | OK |
| 19 | 0.014 | 0.020 | OK |
| 18 | 0.015 | 0.020 | OK |
| 17 | 0.015 | 0.020 | OK |
| 16 | 0.015 | 0.020 | OK |
| 15 | 0.015 | 0.020 | OK |
| 14 | 0.016 | 0.020 | OK |
| 13 | 0.016 | 0.020 | OK |
| 12 | 0.017 | 0.020 | OK |
| 11 | 0.018 | 0.020 | OK |
| 10 | 0.018 | 0.020 | OK |
| 9 | 0.018 | 0.020 | OK |
| 8 | 0.018 | 0.020 | OK |
| 7 | 0.018 | 0.020 | OK |
| 6 | 0.018 | 0.020 | OK |
| 5 | 0.017 | 0.020 | OK |
| 4 | 0.017 | 0.020 | OK |
| 3 | 0.016 | 0.020 | OK |
| 2 | 0.014 | 0.020 | OK |
| 1 | 0.008 | 0.020 | OK |

### 2.5.5 Reduced Beam Section (RBS) Design

Frame girders are also designed with reduced beam sections (RBS) in accordance to the Steel Construction Manual [43] and by following a procedure outlined in STEEL TIPS Design of RBS Moment Frame Connections [51] (Figure 11). The idea is that by removing sections of the top and bottom flanges of the beam by cutting a depth *c* into the beam over a length *b* at a distance *a* from the face of the column the moment on the face of the column is drastically reduced compared to a non RBS beam-column moment connection type. This will protect the connection area, more specifically, the welds from detrimental stress concentrations. The *a*,*b*, and *c* specifications are based on a percent of the beam flange width, $b_f$ and the depth of section *d*. These percentages are constant for all of the girders. See Figure 11 for a depiction of a typical

RBS section. Furthermore, by reducing the strength of the beam at a discrete location away from the column the likelihood of a plastic hinge forming first at the beam-column connection instead of at the reduced beam section under an intense seismic event is significantly reduced.

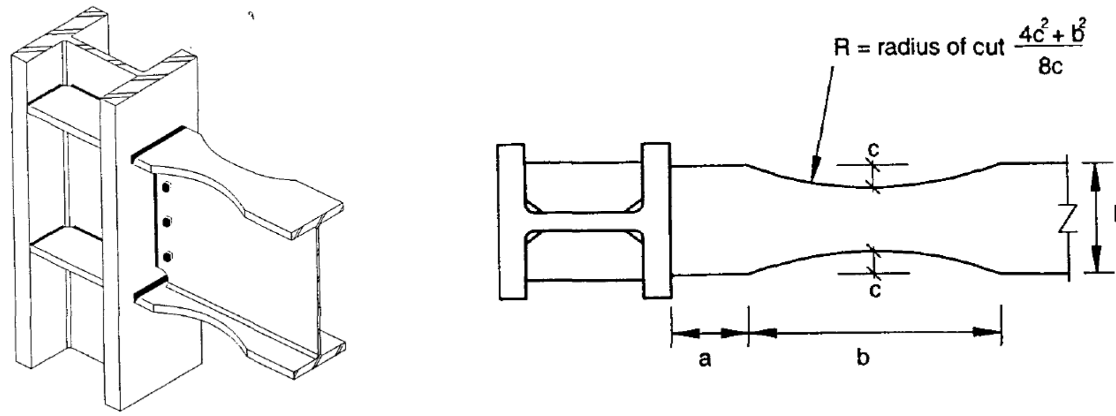


Figure 11: RBS example with plan view of dimension cuts [51].

The critical areas of the RBS design are the moment and shear at the center of the reduced beam section ($M_{RBS}$ and $V_{RBS}$ respectively) as well as the moment at the face of the column $M_f$. These are shown in Figure 12. They are checked against the girder plastic moment capacity, $M_p$, and as well as the RBS plastic moment, $M_{p,RBS}$, and the girder shear capacity $V_n$. See the following table for a typical RBS design strength checks.

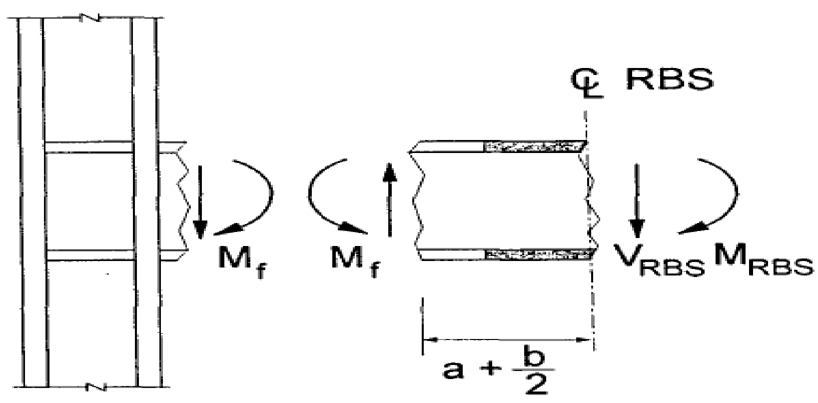


Figure 12: Critical design sections of RBS moment connection [51].

Table 15: RBS Design Coefficients and Factored Moments and Shear.

| Floor | Section | a (in) | b (in) | c (in) | $M_{u,RBS}$ (kip-in) | $V_{u,RBS}$ (kip) | $M_{u,f}$ (kip-in) |
|---|---|---|---|---|---|---|---|
| 20 | W24X94 | 5.62 | 18.20 | 2.25 | 1,034 | 122 | 12,035 |
| 19 | W24X62 | 4.36 | 17.75 | 1.75 | 1,320 | 79 | 7,718 |
| 18 | W24X62 | 4.36 | 17.75 | 1.75 | 1,747 | 79 | 7,716 |
| 17 | W24X62 | 4.36 | 17.75 | 1.75 | 1,923 | 79 | 7,716 |
| 16 | W24X146 | 8.00 | 18.50 | 3.20 | 3,195 | 197 | 19,418 |
| 15 | W24X146 | 8.00 | 18.50 | 3.20 | 3,345 | 196 | 19,409 |
| 14 | W24X146 | 8.00 | 18.50 | 3.20 | 3,622 | 195 | 19,395 |
| 13 | W24X146 | 8.00 | 18.50 | 3.20 | 3,994 | 195 | 19,379 |
| 12 | W24X146 | 8.00 | 18.50 | 3.20 | 4,430 | 193 | 19,359 |
| 11 | W24X131 | 8.00 | 18.35 | 3.20 | 4,604 | 171 | 17,191 |
| 10 | W24X131 | 8.00 | 18.35 | 3.20 | 5,025 | 170 | 17,168 |
| 9 | W24X131 | 8.00 | 18.35 | 3.20 | 5,474 | 169 | 17,162 |
| 8 | W24X131 | 8.00 | 18.35 | 3.20 | 5,851 | 170 | 17,173 |
| 7 | W24X131 | 8.00 | 18.35 | 3.20 | 6,131 | 171 | 17,187 |
| 6 | W24X131 | 8.00 | 18.35 | 3.20 | 6,384 | 172 | 17,202 |
| 5 | W24X146 | 8.00 | 18.50 | 3.20 | 7,602 | 196 | 19,397 |
| 4 | W24X146 | 8.00 | 18.50 | 3.20 | 7,542 | 194 | 19,375 |
| 3 | W24X146 | 8.00 | 18.50 | 3.20 | 7,358 | 193 | 19,350 |
| 2 | W24X146 | 8.00 | 18.50 | 3.20 | 6,915 | 192 | 19,339 |
| 1 | W24X146 | 8.00 | 18.50 | 3.20 | 5,521 | 192 | 19,328 |

Table 16: Demand to Capacity Ratios for the Column Face Moment, Shear and Moment at Center of RBS.

| Floor | $\frac{M_{u,f}}{M_p}$ | $\frac{M_{u,f}}{M_p} \leq 1$ | $\frac{V_{u,RBS}}{V_{n,RBS}}$ | $\frac{V_{u,RBS}}{V_{n,RBS}} \leq 1$ | $\frac{M_{u,RBS}}{M_{p,RBS}}$ | $\frac{M_{u,RBS}}{M_{p,RBS}} \leq 1$ |
|---|---|---|---|---|---|---|
| 20 | 0.86 | OK | 0.35 | OK | 0.13 | OK |
| 19 | 0.92 | OK | 0.27 | OK | 0.25 | OK |
| 18 | 0.92 | OK | 0.27 | OK | 0.33 | OK |
| 17 | 0.92 | OK | 0.27 | OK | 0.36 | OK |
| 16 | 0.84 | OK | 0.45 | OK | 0.25 | OK |
| 15 | 0.84 | OK | 0.45 | OK | 0.26 | OK |
| 14 | 0.84 | OK | 0.45 | OK | 0.29 | OK |
| 13 | 0.84 | OK | 0.44 | OK | 0.32 | OK |
| 12 | 0.84 | OK | 0.44 | OK | 0.35 | OK |
| 11 | 0.84 | OK | 0.42 | OK | 0.41 | OK |
| 10 | 0.84 | OK | 0.41 | OK | 0.45 | OK |
| 9 | 0.84 | OK | 0.41 | OK | 0.49 | OK |
| 8 | 0.84 | OK | 0.41 | OK | 0.52 | OK |
| 7 | 0.84 | OK | 0.42 | OK | 0.54 | OK |
| 6 | 0.85 | OK | 0.42 | OK | 0.57 | OK |
| 5 | 0.84 | OK | 0.45 | OK | 0.60 | OK |
| 4 | 0.84 | OK | 0.44 | OK | 0.60 | OK |
| 3 | 0.84 | OK | 0.44 | OK | 0.58 | OK |
| 2 | 0.84 | OK | 0.44 | OK | 0.55 | OK |
| 1 | 0.84 | OK | 0.44 | OK | 0.44 | OK |

### 2.5.6 Perimeter Frame Column Design

The perimeter frame columns that form part of the moment-resisting frame are all W36 shapes. Other shapes ranging from W14 to W33 were considered however, in order to meet the strong column weak beam (SCWB) moment ratio check from the AISC Seismic Provisions [41] and because large girders are required to meet code drift limitations for such a tall structure this frame design requires deep and heavy column shapes. Overall, the SCWB moment ratio controls the column member sizes for this frame. In the presence of seismic forces this check tries to ensure that columns are stronger relative to beams such that any yielding that occurs or any plastic hinges that form will first take place in the beams rather than the columns thereby avoiding undesirable story mechanisms that may potentially lead to a global collapse scenario for the floors above the column story failure. Figure 13 shows a depiction of a beam-hinge mechanism for a moment resisting frame properly designed based on SCWB criteria. The red dots are where plastic hinges are located.

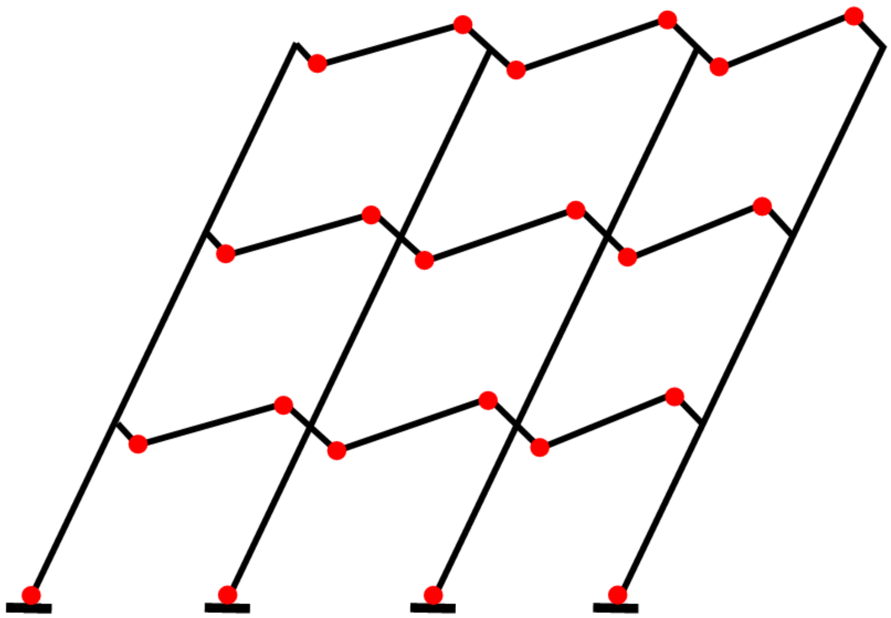

Figure 13: Beams yielding before columns in a three-story building. Figure is modified. [52].

The SCWB ratio is calculated by the following equation. See Table 20 for SCWB checks for the frame.

$$\frac{\sum M_{pc}^*}{\sum M_{pb}^*} > 1 \tag{2.14}$$

Where:

$\sum M_{pc}^*$ : The Sum of the Projections of the Nominal Flexural Strength of the Columns, kip-in.

$\sum M_{pb}^*$: The Sum of the Projections of the Expected Nominal Flexural Strength of the Beams at Plastic Hinge Locations, kip-in.

Column design follows these steps: the initial design is based on assuming W36 shapes such that calculated drift limits and SCWB criteria are met based on estimated story shears following a design approach used by a former graduate student Josh Clayton. Then, the ETABS analytical model is analyzed under design loads and checked for strength capacity, drift limits and strong column weak beam (SCWB) ratio checks until satisfactory member sizes are achieved. See the following tables for final exterior and interior column sizes, compactness, strength and SCWB checks for the E-W frame.

Table 17: Exterior Column Factored Axial Force, Moment and Governing Axial & Moment Interaction Equation from the AISC Steel Construction Manual [43].

| Floor | Section | $P_u$ | $M_u$ | EQ H1-1a/b | H1-1a/b ≤1 |
|---|---|---|---|---|---|
| 20 | W36X170 | 109 | 729 | 0.059 | OK |
| 19 | W36X170 | 222 | 1,032 | 0.12 | OK |
| 18 | W36X170 | 339 | 1,583 | 0.184 | OK |
| 17 | W36X170 | 458 | 2,271 | 0.248 | OK |
| 16 | W36X170 | 582 | 1,932 | 0.314 | OK |
| 15 | W36X194 | 707 | 1,819 | 0.334 | OK |
| 14 | W36X194 | 834 | 1,907 | 0.394 | OK |
| 13 | W36X194 | 965 | 2,051 | 0.456 | OK |
| 12 | W36X194 | 1,099 | 2,169 | 0.519 | OK |
| 11 | W36X194 | 1,236 | 2,477 | 0.584 | OK |
| 10 | W36X194 | 1,377 | 2,830 | 0.651 | OK |
| 9 | W36X231 | 1,523 | 3,227 | 0.545 | OK |
| 8 | W36X231 | 1,672 | 3,318 | 0.598 | OK |
| 7 | W36X231 | 1,824 | 3,640 | 0.652 | OK |
| 6 | W36X231 | 1,978 | 4,220 | 0.707 | OK |
| 5 | W36X330 | 2,140 | 4,627 | 0.534 | OK |
| 4 | W36X330 | 2,295 | 4,779 | 0.573 | OK |
| 3 | W36X330 | 2,454 | 5,682 | 0.613 | OK |
| 2 | W36X330 | 2,610 | 7,474 | 0.652 | OK |
| 1 | W36X330 | 2,755 | 18,279 | 0.712 | OK |

Table 18: Exterior Column Final Factored Axial Force with Overstrength Consideration.

| Floor | Section | $P_u$ | $\frac{P_u}{P_c}$ | $\frac{P_u}{P_c} \leq 1$ |
|---|---|---|---|---|
| 20 | W36X170 | 118 | 0.064 | OK |
| 19 | W36X170 | 245 | 0.133 | OK |
| 18 | W36X170 | 382 | 0.207 | OK |
| 17 | W36X170 | 523 | 0.283 | OK |
| 16 | W36X170 | 694 | 0.375 | OK |
| 15 | W36X194 | 864 | 0.408 | OK |
| 14 | W36X194 | 1,037 | 0.490 | OK |
| 13 | W36X194 | 1,219 | 0.576 | OK |
| 12 | W36X194 | 1,409 | 0.666 | OK |
| 11 | W36X194 | 1,604 | 0.758 | OK |
| 10 | W36X194 | 1,807 | 0.855 | OK |
| 9 | W36X231 | 2,019 | 0.722 | OK |
| 8 | W36X231 | 2,240 | 0.801 | OK |
| 7 | W36X231 | 2,467 | 0.882 | OK |
| 6 | W36X231 | 2,698 | 0.965 | OK |
| 5 | W36X330 | 2,950 | 0.736 | OK |
| 4 | W36X330 | 3,204 | 0.800 | OK |
| 3 | W36X330 | 3,455 | 0.863 | OK |
| 2 | W36X330 | 3,697 | 0.923 | OK |
| 1 | W36X330 | 3,906 | 1.009 | OK* |

* Note: The axial demand to capacity ratio for the first story is slightly exceeded however it is acceptable by common engineering practice.

Table 19: Exterior Column Seismic Compactness Checks

| Floor | Section | $\frac{1}{2}\frac{b_f}{t_f}$ | Flange Thickness Ratio Flexure ≤ 7.22 | $\frac{h}{t_w}$ | $\frac{h}{t_w}$ Limit | Web Thickness Ratio ≤ Limit |
|---|---|---|---|---|---|---|
| 20 | W36X170 | 5.45 | OK | 47.7 | 56.4 | OK |
| 19 | W36X170 | 5.45 | OK | 47.7 | 53.6 | OK |
| 18 | W36X170 | 5.45 | OK | 47.7 | 51.5 | OK |
| 17 | W36X170 | 5.45 | OK | 47.7 | 50.6 | OK |
| 16 | W36X170 | 5.45 | OK | 47.7 | 49.5 | OK |
| 15 | W36X194 | 4.80 | OK | 42.4 | 49.2 | OK |
| 14 | W36X194 | 4.80 | OK | 42.4 | 48.3 | OK |
| 13 | W36X194 | 4.80 | OK | 42.4 | 47.4 | OK |
| 12 | W36X194 | 4.80 | OK | 42.4 | 46.4 | OK |
| 11 | W36X194 | 4.80 | OK | 42.4 | 45.4 | OK |
| 10 | W36X194 | 4.80 | OK | 42.4 | 44.4 | OK |
| 9 | W36X231 | 6.55 | OK | 42.2 | 45.1 | OK |
| 8 | W36X231 | 6.55 | OK | 42.2 | 44.2 | OK |
| 7 | W36X231 | 6.55 | OK | 42.2 | 43.3 | OK |
| 6 | W36X231 | 6.55 | OK | 42.2 | 42.4 | OK |
| 5 | W36X330 | 4.49 | OK | 31.4 | 45.2 | OK |
| 4 | W36X330 | 4.49 | OK | 31.4 | 44.6 | OK |
| 3 | W36X330 | 4.49 | OK | 31.4 | 43.9 | OK |
| 2 | W36X330 | 4.49 | OK | 31.4 | 43.2 | OK |
| 1 | W36X330 | 4.49 | OK | 31.4 | 42.6 | OK |

Table 20: Strong Column Weak Beam Check for Exterior Columns.

| Floor | Section | $\sum M_{pc}^{*}$ | $\sum M_{pb}^{*}$ | SCWB Ratio | Check > 1 |
|---|---|---|---|---|---|
| 19 | W36X170 | 71,056 | 9,157 | 7.76 | OK |
| 18 | W36X170 | 66,741 | 9,151 | 7.29 | OK |
| 17 | W36X170 | 62,314 | 9,153 | 6.81 | OK |
| 16 | W36X170 | 57,384 | 22,980 | 2.50 | OK |
| 15 | W36X194 | 63,514 | 22,992 | 2.76 | OK |
| 14 | W36X194 | 57,957 | 22,963 | 2.52 | OK |
| 13 | W36X194 | 52,166 | 22,929 | 2.28 | OK |
| 12 | W36X194 | 46,079 | 22,888 | 2.01 | OK |
| 11 | W36X194 | 39,792 | 20,309 | 1.96 | OK |
| 10 | W36X194 | 33,288 | 20,261 | 1.64 | OK |
| 9 | W36X231 | 46,519 | 20,249 | 2.30 | OK |
| 8 | W36X231 | 39,089 | 20,273 | 1.93 | OK |
| 7 | W36X231 | 31,486 | 20,300 | 1.55 | OK |
| 6 | W36X231 | 23,733 | 20,333 | 1.17 | OK |
| 5 | W36X330 | 65,638 | 23,083 | 2.84 | OK |
| 4 | W36X330 | 56,849 | 23,037 | 2.47 | OK |
| 3 | W36X330 | 48,187 | 22,985 | 2.10 | OK |
| 2 | W36X330 | 39,822 | 22,962 | 1.73 | OK |
| 1 | W36X330 | 31,817 | 22,940 | 1.39 | OK |

Table 21: Interior Column Factored Axial Force, Moment and Governing Axial & Moment Interaction Equation from the AISC Steel Construction Manual [43].

| Floor | Section | $P_u$ | $M_u$ | EQ H1-1a/b | H1-1a/b ≤1 |
|---|---|---|---|---|---|
| 20 | W36X160 | 87 | 987 | 0.043 | OK |
| 19 | W36X160 | 173 | 1,689 | 0.096 | OK |
| 18 | W36X160 | 259 | 2,530 | 0.154 | OK |
| 17 | W36X210 | 345 | 4,649 | 0.182 | OK |
| 16 | W36X210 | 440 | 4,164 | 0.191 | OK |
| 15 | W36X210 | 533 | 3,780 | 0.309 | OK |
| 14 | W36X210 | 624 | 3,903 | 0.353 | OK |
| 13 | W36X210 | 714 | 4,066 | 0.398 | OK |
| 12 | W36X210 | 801 | 4,094 | 0.439 | OK |
| 11 | W36X210 | 885 | 4,432 | 0.486 | OK |
| 10 | W36X210 | 965 | 4,689 | 0.531 | OK |
| 9 | W36X210 | 1,043 | 5,190 | 0.578 | OK |
| 8 | W36X210 | 1,122 | 5,341 | 0.617 | OK |
| 7 | W36X210 | 1,198 | 5,573 | 0.658 | OK |
| 6 | W36X210 | 1,273 | 6,140 | 0.707 | OK |
| 5 | W36X210 | 1,339 | 5,926 | 0.729 | OK |
| 4 | W36X210 | 1,402 | 6,054 | 0.756 | OK |
| 3 | W36X231 | 1,470 | 6,820 | 0.667 | OK |
| 2 | W36X231 | 1,538 | 7,439 | 0.703 | OK |
| 1 | W36X231 | 1,606 | 12,938 | 0.861 | OK |

Table 22: Interior Column Final Factored Axial Force with Overstrength Consideration.

| Floor | Section | $P_u$ | $\frac{P_u}{P_c}$ | $\frac{P_u}{P_c} \leq 1$ |
|---|---|---|---|---|
| 20 | W36X160 | 89 | 0.052 | OK |
| 19 | W36X160 | 174 | 0.101 | OK |
| 18 | W36X160 | 257 | 0.149 | OK |
| 17 | W36X210 | 343 | 0.149 | OK |
| 16 | W36X210 | 447 | 0.194 | OK |
| 15 | W36X210 | 546 | 0.237 | OK |
| 14 | W36X210 | 644 | 0.280 | OK |
| 13 | W36X210 | 738 | 0.321 | OK |
| 12 | W36X210 | 829 | 0.360 | OK |
| 11 | W36X210 | 914 | 0.397 | OK |
| 10 | W36X210 | 994 | 0.432 | OK |
| 9 | W36X210 | 1,070 | 0.465 | OK |
| 8 | W36X210 | 1,151 | 0.500 | OK |
| 7 | W36X210 | 1,228 | 0.534 | OK |
| 6 | W36X210 | 1,301 | 0.566 | OK |
| 5 | W36X210 | 1,357 | 0.590 | OK |
| 4 | W36X210 | 1,410 | 0.613 | OK |
| 3 | W36X231 | 1,462 | 0.523 | OK |
| 2 | W36X231 | 1,513 | 0.541 | OK |
| 1 | W36X231 | 1,560 | 0.579 | OK |

Table 23: Interior Column Seismic Compactness Checks

| Floor | Section | $\frac{1}{2}\frac{b_f}{t_f}$ | Flange Thickness Ratio Flexure $\leq 7.22$ | $\frac{h}{t_w}$ | $\frac{h}{t_w}$ Limit | Web Thickness Ratio $\leq$ Limit |
|---|---|---|---|---|---|---|
| 20 | W36X160 | 5.88 | OK | 49.9 | 56.7 | OK |
| 19 | W36X160 | 5.88 | OK | 49.9 | 54.5 | OK |
| 18 | W36X160 | 5.88 | OK | 49.9 | 52.3 | OK |
| 17 | W36X210 | 4.49 | OK | 39.1 | 52.2 | OK |
| 16 | W36X210 | 4.49 | OK | 39.1 | 51.4 | OK |
| 15 | W36X210 | 4.49 | OK | 39.1 | 50.8 | OK |
| 14 | W36X210 | 4.49 | OK | 39.1 | 50.2 | OK |
| 13 | W36X210 | 4.49 | OK | 39.1 | 49.6 | OK |
| 12 | W36X210 | 4.49 | OK | 39.1 | 49.0 | OK |
| 11 | W36X210 | 4.49 | OK | 39.1 | 48.4 | OK |
| 10 | W36X210 | 4.49 | OK | 39.1 | 47.9 | OK |
| 9 | W36X210 | 4.49 | OK | 39.1 | 47.4 | OK |
| 8 | W36X210 | 4.49 | OK | 39.1 | 46.9 | OK |
| 7 | W36X210 | 4.49 | OK | 39.1 | 46.3 | OK |
| 6 | W36X210 | 4.49 | OK | 39.1 | 45.8 | OK |
| 5 | W36X210 | 4.49 | OK | 39.1 | 45.4 | OK |
| 4 | W36X210 | 4.49 | OK | 39.1 | 45.0 | OK |
| 3 | W36X231 | 6.55 | OK | 42.2 | 45.4 | OK |
| 2 | W36X231 | 6.55 | OK | 42.2 | 45.0 | OK |
| 1 | W36X231 | 6.55 | OK | 42.2 | 44.6 | OK |

Table 24: Strong Column Weak Beam Check for Interior Columns.

| Floor | Section | $\sum M_{pc}^{*}$ | $\sum M_{pb}^{*}$ | SCWB Ratio | Check > 1 |
|---|---|---|---|---|---|
| 19 | W36X160 | 68,124 | 18,160 | 3.75 | OK |
| 18 | W36X160 | 65,519 | 18,155 | 3.61 | OK |
| 17 | W36X210 | 87,322 | 18,194 | 4.80 | OK |
| 16 | W36X210 | 84,655 | 45,811 | 1.85 | OK |
| 15 | W36X210 | 81,467 | 45,793 | 1.78 | OK |
| 14 | W36X210 | 78,354 | 45,764 | 1.71 | OK |
| 13 | W36X210 | 75,332 | 45,730 | 1.65 | OK |
| 12 | W36X210 | 72,427 | 45,689 | 1.59 | OK |
| 11 | W36X210 | 69,594 | 40,578 | 1.72 | OK |
| 10 | W36X210 | 67,017 | 40,530 | 1.65 | OK |
| 9 | W36X210 | 64,600 | 40,518 | 1.59 | OK |
| 8 | W36X210 | 62,020 | 40,542 | 1.53 | OK |
| 7 | W36X210 | 59,546 | 40,569 | 1.47 | OK |
| 6 | W36X210 | 57,209 | 40,602 | 1.41 | OK |
| 5 | W36X210 | 55,518 | 45,767 | 1.21 | OK |
| 4 | W36X210 | 53,803 | 45,722 | 1.18 | OK |
| 3 | W36X231 | 65,293 | 45,643 | 1.43 | OK |
| 2 | W36X231 | 63,573 | 45,602 | 1.39 | OK |
| 1 | W36X231 | 60,470 | 45,579 | 1.33 | OK |

### 2.5.7 Panel Zone and Doubler Plates

Once the frame column and beams are sized the beam-column intersection known as the panel zone depicted below must be checked for adequate shear strength under column axial load.

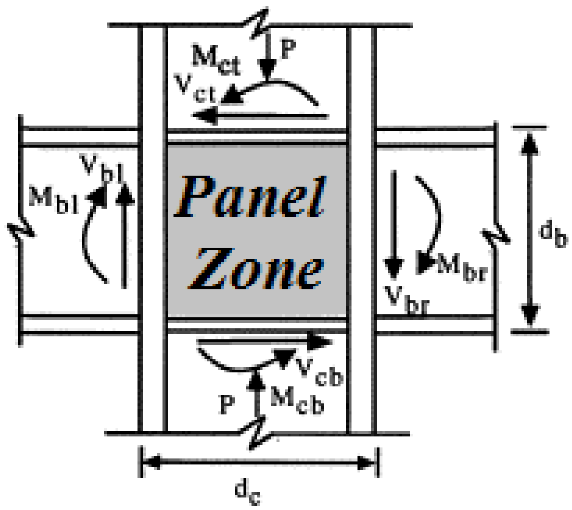


Figure 14: Panel zone location and forces acting on it [53].

The panel zone is important because when a moment frame is subject to strong lateral loads, high shear forces develop. When these forces result in plastic deformations the panel zone exhibits stable hysteretic behavior thus becoming a good source of seismic energy dissipation [54]. However, yielding in beams at RBS connections may not be achieved and the desirable beam-hinge mechanism not obtained. The panel zone is checked according to the requirements from AISC 360-10 Specification for Structural Steel Buildings [42]. The governing equations are the following:

For $P_r \leq 0.75P_c$

$$R_n = 0.60F_y d_c t_w \left[1 + \frac{3b_{cf}t_{cf}^2}{d_b d_c t_w}\right] \tag{2.15}$$

For $P_r > 0.75P_c$

$$R_n = 0.60F_y d_c t_w \left[1 + \frac{3b_{cf}t_{cf}^2}{d_b d_c t_w}\right]\left(1.9 - 1.2\frac{P_r}{P_c}\right) \tag{2.16}$$

Where:

$R_n$ : The Available Strength for Web Panel Zone Shear Yielding, kip.

$F_y$: Specified Minimum Yield Stress of the Column Web, ksi.

$d_c$: Depth of Column, in.

$d_b$: Depth of Beam, in.

$t_w$: Thickness of Column Web, in.

$b_{cf}$: Width of Column Flange, in.

$t_{cf}$: Thickness of Column Flange, in.

$P_r$: Required Axial Strength, kip.

$P_c$: Axial Yield Strength of the Column, kip.

If the panel zone does not meet these strength checks then it is reinforced with steel plates on both sides of the column web called doubler plates. Table 25: Panel Zone and Doubler Platting of Exterior Columns.

Table 26 summarize the panel zone strength checks and doubler plate requirements and dimensions.

Table 25: Panel Zone and Doubler Platting of Exterior Columns.

| Floor | Beam Section | Column Section | $R_u$ | $R_n$ | Doubler Plate? |
|---|---|---|---|---|---|
| 20 | W24X94 | W36X170 | 431 | 792 | No |
| 19 | W24X62 | W36X170 | 281 | 794 | No |
| 18 | W24X62 | W36X170 | 281 | 794 | No |
| 17 | W24X62 | W36X170 | 281 | 794 | No |
| 16 | W24X146 | W36X170 | 688 | 791 | No |
| 15 | W24X146 | W36X194 | 688 | 908 | No |
| 14 | W24X146 | W36X194 | 688 | 908 | No |
| 13 | W24X146 | W36X194 | 688 | 908 | No |
| 12 | W24X146 | W36X194 | 688 | 908 | No |
| 11 | W24X131 | W36X194 | 614 | 908 | No |
| 10 | W24X131 | W36X194 | 614 | 908 | No |
| 9 | W24X131 | W36X231 | 614 | 928 | No |
| 8 | W24X131 | W36X231 | 614 | 928 | No |
| 7 | W24X131 | W36X231 | 614 | 928 | No |
| 6 | W24X131 | W36X231 | 614 | 928 | No |
| 5 | W24X146 | W36X330 | 688 | 1,361 | No |
| 4 | W24X146 | W36X330 | 688 | 1,361 | No |
| 3 | W24X146 | W36X330 | 688 | 1,361 | No |
| 2 | W24X146 | W36X330 | 688 | 1,361 | No |
| 1 | W24X146 | W36X330 | 705 | 1,361 | No |

Table 26: Panel Zone and Doubler Platting of Interior Columns.

| Floor | Beam Section | Column Section | $R_u$ (kip) | $R_n$ (kip) | Doubler Plate? | Side Plate Thickness (in) | Total Plate Thickness (in) |
|---|---|---|---|---|---|---|---|
| 20 | W24X94 | W36X160 | 862 | 748 | Yes | 1/16 | 0.125 |
| 19 | W24X62 | W36X160 | 562 | 749 | No | 0 | 0 |
| 18 | W24X62 | W36X160 | 562 | 749 | No | 0 | 0 |
| 17 | W24X62 | W36X210 | 563 | 1,000 | No | 0 | 0 |
| 16 | W24X146 | W36X210 | 1,376 | 996 | Yes | 3/16 | 0.375 |
| 15 | W24X146 | W36X210 | 1,376 | 996 | Yes | 3/16 | 0.375 |
| 14 | W24X146 | W36X210 | 1,376 | 996 | Yes | 3/16 | 0.375 |
| 13 | W24X146 | W36X210 | 1,376 | 996 | Yes | 3/16 | 0.375 |
| 12 | W24X146 | W36X210 | 1,376 | 996 | Yes | 3/16 | 0.375 |
| 11 | W24X131 | W36X210 | 1,229 | 997 | Yes | 2/16 | 0.250 |
| 10 | W24X131 | W36X210 | 1,229 | 997 | Yes | 2/16 | 0.250 |
| 9 | W24X131 | W36X210 | 1,229 | 997 | Yes | 2/16 | 0.250 |
| 8 | W24X131 | W36X210 | 1,229 | 997 | Yes | 2/16 | 0.250 |
| 7 | W24X131 | W36X210 | 1,229 | 997 | Yes | 2/16 | 0.250 |
| 6 | W24X131 | W36X210 | 1,229 | 997 | Yes | 2/16 | 0.250 |
| 5 | W24X146 | W36X210 | 1,376 | 996 | Yes | 3/16 | 0.375 |
| 4 | W24X146 | W36X210 | 1,376 | 996 | Yes | 3/16 | 0.375 |
| 3 | W24X146 | W36X231 | 1,376 | 928 | Yes | 4/16 | 0.500 |
| 2 | W24X146 | W36X231 | 1,376 | 928 | Yes | 4/16 | 0.500 |
| 1 | W24X146 | W36X231 | 1,410 | 928 | Yes | 4/16 | 0.500 |

### 2.5.8 P-Δ Effects

In a severe earthquake, steel frame structures have the potential to collapse in a sidesway mode due to P- Δ effects. These effects are caused by vertical gravity loads acting on the deformed configuration of the structure [55]. In order to determine whether or not the individual member forces of the frame require P-Δ amplifications the stability coefficient equation from ASCE 7-10 is used. This equation is as follows:

$$\theta = \frac{P_x \Delta I_e}{V_x h_{sx} C_d} \leq \frac{0.5}{\beta C_d} \leq 0.25 \tag{2.17}$$

Where:

$\theta$ : Stability Coefficient Factor, unitless.

$P_x$: Total Vertical Design Load at and Above Level x, kip.

$\Delta$: Design Story Drift, in.

$I_e$: Importance Factor, unitless.

$V_x$: Seismic Shear Force Acting between Levels x and x-1, kip.

$h_{sx}$: Story Height Below Level x, in.

$C_d$: Deflection Amplification Factor, unitless.

$\beta$: Ratio of Shear Demand to Shear Capacity for the Story between Levels x and x-1, unitless.

When the stability coefficient is less than 0.10, P-Δ amplifications are not considered. For this frame the all stories have a stability factor less than 0.10 as can be seen from the following table:

Table 27: Stability Coefficient Check.

| Story | **$\theta$** | **$\theta_{max}$** | **$\theta \leq 0.10 \leq \theta_{max}$** |
|---|---|---|---|
| 20 | 0.03 | 0.25 | OK |
| 19 | 0.03 | 0.25 | OK |
| 18 | 0.03 | 0.20 | OK |
| 17 | 0.02 | 0.25 | OK |
| 16 | 0.02 | 0.25 | OK |
| 15 | 0.02 | 0.25 | OK |
| 14 | 0.02 | 0.25 | OK |
| 13 | 0.02 | 0.25 | OK |
| 12 | 0.02 | 0.25 | OK |
| 11 | 0.02 | 0.25 | OK |
| 10 | 0.02 | 0.25 | OK |
| 9 | 0.02 | 0.25 | OK |
| 8 | 0.02 | 0.24 | OK |
| 7 | 0.02 | 0.23 | OK |
| 6 | 0.01 | 0.23 | OK |
| 5 | 0.01 | 0.24 | OK |
| 4 | 0.01 | 0.23 | OK |
| 3 | 0.01 | 0.22 | OK |
| 2 | 0.01 | 0.21 | OK |
| 1 | 0.01 | 0.25 | OK |

## 2.6 Gravity System Design

The steel moment resisting frame is designed to withstand the combination of design dead and live loads as well as the design level earthquake forces and resist excessive lateral deformations. However, the remaining frame elements in the building must still be designed including interior and perimeter beams and columns. It is assumed that the steel perimeter moment resisting frames resist the lateral forces therefore, these other frame elements must only resist their own tributary gravity loads including design dead and live loads.

### 2.6.1 Gravity Beam Design

The floor system is comprised of a concrete slab cast in a steel ribbed deck made composite to steel beams through steel shear studs. The composite floor system depicted below spans in the North-South direction and is designed in accordance to the composite design specifications of ASCI 360-10 [42] and by following a design procedure in STEEL TIPS LRFD Composite Beam Design with Metal Deck [56]. The steel beams are connected to columns through shear connections such that there is negligible or relatively small moment transfer.

Figure 15: Cross-section of composite steel deck [57].

The floor is designed such that the critical beam-slab section is evaluated, sized and used for rest of the floor sections. The other beam section design calculations can be found in Appendix C. A typical floor beam is depicted below in the plan view of the building.

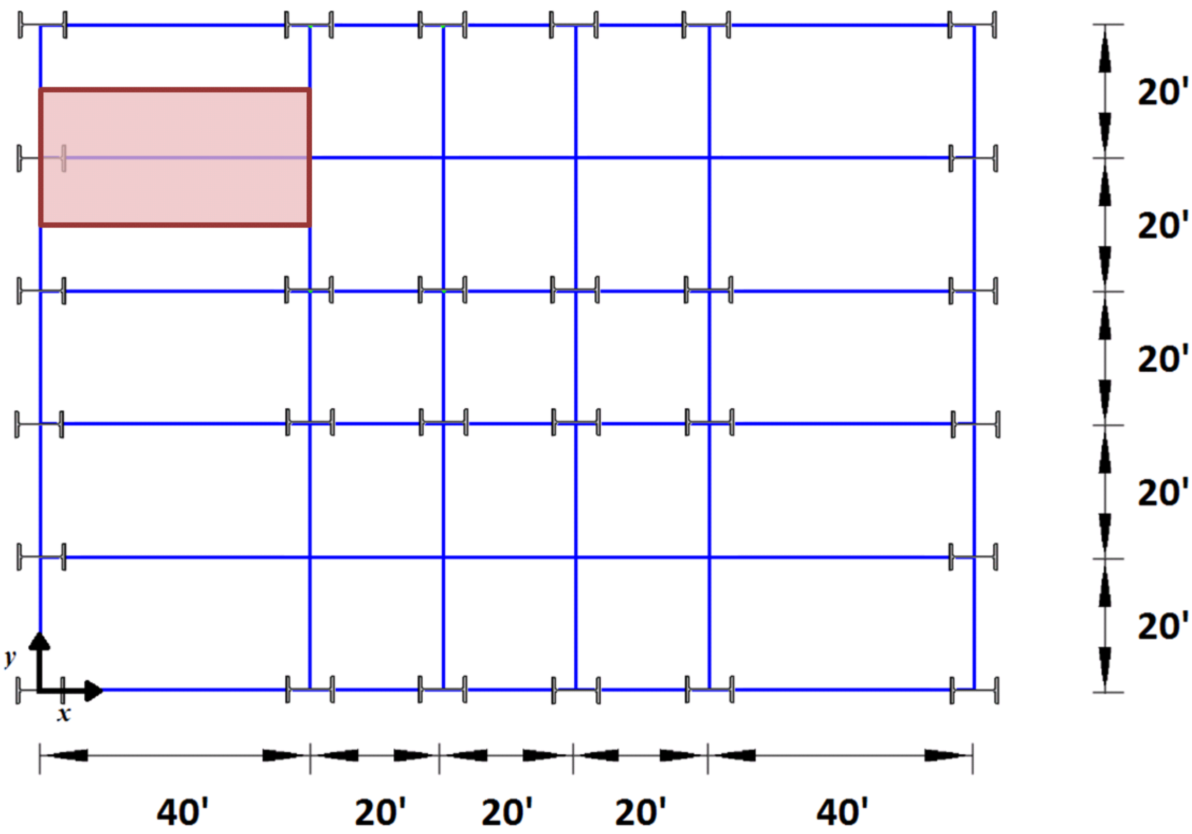


Figure 16: Typical gravity floor beam used for design.

All gravity floor beams are W21X68 with doubled up ¾" shear studs at 12" on center. The concrete slab has a 28 day compressive strength of 3,000 psi. The metal deck runs perpendicular to the steel beams. It is made out of 18 gage steel sheets and has a rib width, $W_r$, of 5 inches. The rib spacing, $S_r$, is 12 inches. The rib height, $h_r$, is 2 inches and the slab height beyond the rib height, $t_s$, is also 2 inches thus giving a total nominal slab depth of 4 inches. The shear studs are

3.5 inches long denoted by $H_s$ with a half inch of clear cover. Figure 17 shows profile and section views for metal deck, shear stud and slab dimensions.

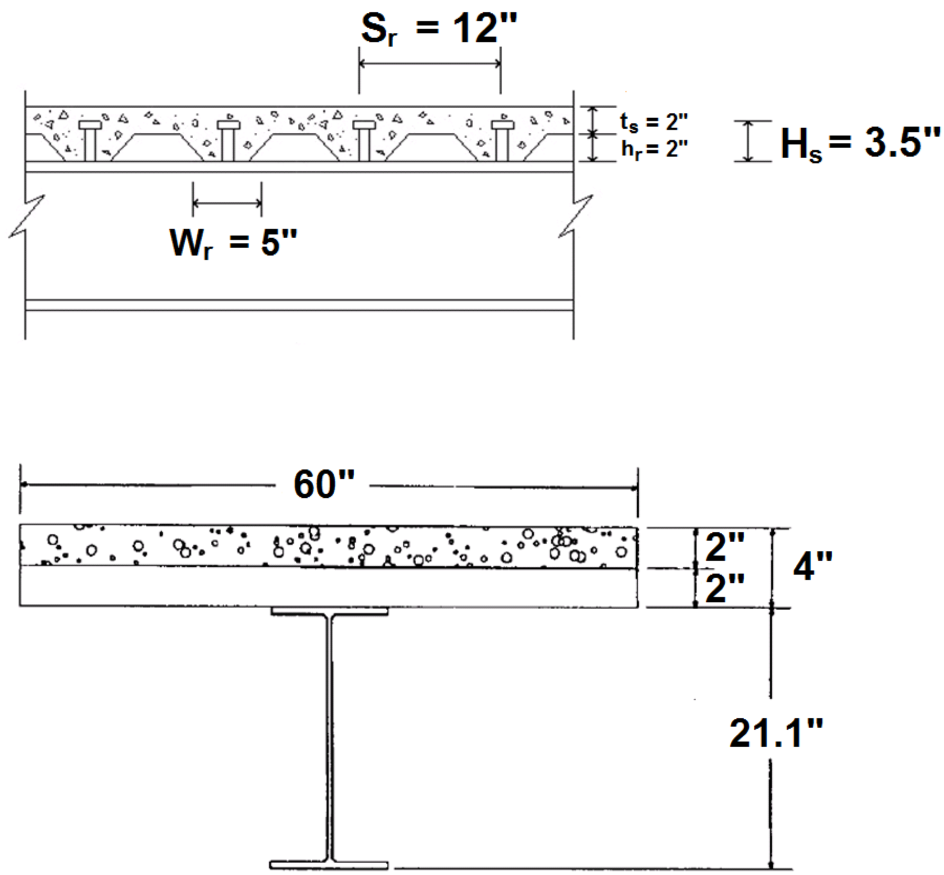


Figure 17: (Top) Cross-section of composite floor deck with ribs perpendicular to steel beam [51]. (Bottom) Cross-section of effective width of W21X68 steel section [51].

The composite section flexure, shear and deflection checks are summarized in the following table:

Table 28: Typical Composite Floor Beam Flexural, Shear and Deflection Checks.

| Section | $M_u$ (kip-ft) | $\varphi M_N$ (kip-ft) | $V_u$ (kip) | $\varphi V_N$ (kip) | Deflection (inches) | L/360 (inches) | Check Limit |
|---|---|---|---|---|---|---|---|
| W21X68 | 756 | 820 | 76 | 272 | 1.324 | 1.333 | OK |

### 2.6.2 Gravity Column Design

Gravity columns are designed according to ASCI 360-10 [42] for design dead and live loads. The live loads are reduced according to ASCE 7-10. There are three column lines including two interior and a corner all with differing tributary areas. All of the columns connect to floor beams through shear connections. Only the column with tributary area $G_1$ will be shown here (see Figure 18) while the rest of the column checks can be found in Appendix C.

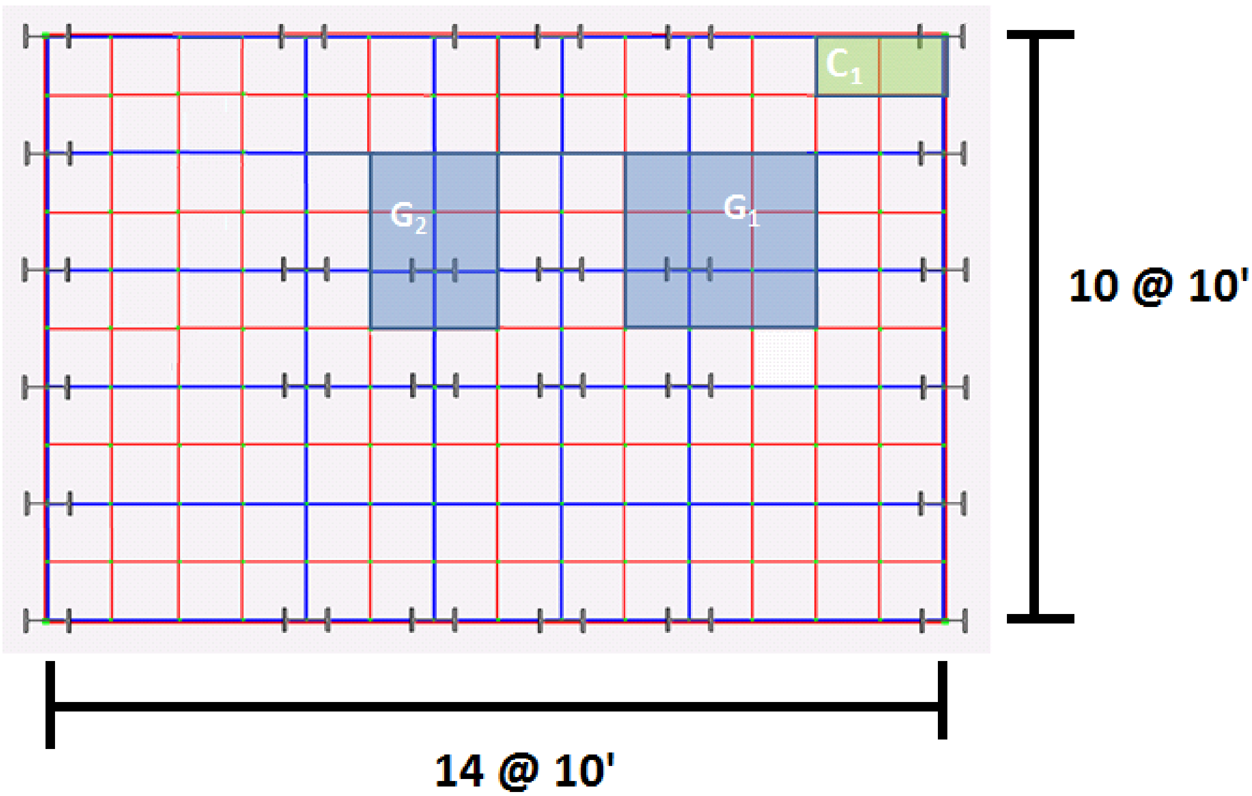


Figure 18: Tributary area and location of gravity columns.

Table 29: Interior Column Strength Checks.

| Floor | Design $P_u$ (kips) | ETABS $P_u$ (kips) | Section | $\frac{P_u}{\phi P_n}$ | $\frac{P_u}{\phi P_n} \leq 1$ |
|---|---|---|---|---|---|
| 20 | 137 | 129 | W14X53 | 0.32 | OK |
| 19 | 276 | 266 | W14X53 | 0.64 | OK |
| 18 | 412 | 402 | W14X53 | 0.95 | OK |
| 17 | 549 | 539 | W14X74 | 0.75 | OK |
| 16 | 686 | 676 | W14X74 | 0.93 | OK |
| 15 | 823 | 814 | W14X90 | 0.79 | OK |
| 14 | 960 | 951 | W14X90 | 0.92 | OK |
| 13 | 1,096 | 1,089 | W14X109 | 0.87 | OK |
| 12 | 1,233 | 1,227 | W14X109 | 0.97 | OK |
| 11 | 1,370 | 1,365 | W14X132 | 0.89 | OK |
| 10 | 1,507 | 1,504 | W14X132 | 0.98 | OK |
| 9 | 1,644 | 1,642 | W14X159 | 0.87 | OK |
| 8 | 1,780 | 1,781 | W14X159 | 0.95 | OK |
| 7 | 1,917 | 1,920 | W14X176 | 0.92 | OK |
| 6 | 2,054 | 2,060 | W14X176 | 0.98 | OK |
| 5 | 2,191 | 2,199 | W14X211 | 0.87 | OK |
| 4 | 2,328 | 2,339 | W14X211 | 0.93 | OK |
| 3 | 2,464 | 2,478 | W14X257 | 0.80 | OK |
| 2 | 2,601 | 2,618 | W14X257 | 0.85 | OK |
| 1 | 2,738 | 2,758 | W14X257 | 0.92 | OK |

Table 30: Interior Column Strength Checks.

| Floor | Section | $\frac{1}{2}\frac{b_f}{t_f}$ | Flange Thickness Ratio Flexure $\leq 13.49$ | $\frac{h}{t_w}$ | Web Thickness Ratio $\leq 35.9$ |
|---|---|---|---|---|---|
| 20 | W14X53 | 6.11 | OK | 30.9 | OK |
| 19 | W14X53 | 6.11 | OK | 30.9 | OK |
| 18 | W14X53 | 6.11 | OK | 30.9 | OK |
| 17 | W14X74 | 6.43 | OK | 25.4 | OK |
| 16 | W14X74 | 6.43 | OK | 25.4 | OK |
| 15 | W14X90 | 10.21 | OK | 25.9 | OK |
| 14 | W14X90 | 10.21 | OK | 25.9 | OK |
| 13 | W14X109 | 8.49 | OK | 21.7 | OK |
| 12 | W14X109 | 8.49 | OK | 21.7 | OK |
| 11 | W14X132 | 7.14 | OK | 17.7 | OK |
| 10 | W14X132 | 7.14 | OK | 17.7 | OK |
| 9 | W14X159 | 6.55 | OK | 15.3 | OK |
| 8 | W14X159 | 6.55 | OK | 15.3 | OK |
| 7 | W14X176 | 5.99 | OK | 13.7 | OK |
| 6 | W14X176 | 5.99 | OK | 13.7 | OK |
| 5 | W14X211 | 5.06 | OK | 11.6 | OK |
| 4 | W14X211 | 5.06 | OK | 11.6 | OK |
| 3 | W14X257 | 4.23 | OK | 9.71 | OK |
| 2 | W14X257 | 4.23 | OK | 9.71 | OK |
| 1 | W14X257 | 4.23 | OK | 9.71 | OK |

CHAPTER 3

# MODELING AND ANALYSIS

## 3.1 Structural Analysis Software

In order to accurately capture component acceleration demands through floor response spectra, the out-of-plane flexibility of the floor must be realistically modeled. To achieve this goal, a three-dimensional model must be used. For this purpose, the 20-story building is modeled and designed three-dimensionally using ETABS v9.7.3 [58]. ETABS is used over other structural analysis packages because it is specifically created for modeling, designing and analyzing buildings rather than a general all-purpose finite element package. While ETABS is great for general structural modeling and analysis, SAP2000 v15 [11] has a better user interface when it comes to advanced structural analysis capabilities. However, modeling buildings in SAP2000 is not as efficient or intuitive as it is in ETABS. Since Computers and Structures Inc. produces both of these software packages, the 20-story building was easily modeled, and designed in ETABS and then the final design was exported to SAP2000 in order to generate response spectrum curves in a more efficient manner.

## 3.2 Computational Model and Meshing

The base of the steel moment frames are assumed to be fixed while the rest of the columns are considered as pin connections. The building is comprised of frame (line) elements for the beams and columns. The beam-column connections of the interior gravity frames are shear connections. The only connections to have moment resistance are the beam-column connections in the perimeter steel moment frames. Each column frame element is discretized into two elements for a total of three nodes. The model is modified so that columns are further discretized to 10 elements and response spectra for a selected number of time histories are compared to the two element discretization to check the need for further meshing. The result of this comparison is a 2% difference in response spectra acceleration values between the two column meshes. In an effort to reduce computational time, the two element mesh is used over the higher resolution mesh. The floor system is meshed at five foot intervals. The beam and slab are both meshed at the same five foot interval so that connectivity is preserved. Various meshes at 10-, 5-, and 2.5-foot intervals are also considered and evaluated by looking at the summed dynamic vertical modal mass participation. These evaluations are plotted in Figure 19..

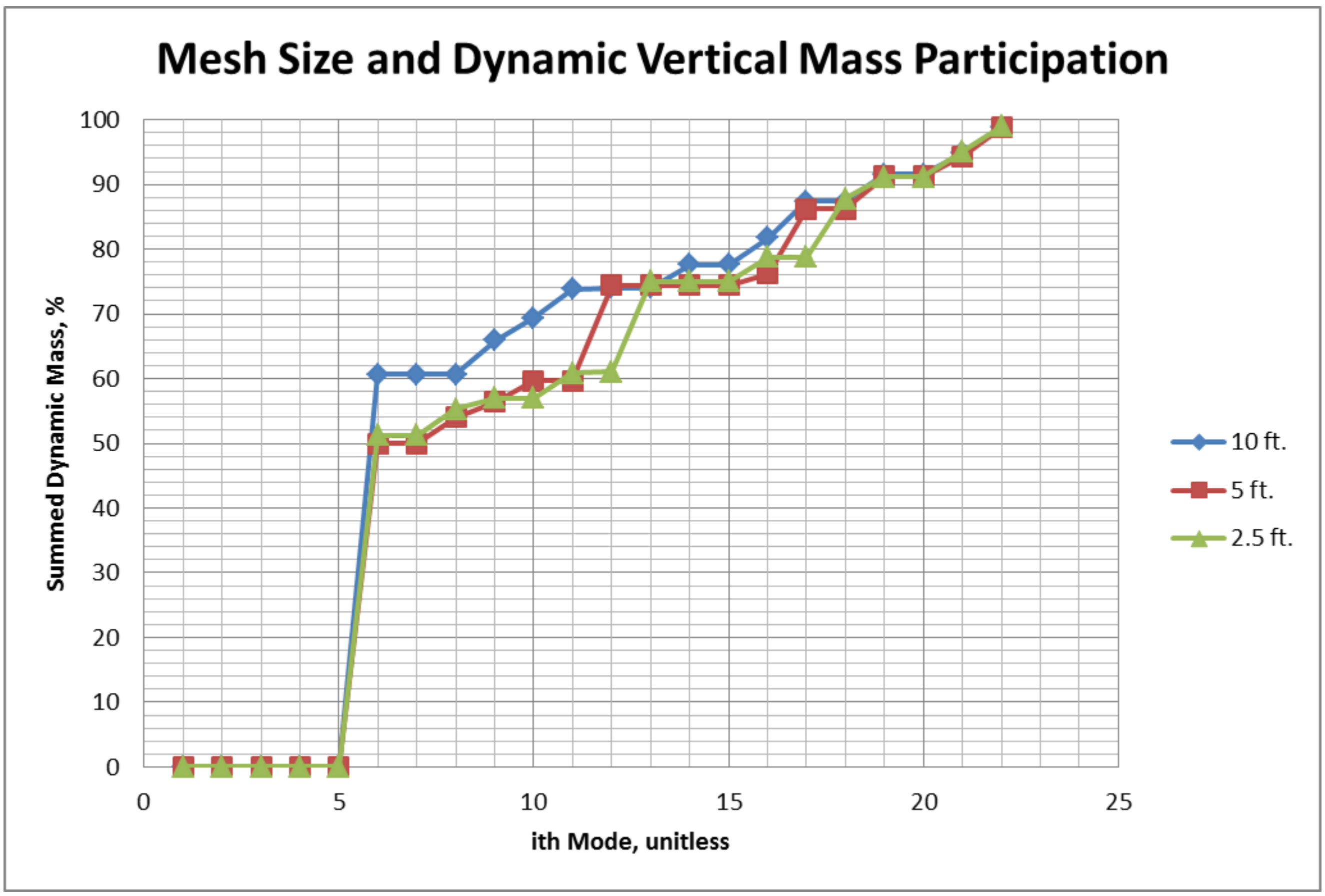


Figure 19: Effect of mesh size on the summed total dynamic vertical mass participation.

As can be seen from Figure 19, the finer meshes at 5 and 2.5 feet give approximately the same shape and cumulative modal mass participation. However, the computational time required to run one simulation at the 2.5 foot mesh is about 6 and 2 times longer than compared to the 10 and 5 foot meshes respectively. Furthermore, the fundamental vertical mode which occurs at mode 6 changes very little between the 5 and 2.5 foot meshes resulting in fundamental frequency values of 2.19 Hz and 2.23 Hz respectively (2% relative difference). Therefore, additional meshing refinements do not yield significant differences in the dynamic behavior of the building model. The final dynamic characteristics of the building in the vertical direction are as follows:

Table 31: Effective Modal Mass Percent in the Z Direction.

| Mode | Period (s) | Frequency (Hz) | UZ | ΣUZ |
|---|---|---|---|---|
| 6 | 0.457 | 2.19 | 49.94 | 49.9 |
| 8 | 0.396 | 2.53 | 4.05 | 54.0 |
| 9 | 0.387 | 2.59 | 2.37 | 56.4 |
| 10 | 0.380 | 2.63 | 3.34 | 59.7 |
| 12 | 0.316 | 3.17 | 14.74 | 74.4 |
| 16 | 0.217 | 4.60 | 1.79 | 76.3 |
| 17 | 0.171 | 5.87 | 9.94 | 86.2 |
| 19 | 0.145 | 6.91 | 5.13 | 91.3 |
| 21 | 0.103 | 9.69 | 3.02 | 94.3 |
| 22 | 0.051 | 19.57 | 4.49 | **98.8** |

Four thin shell elements with 6 degrees of freedom are used in order to model the out-of-plane flexibility of the floor. SAP2000 allows the user to input different shell thicknesses in order to provide different in-plane and out-of-plane element stiffnesses. AutoCAD is used in order to determine the appropriate thickness of an equivalent shell floor system. Note that only the concrete filled sections of the metal deck including the ribs are used to find an equivalent rectangular section. The steel beams are not used in this calculation. AutoCAD is used to turn a drawing obtained from ASC Steel Deck [59] of the assumed cross-section of the composite metal deck designed for this study into a region, and then obtain its geometric properties. These can be seen in the following table.

Table 32: Geometric Properties of the Composite Deck from AutoCAD.

| Geometric Property | Symbol | Value | Units |
|---|---|---|---|
| Horizontal Length | $L_X$ | 238 | in |
| Area | $A$ | 696 | in$^2$ |
| Perimeter | $P$ | 545 | in |
| X Centroid | $\bar{X}$ | 119 | in |
| Y Centroid | $\bar{Y}$ | 2.36 | in |
| XY Inertia | $I_{XY}$ | 169,765 | in$^4$ |
| X Inertia | $I_{X,0}$ | 804 | in$^4$ |
| Y Inertia | $I_{Y,0}$ | 3,275,613 | in$^4$ |
| X Radius Gyration | $r_X$ | 2.31 | in |
| Y Radius Gyration | $r_Y$ | 137 | in |

A shell element having an in-plane thickness of 2.9 inches and a bending thickness of 3.4 inches produces a floor system with equivalent geometric parameters. The percent difference of the moment of inertia around the x axis between the actual floor system and the equivalent shell system is less than 1% at 0.04%. SAP2000® gives the user the ability to choose between thick and thin shell stiffness formulations. A general rule of thumb in determining whether to use thick or thin shells depends on the depth to minimum in-plan-orthogonal side ratio [60].

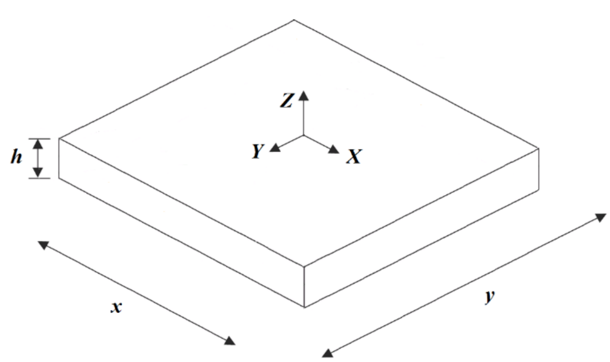


Figure 20: Shell element.

$$\text{Thin Shells:} \quad \frac{h}{\text{minimum}(x \text{ or } y)} < \frac{1}{10} \tag{3.1}$$

$$\text{Thick Shells:} \quad \frac{h}{\text{minimum}(x \text{ or } y)} > \frac{1}{10} \tag{3.2}$$

Where:

$h$ : Vertical Thickness of Shell, in.

$x$ : Shell Length Along X Direction, in.

$y$ : Shell Length Along Y Direction, in.

For this study modeling the floor system with the thin shells is a valid assumption due to equation 3.1 controlling for example $\frac{3.435''}{60''} = 0.05725 < 0.10$. Each floor level is assigned its own rigid diaphragm in the z plane. This is because floor systems in buildings exhibit composite behavior due to the concrete, rebar, and beams tying everything together. In an effort to model the floor as realistically as possible, the deck is raised above the beams. In the SAP2000 model this is done by lowering the frames through the use of insertion points. Insertion points allow the beam-slab connection to remain compatible with respect to displacements thereby allowing the beam-slab to deform together achieving the assumed composite behavior.

## 3.3 Ground Motion Selection

Ground motion acceleration time histories are selected using the Pacific Earthquake Engineering Research Next Generation Attenuation (PEER NGA) [61] strong motion database. The criteria for selection is as follows: ground motions with a moment magnitude ranging from 6.5 to 8, excluding acceleration recording at dam abutments, source-to-fault-rupture distance between 0 and 30 kilometers, and soil site class D. These specifications produce 106 unscaled ground motions which are detailed in Appendix B.

## 3.4 Linear Modal Time History and Response Spectrum Analysis

To solve the equation of motion for each ground motion at every time instance SAP2000 uses linear modal methods instead of a direct integration scheme. For this study this method is preferable since this is an elastic analysis. In order to ensure an accurate solution for each mode when conducting the linear modal time history analysis, the time step $\Delta t$ must be sufficiently small. A general rule of thumb is that the following equation should be satisfied: [62]

$$\Delta t \leq 0.1 T_N \tag{3.3}$$

Where:

$\Delta t$ : Time Step, s.

$T_N$ : Highest Mode Period, s.

For this study $\Delta t \leq 0.1(0.0511) \leq 0.00511$ seconds. The time step for each ground motion run is at 0.005 or less seconds; thus, meeting the requirement. Once the linear modal time history for each ground motion has been performed, response spectrum curves can be generated. These curves produce the maximum acceleration experienced by a NSC modeled as a single-degree-of-freedom (SDOF) system plotted against the frequency of the component. In an effort to take advantage of the symmetry of the floor plan to reduce the total number of data points to generate floor response spectra, only the locations depicted by the purple and yellow circles in Figure 21 are used.

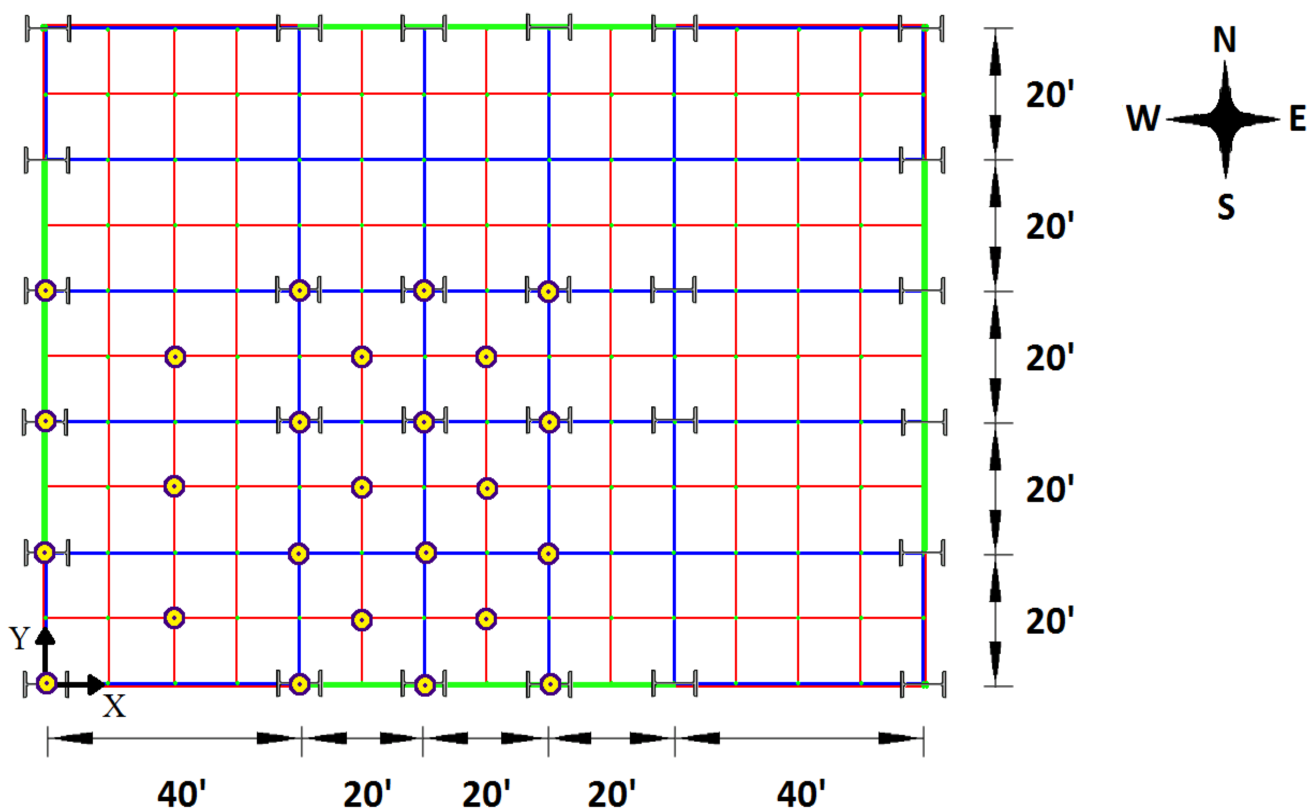


Figure 21: Floor plan of the building with response spectrum curve indicators.

The response spectrum curves generated for these points assume 5% of critical damping. These curves will be presented and discussed in the next chapter.

# CHAPTER 4

# RESULTS & DISCUSSION

This chapter presents typical floor acceleration response spectra gathered from running various ground motions. At certain locations throughout the floor plan and along the height of the building median peak vertical floor accelerations are calculated and presented. By visualizing the magnitude of the acceleration along the height of the building this work can be directly compared to both similar work and to the design requirements of ASCE 7-10.

## 4.1 Floor Response Spectra

The floor acceleration response spectrum (FRS) for a floor system are important because they are useful in design when the period of the component is known (it is usually provided by the manufacturer) since the FRS gives the maximum corresponding acceleration the particular component will experience due to a particular earthquake ground motion. This maximum acceleration is then turned into a maximum inertial force using the mass of the component. This seismic force then allows engineers to properly design the anchorage of the component and complete their design.

In order to develop the FRS the vertical component of acceleration from a suite of 106 strong ground motions is used to excite the building using SAP2000 v15. FRS are obtained at discrete points located throughout the building. These points are broken down and classified based on plan view location. These categories include whether the component is located on an exterior or interior column line or whether it is located in the middle of a large versus small slab section.

The large bays are 40ft in length and the smaller slab sections are 20ft in length. See Figure 22 for the breakdown:

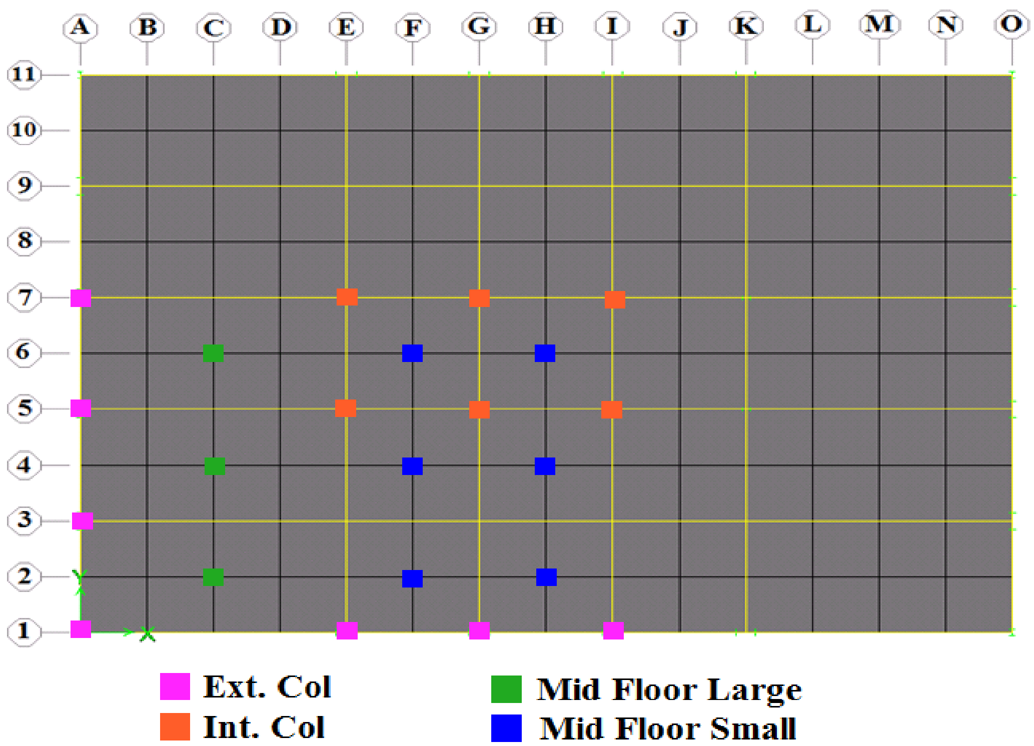


Figure 22: Floor plan with floor point classification.

These points also have alphabetic and numeric descriptions based on the figure from above:

Table 33: General FRS Categories.

| Classification | Points | Description |
|---|---|---|
| Mid Large | C6, C4, C2 | Middle of the 40 foot bay |
| Mid Small | F6, F4, F2<br>H6, H4, H2 | Middle of the 20 foot bay |
| Ext. Col | A1, A3, A5, A7<br>E1, G1, I1 | On an exterior column |
| Int. Col | E7, E5, G7, G5, I7, I5 | On an interior column |

The following floor response spectrum graphs depict the median response of the points on the floor, which are grouped into the aforementioned categories, to the ground motions.

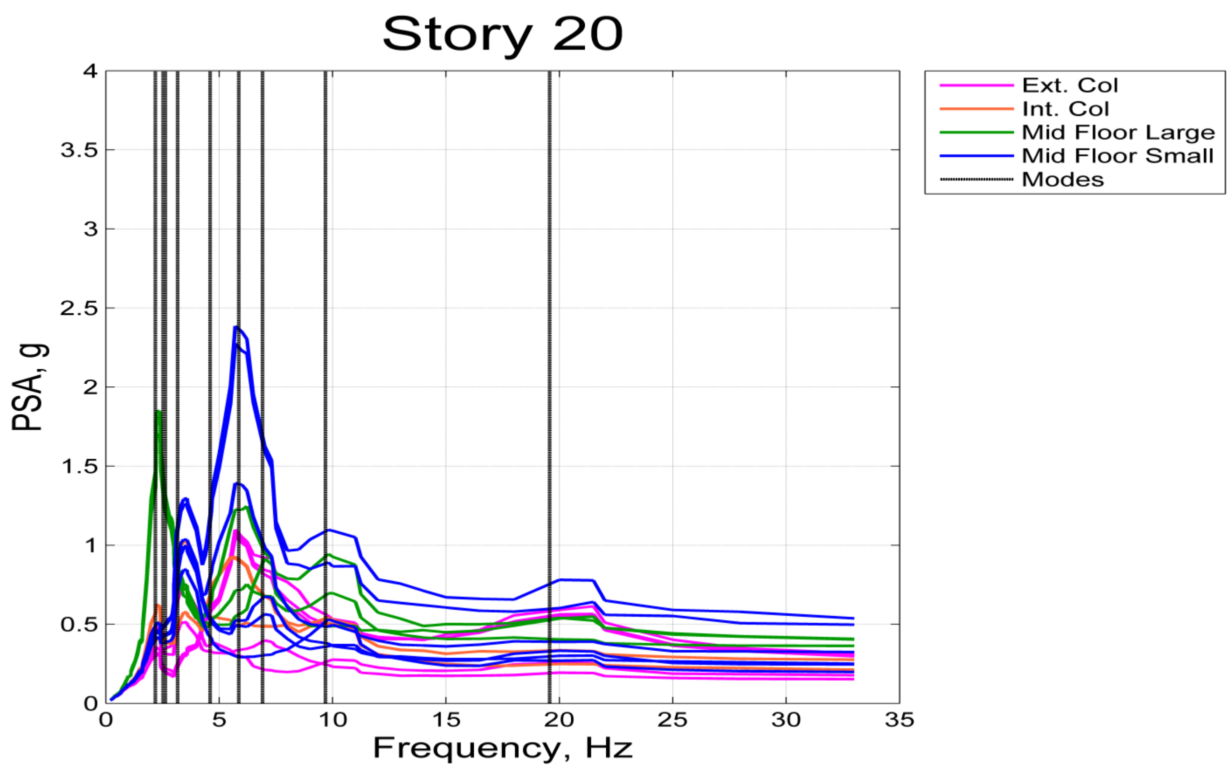


Figure 23: 20th story floor response spectra for selected locations.

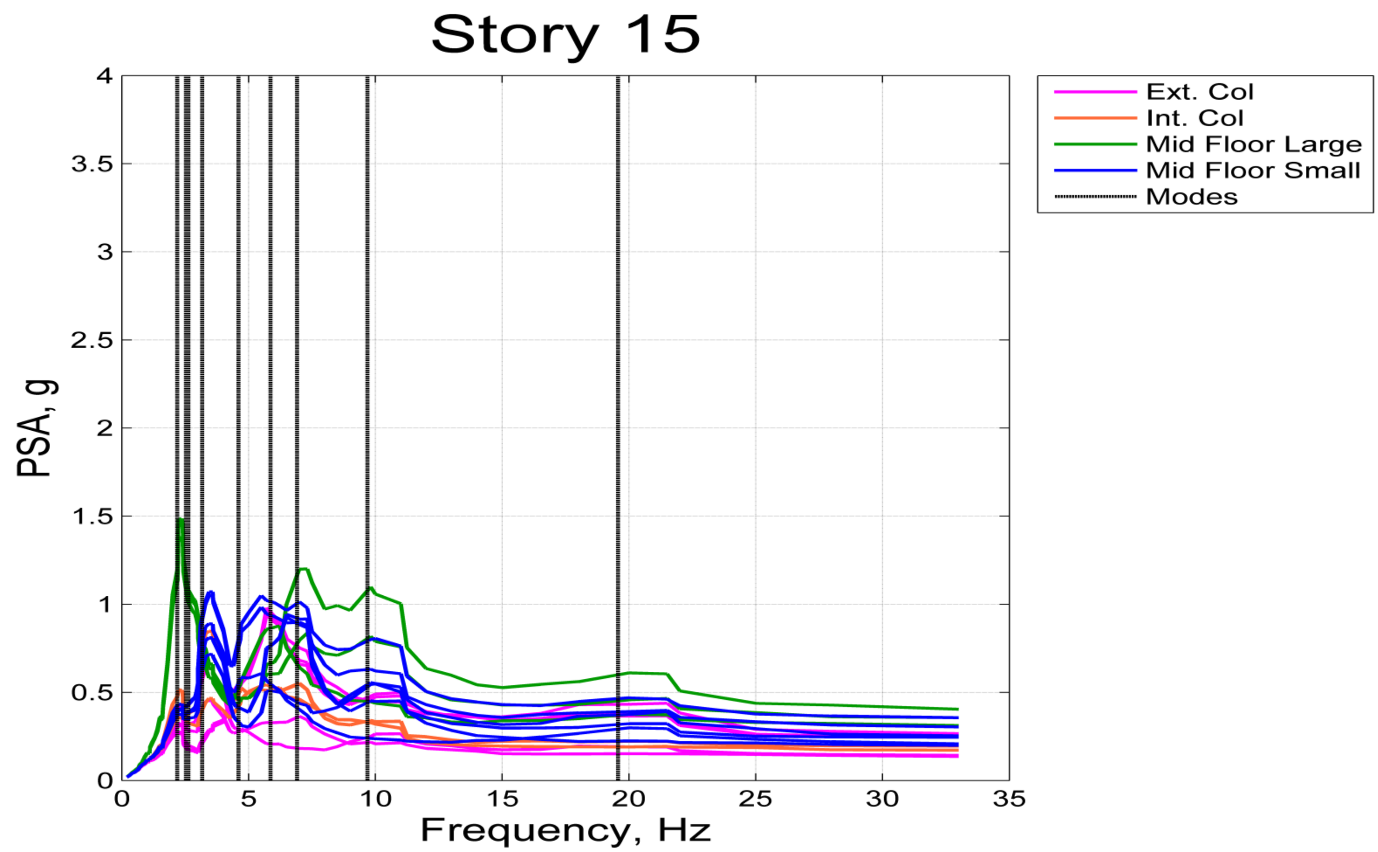


Figure 24: 15th story floor response spectra for selected locations.

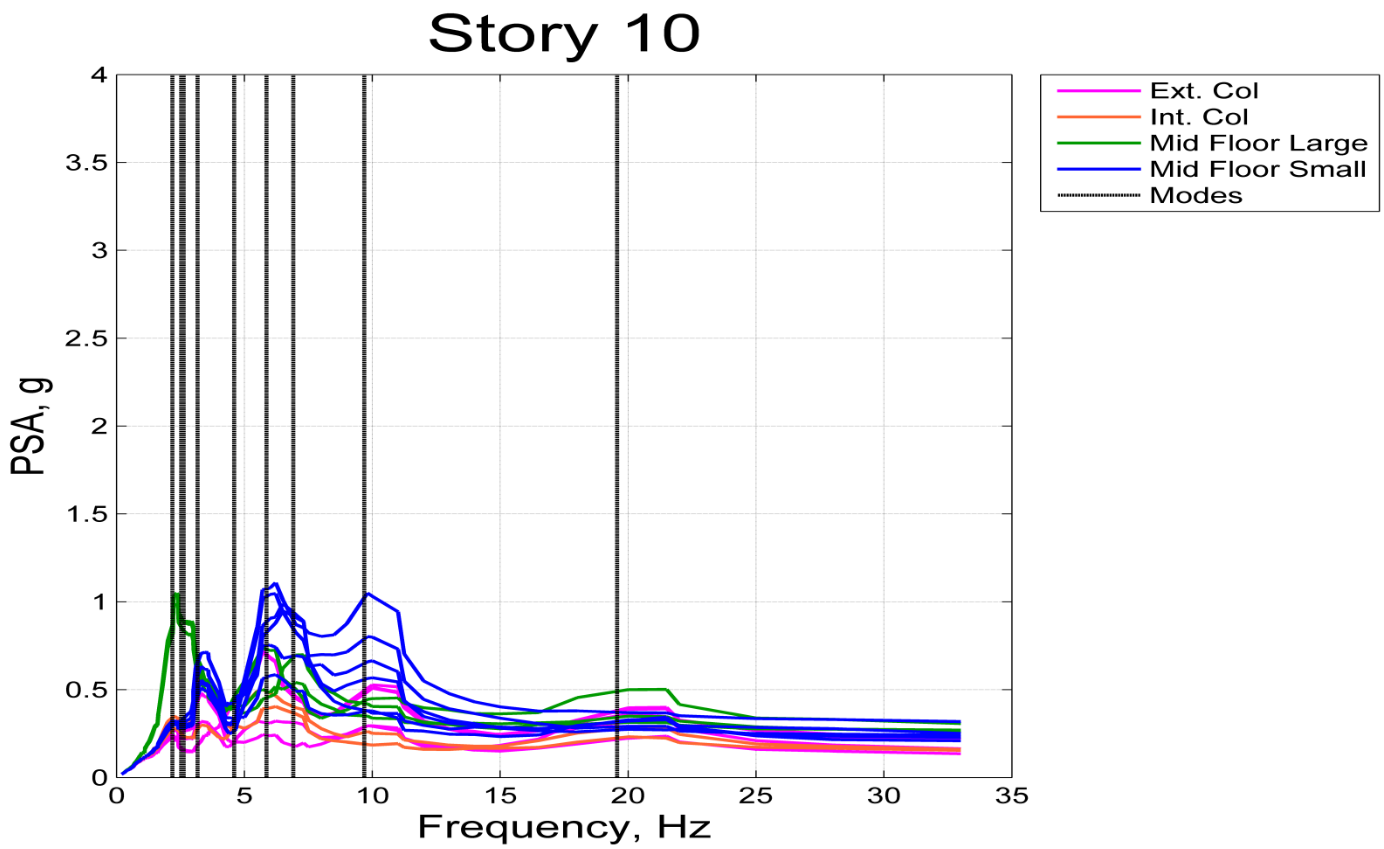


Figure 25: 10th story floor response spectra for selected locations.

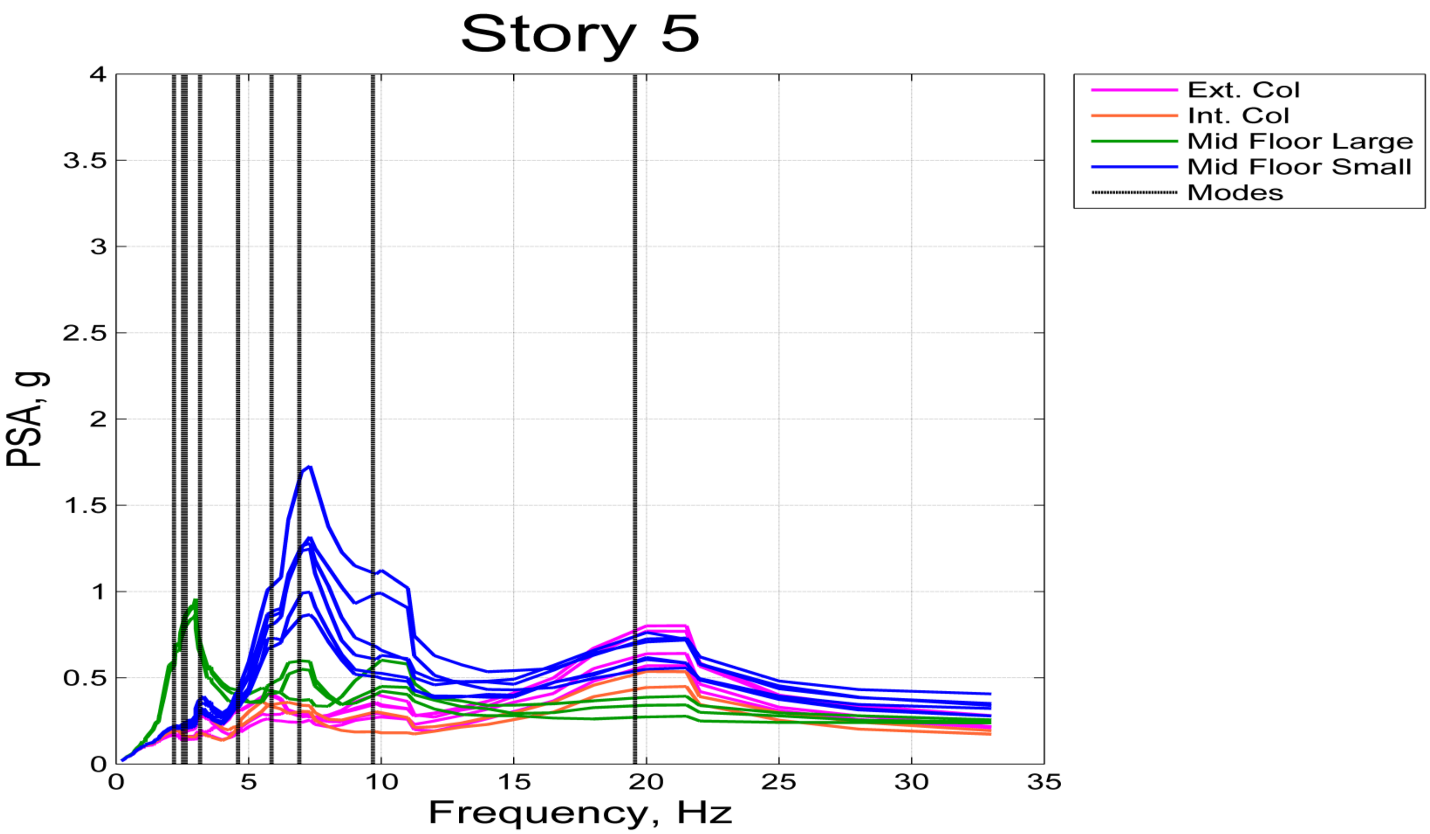


Figure 26: 5th story floor response spectra for selected locations.

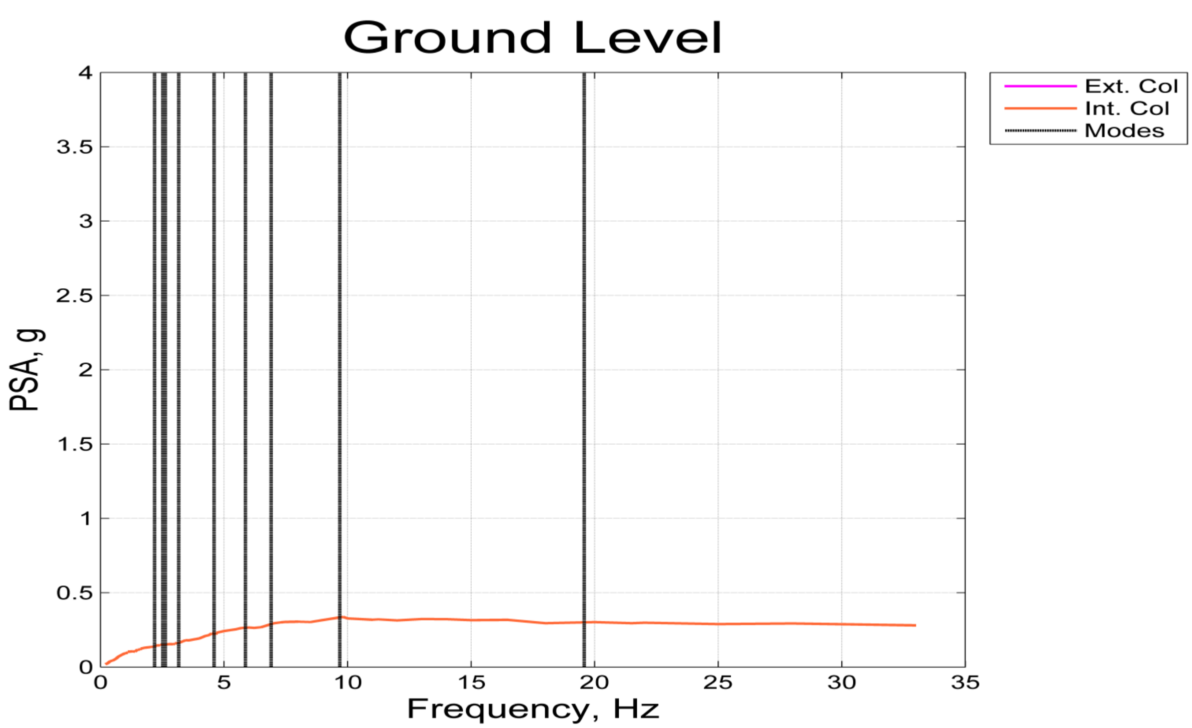


Figure 27: Ground floor response spectra.

As can be seen from the plots both the exterior and interior columns and some of the larger open slab sections of the floor see an increase in acceleration around 22 Hz. This frequency is close to the 22$^{nd}$ mode (19.6 Hz) of the structure; the last vertical mode considered in the analysis. The 22$^{nd}$ mode shape corresponds to columns moving out of phase with the interior slab sections which may explain the increase in floor response spectral acceleration.

The acceleration is greatest in the bottom floors of the building then recedes towards the middle and picks back up towards the roof level. This acceleration increase throughout the height of the structure may be the result of component frequencies interacting with the higher mode frequencies of the ground motions used in this study. The ground motions here have an average highest usable frequency of approximately 40Hz. Therefore, the frequency range beyond the last vertical mode is approximately 20Hz. It is possible that frequencies in this range have a disproportionate effect on the acceleration response of components compared to lower frequencies since it has been reported that vertical component accelerations are sensitive to higher modes.

From the ground floor to the roof the slab sections see an increase in acceleration in the first 10 Hz as the floor height increases. The vertical lines in Figure 23 through Figure 27 represent the modal frequencies in the vertical direction as shown in Table 31. In the Figures above, many of the peaks in acceleration of the slab sections coincide with the vertical frequencies of the structure. A good example of this is found in Figure 25, the 10$^{th}$ floor, where the larger slab section has peaks coinciding with the 1,2,3,4 and 6$^{th}$ modes. The remaining story FRS figures can be seen in Appendix D.

The peak vertical floor acceleration (PVFA) is also important because typically components are well anchored to the floor, columns, or walls of the primary structure since in most cases equipment is desired to remain stationary. The PVFA is taken at 33 Hz and can be seen along the height of the building in the following figures.

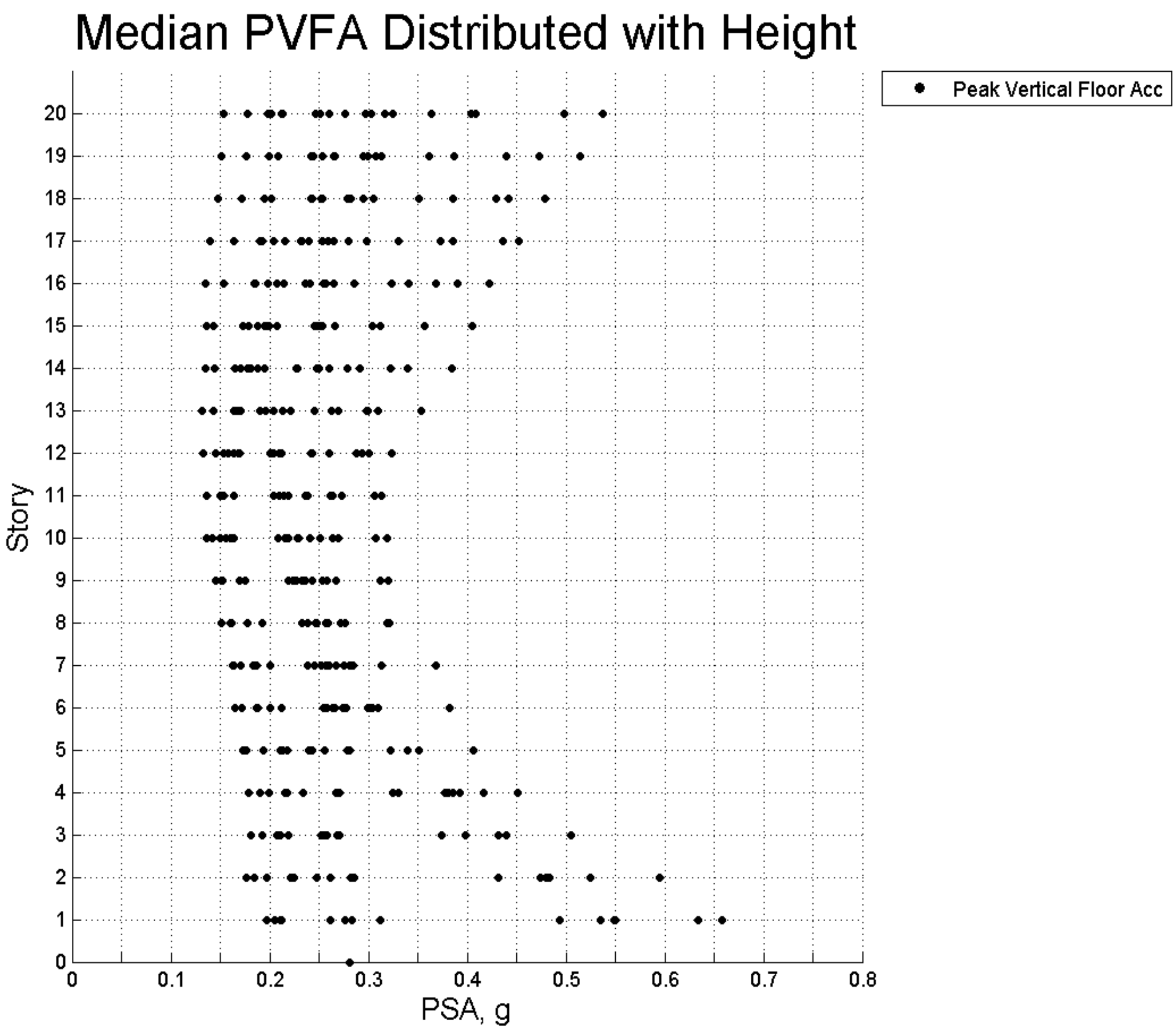


Figure 28: Median PVFA values.

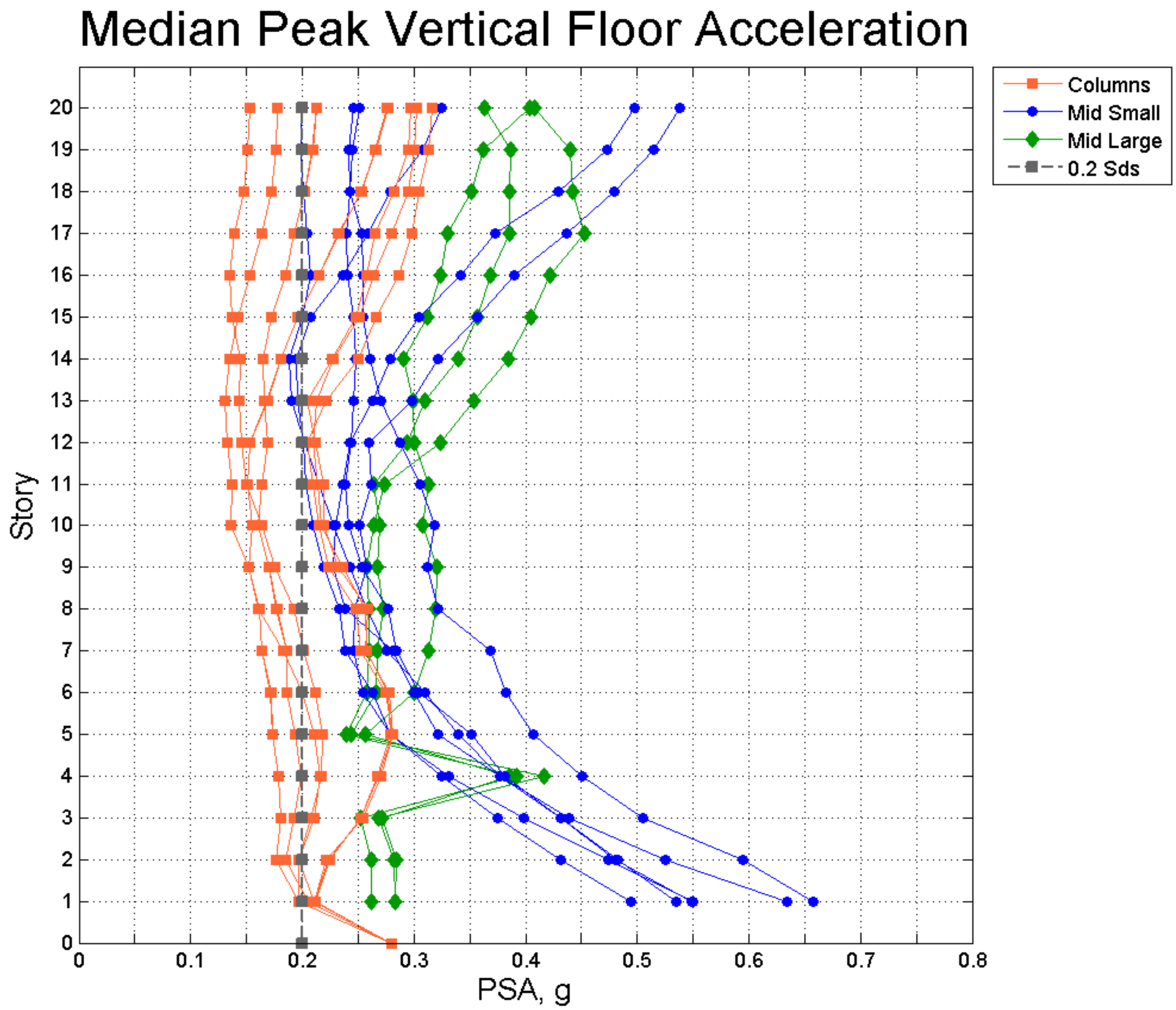


Figure 29: Median PVFA values classified by location in floor plan.

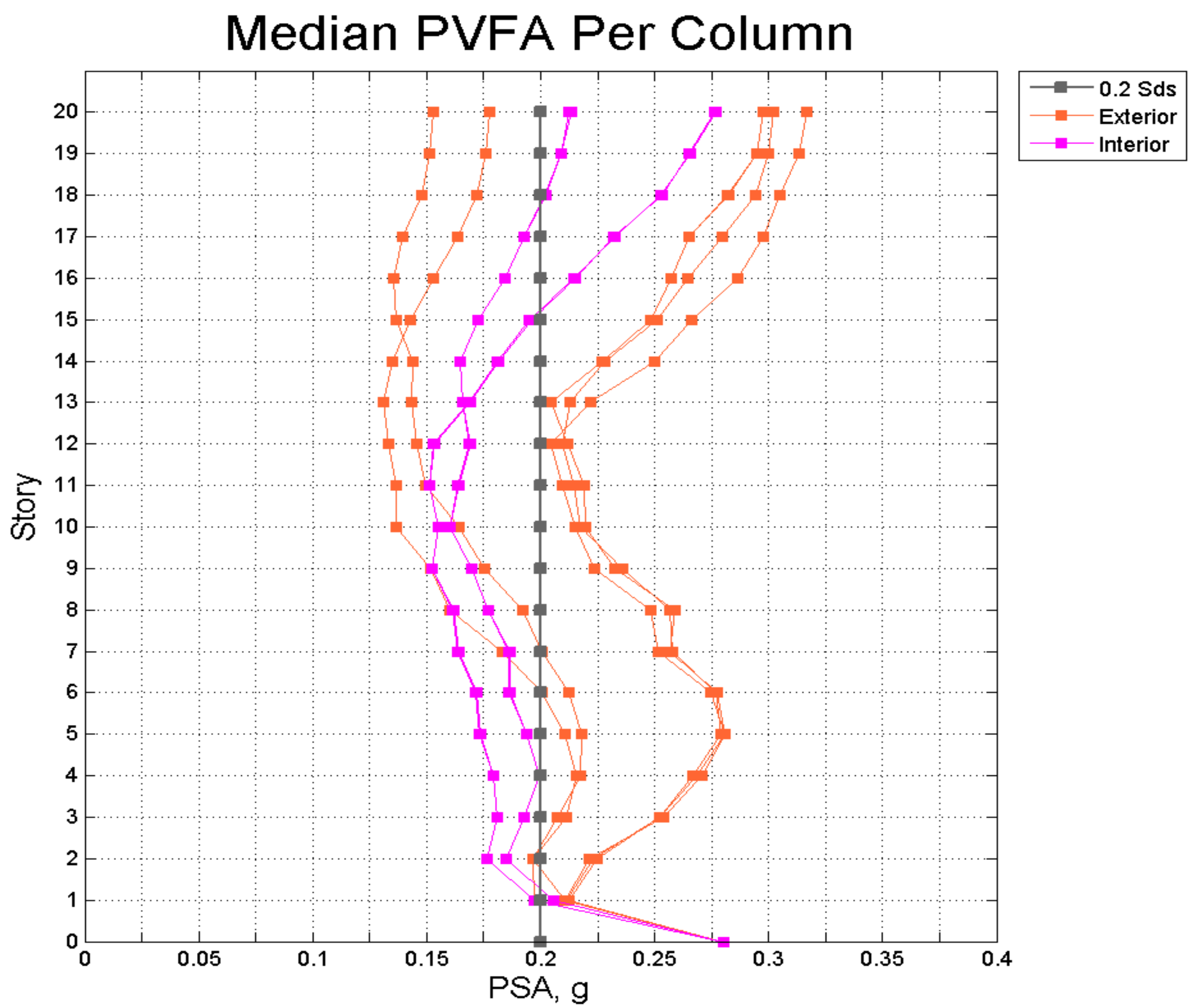


Figure 30: Median PFA values at exterior and interior columns.

Generally, the larger slab sections see an increasing trend in the median peak vertical floor accelerations (PVFA) except for the roof and the discontinuity in the 4th story. This large increase in acceleration in the 4th floor exists for all of the large slab sections. It is also found only in the larger slab sections.  On the other hand, the smaller slab sections experience large accelerations at the bottom and top of the structure producing a “C” shaped response over the whole height. The median PVFA of points on the smaller slab sections tends to be much larger than all of the other sections. The only exceptions to this observation are in floors 7 through 11 where the larger slab sections dominate all but one of the smaller slab sections and in floors 11 through 17 where the larger slab section accelerations tend to overcome the smaller section response. In the remaining top floors of the building the small slab sections dominate and approach the large levels found in the bottom stories. The column accelerations over the height of the building do not resemble either the small or large slab sections and there are differences even between the interior and exterior columns. In the exterior columns accelerations are generally larger which may be due to the fact that generally, the exterior columns are larger and stiffer W sections. About half of the column PVFA fall below the ASCE 7-10 design limitation of $0.20S_{ds}$ which for this case becomes 0.20 g and is shown in Figure 29 and Figure 30 as a vertical line. The vast majority of all mid slab section points are greater than the prescribed ASCE 7-10 limit. This suggests that the limit required by ASCE 7-10 may be unconservative.

The horizontal earthquake design force equation from ASCE 7-10 incorporates a component that accounts for ground and floor amplification over the height. The code uses a linear characterization over the height where the roof level experiences the highest amplification. The underlying assumption is that, buildings are very stiff in the vertical direction and as a result ASCE 7-10 does not require a similar component which amplifies the ground to floor acceleration when estimating design vertical earthquake forces. To investigate whether this 20-story building experiences ground amplification throughout the height, all of the peak vertical acceleration values have been normalized to the peak ground acceleration.

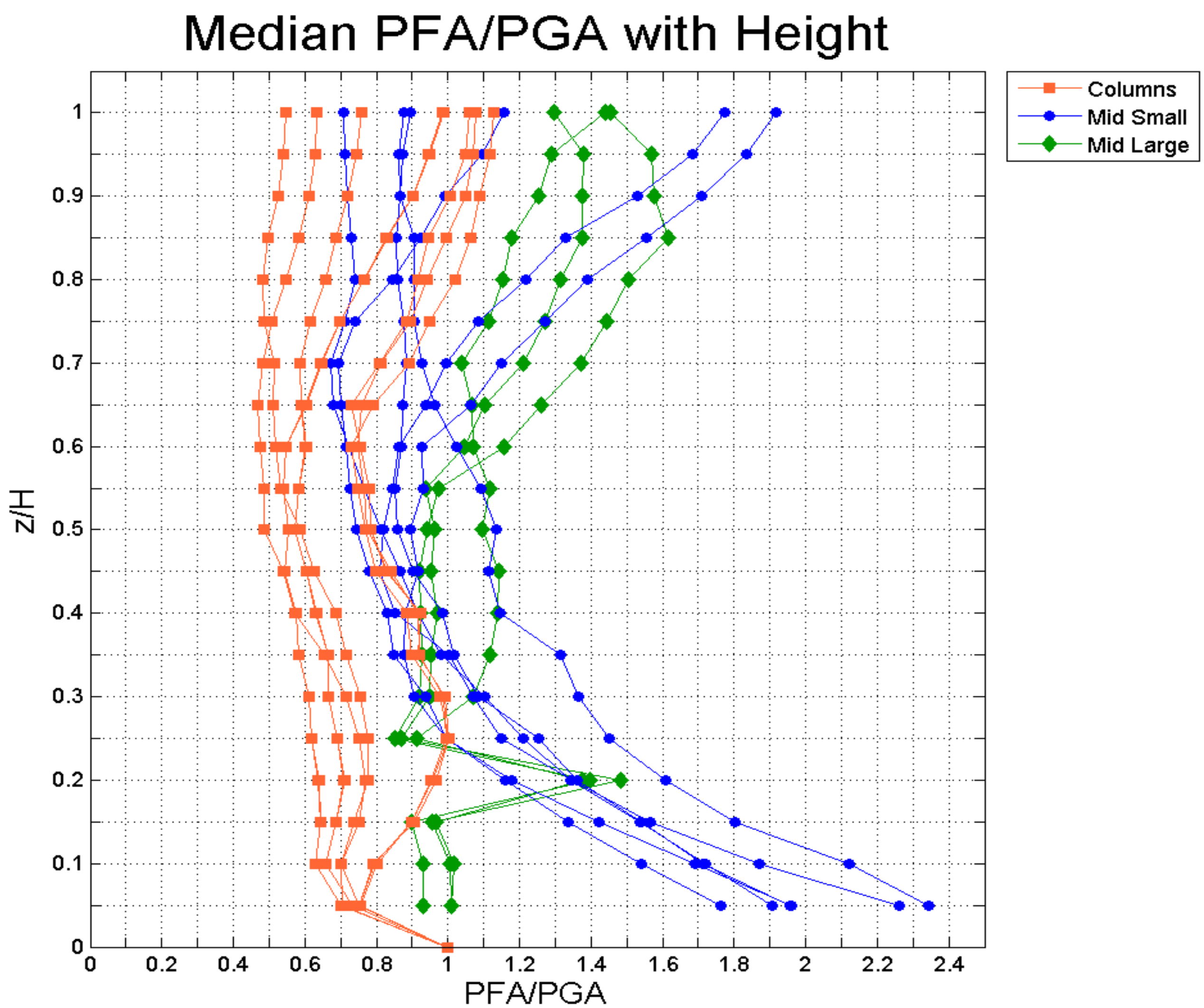


Figure 31: Median PFA/PGA values by location in floor plan.

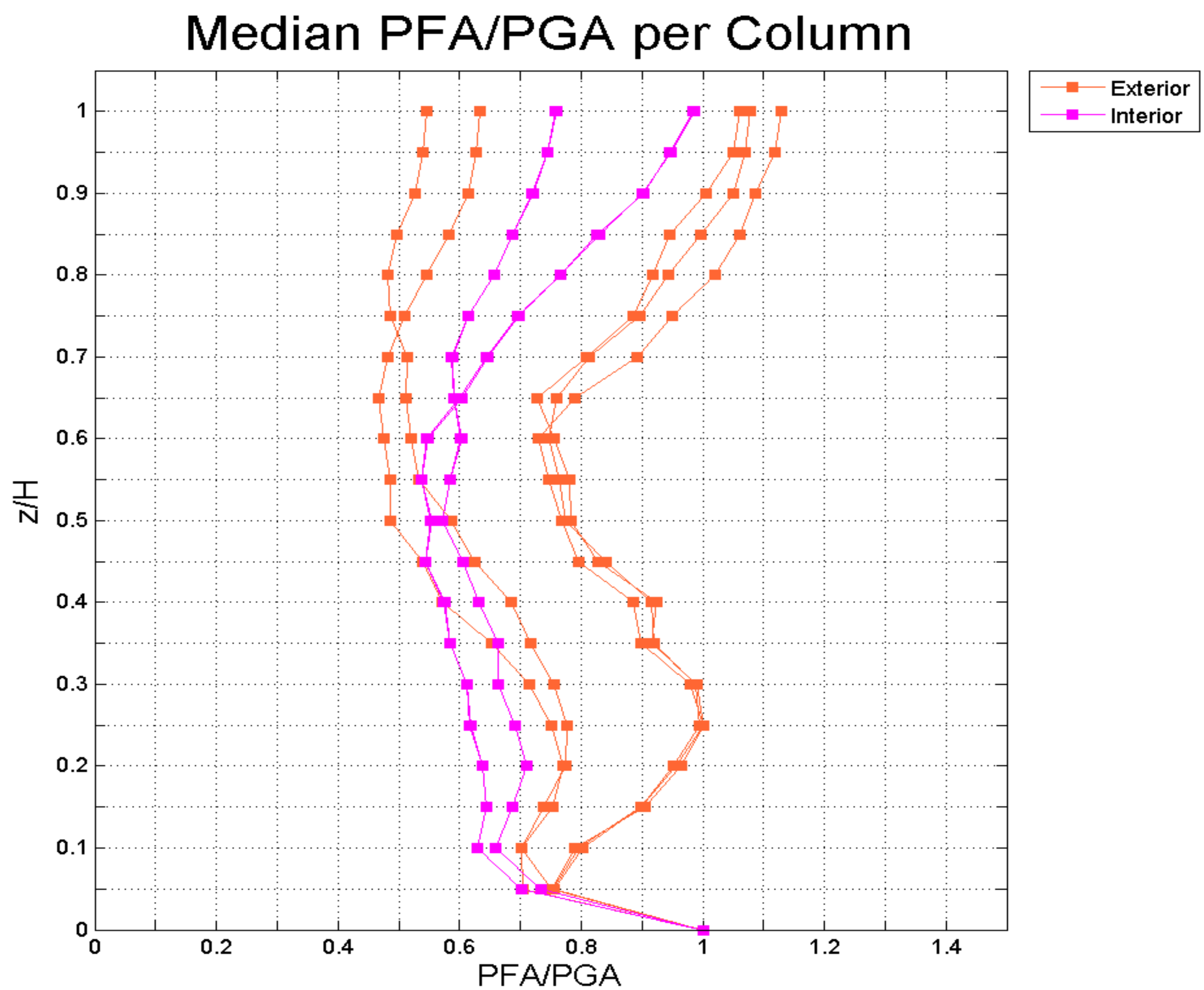

Figure 32: Median PFA/PGA values on the exterior and interior columns.

It can be seen from Figure 31 and Figure 32 the ratio of PVFA/PGA changes over the height of the building. While column acceleration demands increase in the very top floors the interior column demands never overcome the ground acceleration whereas some exterior columns do overcome the ground acceleration by approximately 10% for a PGA of 0.281g. The large and small slab sections median PVFA/PGA ratios vary from about 0.7 to 2.3. The largest values amplified with respect to ground are found in the smaller slab section. These sections are stiffer because of shorter unsupported lengths, which attract larger accelerations.

## 4.2 Comparison with Studies on the LA SAC 20-story Structure

Peak vertical floor acceleration demands for columns are similar to those obtained from Pekcan et al. [4] For instance, the variation of PFVA/PGA along the height of the building shows an increasing trend that can be observed in the upper stories as seen in Figure 33. This trend is consistent with the one observed in this study (Figures 31 to 32). Median values compare reasonably well too. However, PVFA/PGA ratios for the LA office building are between 0.5 and 1.1, whereas values around 1.0 are observed for the SAC 20-story structure (see Figure 33).

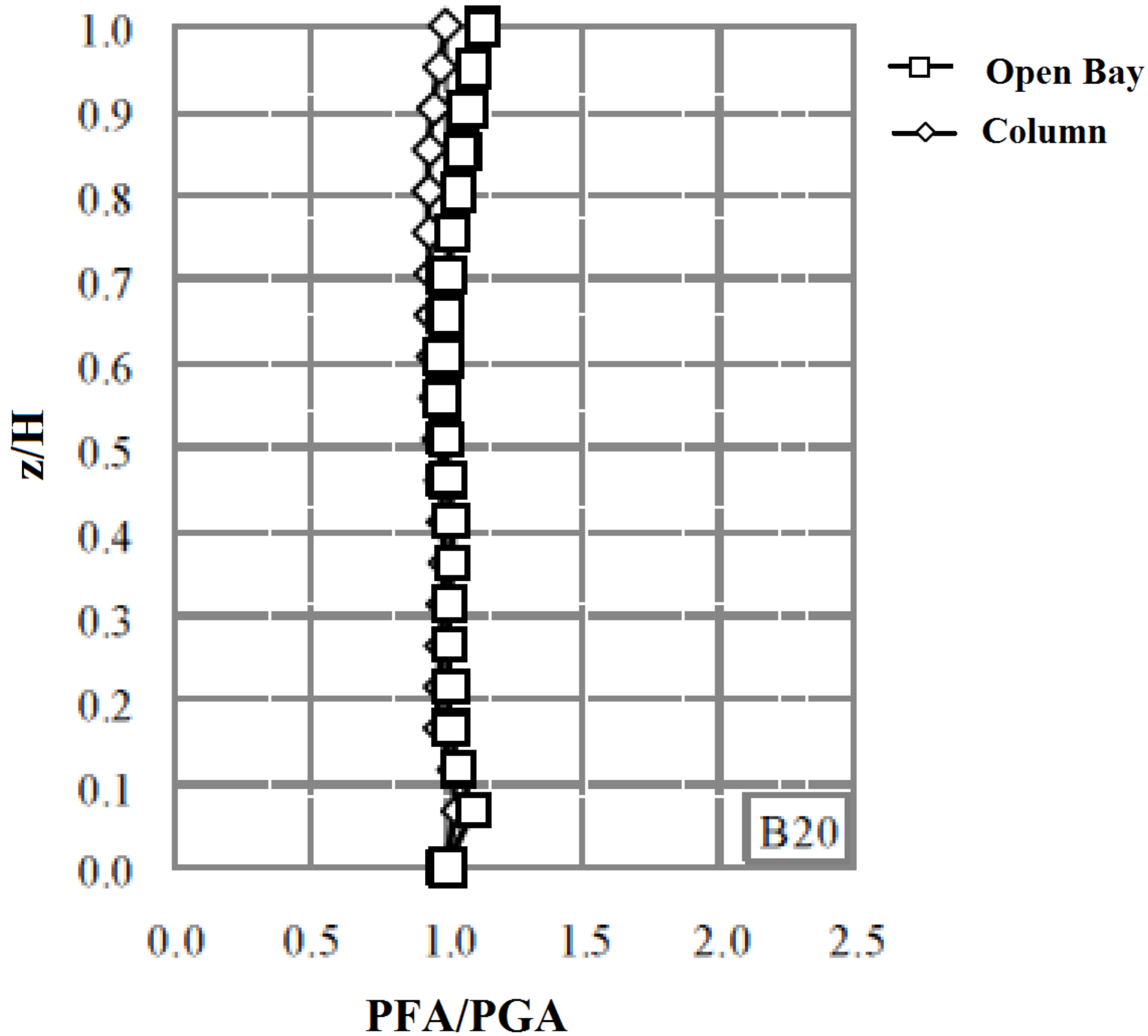

Figure 33: Median PFA/PGA values for the SAC 20-story office building. [4]

The similarity and uniformity between the column and slab vertical accelerations lead Pekcan et al. [4] to conclude that the column "axial stiffness is sufficiently great to provide essentially rigid body motion in the vertical direction." However, the slab accelerations normalized to ground for the building presented in this study take on a "C" shape over the height with slab to ground median amplification values between 0.5 and 2.4. The SAC building on the other hand has a height wise shape resembling a straight line with an acceleration range approximately between 1 and 1.1.

This discrepancy may be explained by differences in the plan layout, column sections, floor diaphragm out-of-plane flexibilities, as well as the approach taken to model the floor system. Figure 34 presents results obtained from statistics on the smaller group of ground motion recordings used by Pekcan et al. [4] It can be seen that values and trends in the variation of vertical acceleration responses are still consistent with the ones obtained using the larger ground motion set in this study.

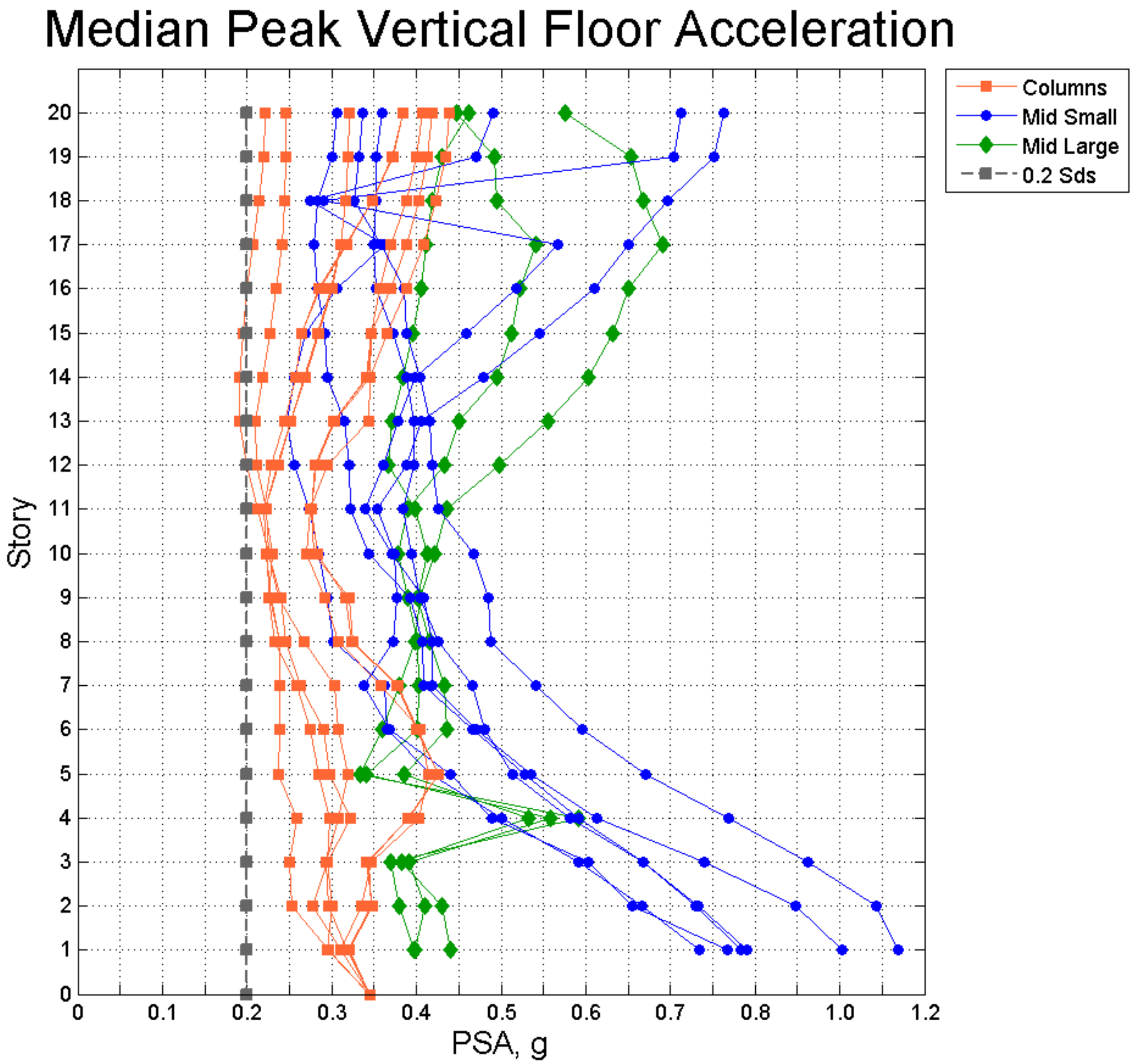


Figure 34: Median PVFA values produced by the ground motions used in Pekcan et al. study.

A closer look at Figure 34 indicates that using the ground motions from the University of Nevada- Reno study produces median vertical floor acceleration demands that are slightly larger than the median results of the 106 ground motions used in this study. This is due to the smaller sample size; however, the trends in the variation of floor accelerations along the height are still consistent between the two data sets.

Differences between the two office buildings plan view floor layout may help explain some of the differences found in these two studies. The layout of the SAC office building is 6 bays at 20 foot in the East-West direction and 5 bays at 20 foot in the North-South direction. The bays are uniform and the overall aspect ratio of the SAC office building is 1.2. The floor plan is relatively uniform and the median PFA/PGA values shown in Figure 33 are also fairly uniform along the height of the building.

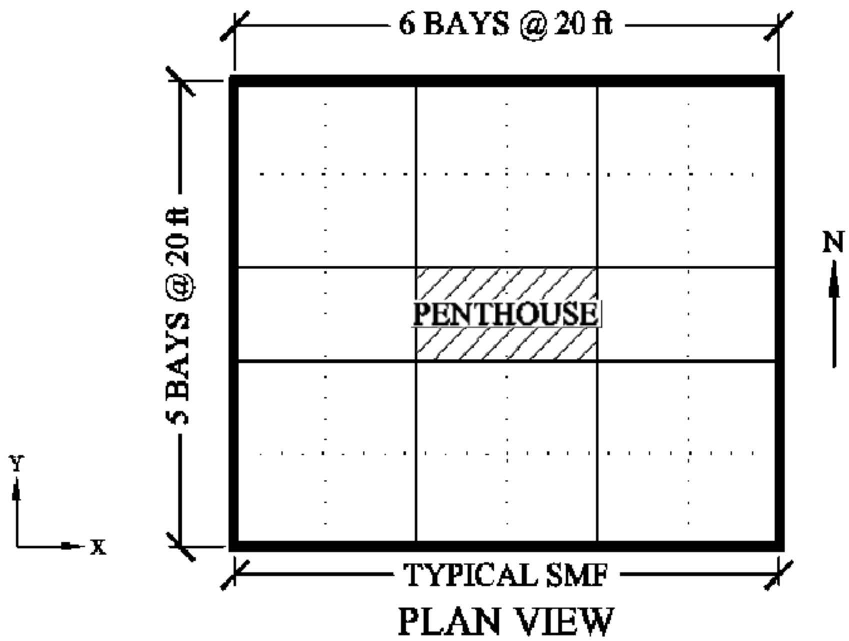


Figure 35: Roof plan view, 20-story office building used in Pekcan et al. study.

In this study the bay size is nonuniform (20-by-20 and 40-by-20 foot). The out-of-plane stiffness of the shorter bay is approximately 2.08 times greater than the out-of-plane stiffness of the larger bay. This stiffness comparison rests on many simplifying assumptions such as analyzing the concrete bays as simply supported (at all edges) rectangular plates bending out-of-plane under uniform loading. This nonuniformity in the out-of-plane stiffness of the floor may partially explain the lack of uniformity in the PVFA results from Figure 31.

The larger slab sections, rather than the smaller ones with the exact same dimensions, more closely resemble the 20-by-20 foot section acceleration responses of the SAC building. The SAC building has more bays, and hence, more columns. Since vertical inertia forces are transferred to the floor system through the columns, an increase in the number of columns may provide a more uniform “loading” to the floor, thereby yielding floor acceleration results that are more similar to the column output.

Differences in the overall dynamic characteristics between the buildings may also help explain the differences in vertical acceleration values. The SAC building has a fundamental period of approximately 3.9 seconds while building considered in this study has a fundamental period of 5.5 seconds. This building is more flexible when it comes to the vertical direction as well with a fundamental period of 0.46 seconds (2.2 Hz) while the SAC building has 0.28 second (3.6 Hz) vertical fundamental period. The largest frequency obtained for the structure used in this study is of 19.6 Hz, which corresponds to mode 22. This frequency is lower than the highest corner frequency used to correct the ground motion recordings used in this study (i.e., 20 to 60 Hz.) However, if the building were more rigid, as it is the case for the SAC building; then, it would have higher modes with higher frequencies. In that case, it is conceivable that some ground motions may not have the frequency content to adequately excite the whole structure or certain higher modes that have significant modal mass contributions. Therefore, the estimated vertical floor accelerations may be smaller. Admittedly, without an effective modal mass breakdown for the SAC building analysis, it is difficult to evaluate whether higher mode effects may explain some of the differences in acceleration results.

Another relevant difference between the two buildings is the design of the floor system and how it is modeled. The SAC building analysis uses shell elements with large thicknesses in order to account for the composite action between the floor slab and secondary beams, and hence, does not explicitly model the secondary beams. The actual mass of the system is manually added to each node. In principle, this method of modeling should reasonably capture the out-of-plane flexibility and the global dynamic behavior of the floor system. However, by refining the model through the use of separate beam and slab elements, as well as by ensuring compatibility through displacement constraints, the local dynamic behavior of the model could be greatly improved. With these changes, the mass of the system is more realistically distributed. Improvements in the local dynamic behavior of the model will be reflected in more realistic floor response spectra (FRS). The latter more refined approach is used in this report and may also help explain the differences in acceleration results when compared to the Pekcan et al. [4] study.

There is also evidence to suggest that for shorter buildings, the PVFA shows an increasing trend that contrasts the uniform vertical acceleration found in very axially stiff column systems. Based on the floor plan of the 20-story office building used in this study, a series of simplified multiple-degree-of-freedom (MDOF) systems (i.e., stick models) having various building heights including 5, 10, 15, and 20 stories are modeled. These stick models lump the entire floor mass at one level and frame elements are used to connect all of the masses. The vertical stiffness of each story frame is taken as the summation of the in-plan column properties (i.e., the total cross-sectional area of each column at each story level.) While these models are simple, they can be used to provide a general idea of column dynamic behavior with little computational time. A 27-ground motion subset of the total 106 set is used on each model and floor response spectra are obtained. The PVFA is plotted against the height of each building and all stories show an increasing trend with height (Figure 36 to Figure 40).

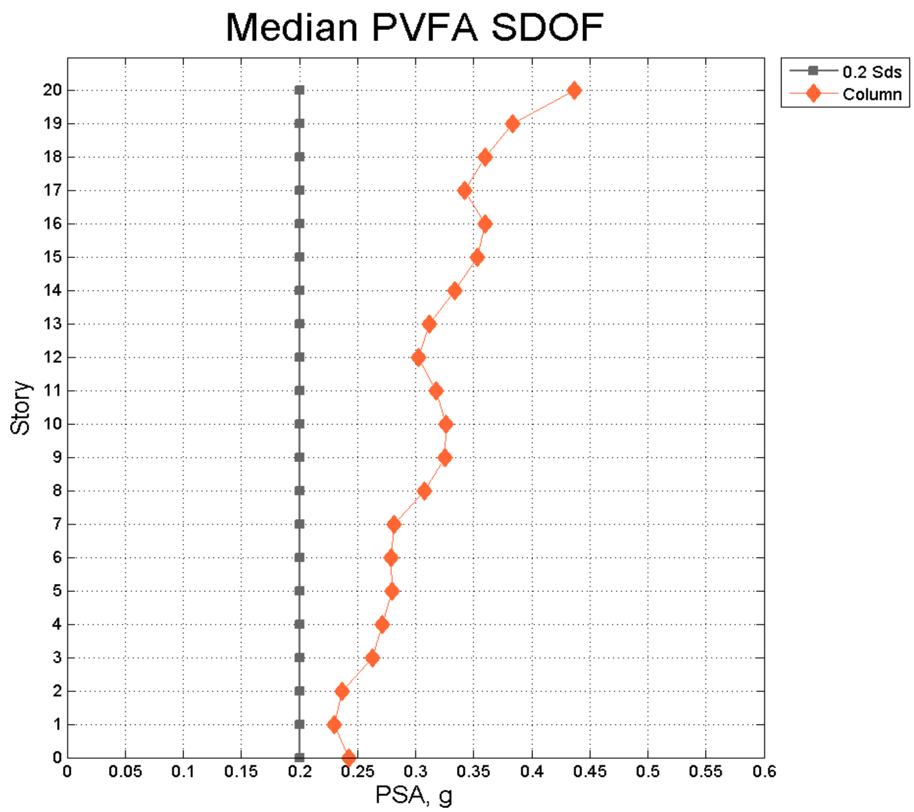

Figure 36: Median PVFA, simplified 20-story stick model.

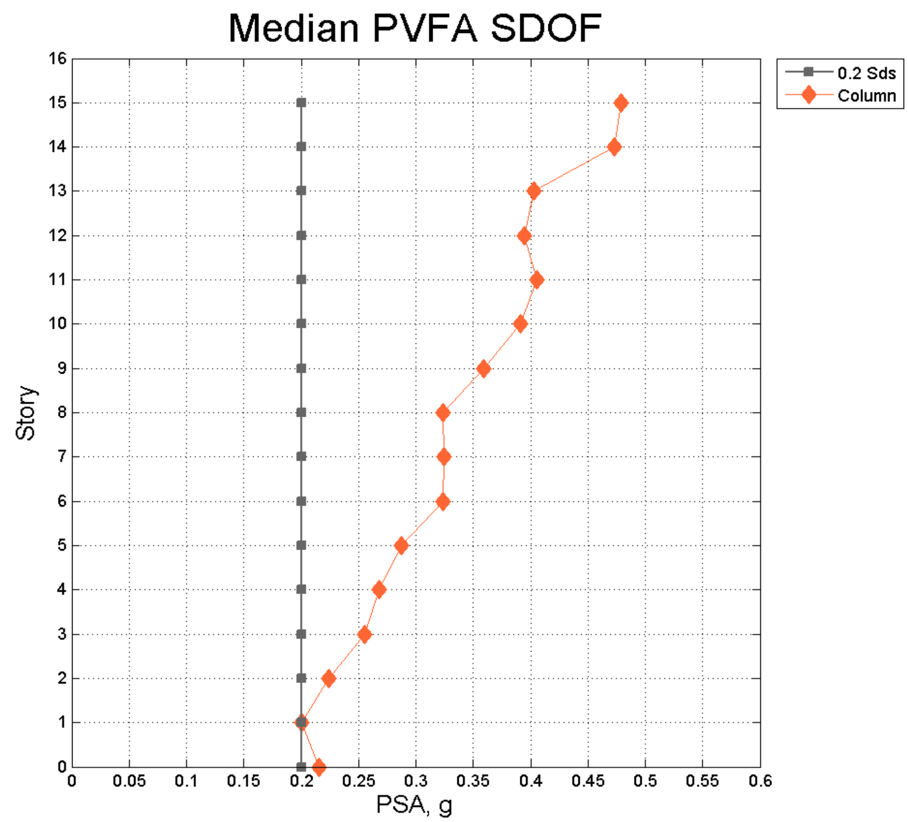


Figure 37: Median PVFA, simplified 15-story stick model.

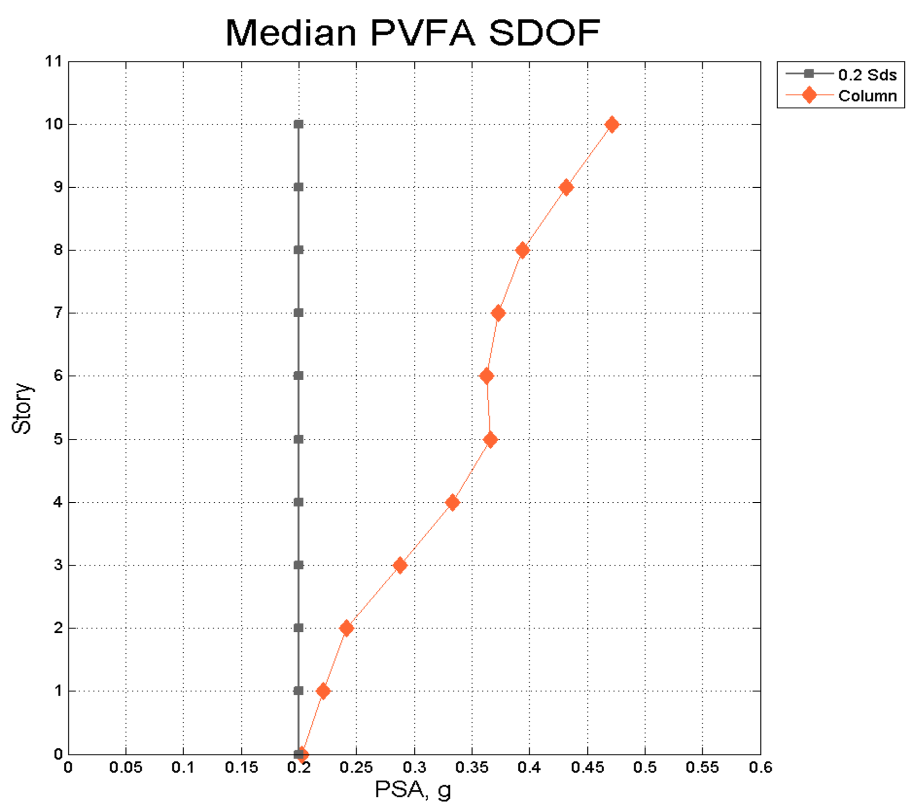


Figure 38: Median PVFA, simplified 10-story stick model.

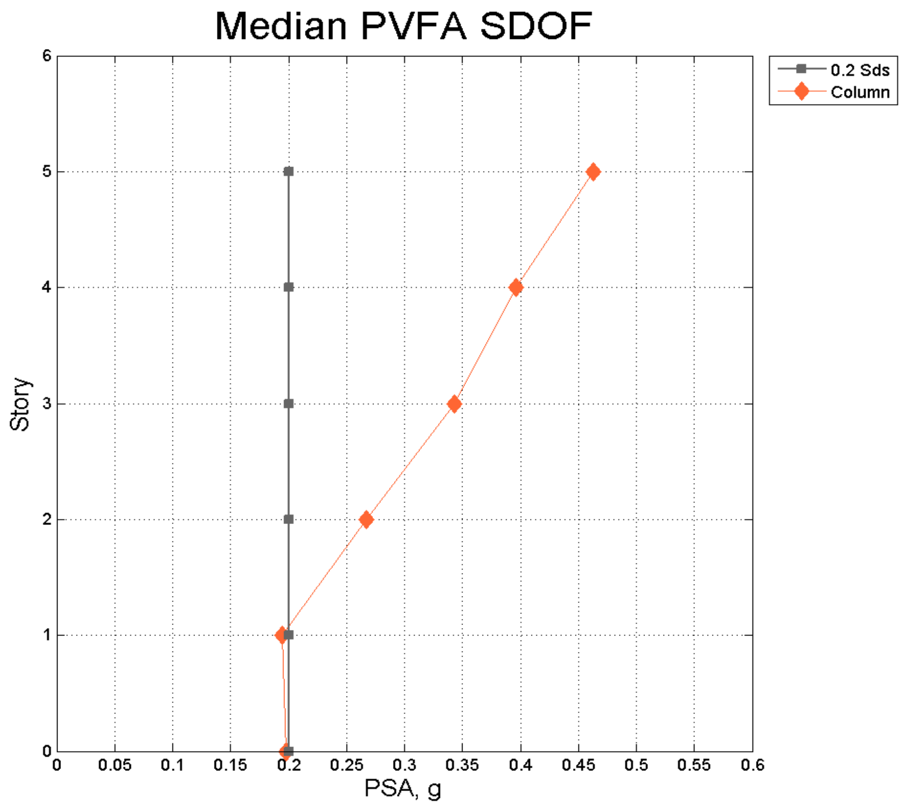


Figure 39: Median PVFA, simplified 5-story stick model.

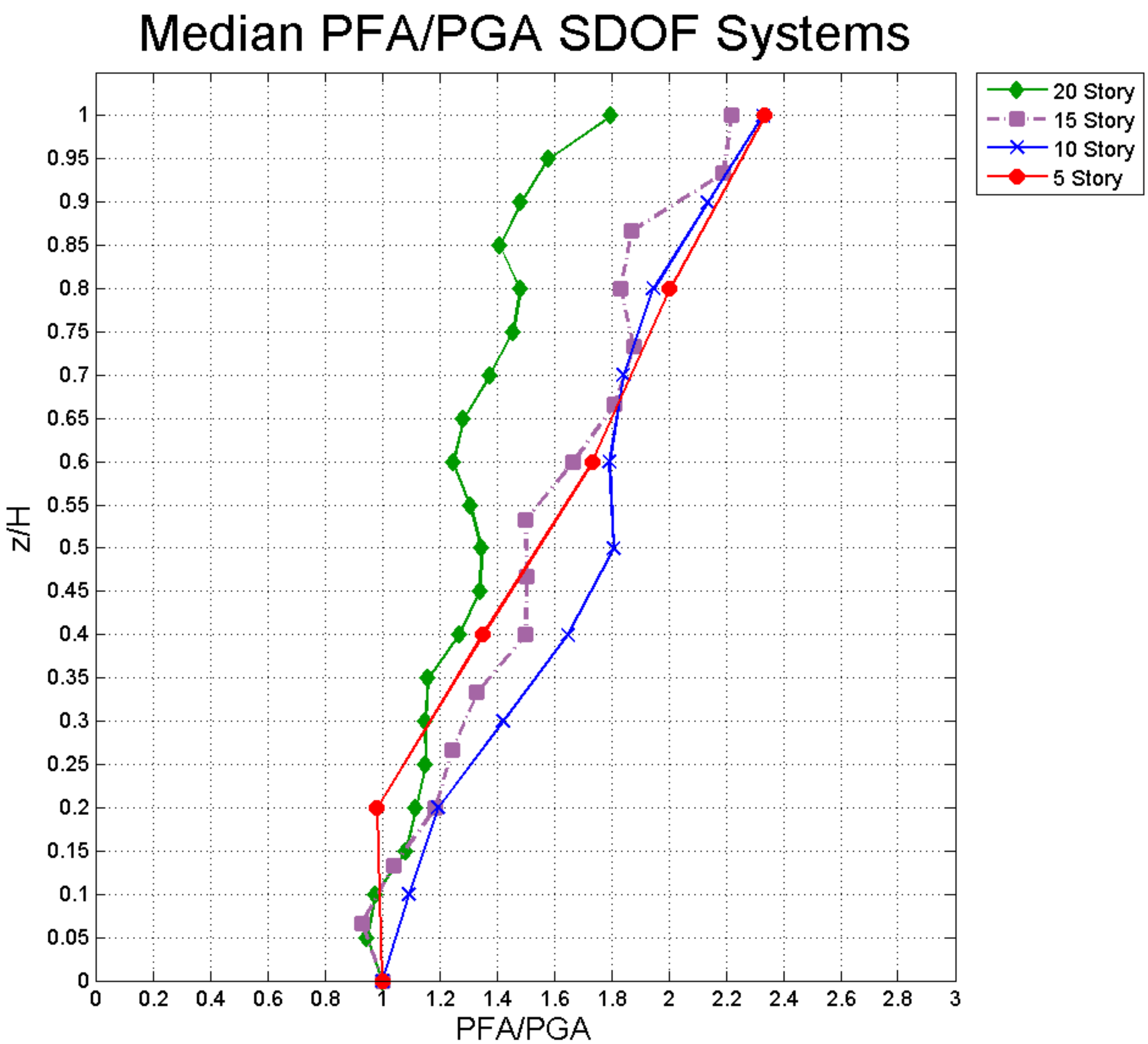

Figure 40: Median PVFA/PGA, all stick models.

As can be seen from the figures above, all of the models show a similar increasing acceleration trend along the height of the building with roof vertical acceleration values ranging from 1.8 to 2.3 times the PGA. The shorter story buildings from the /university of Nevada-Reno study including the 3- and 9-story structures show a similar trend (Figure 41).

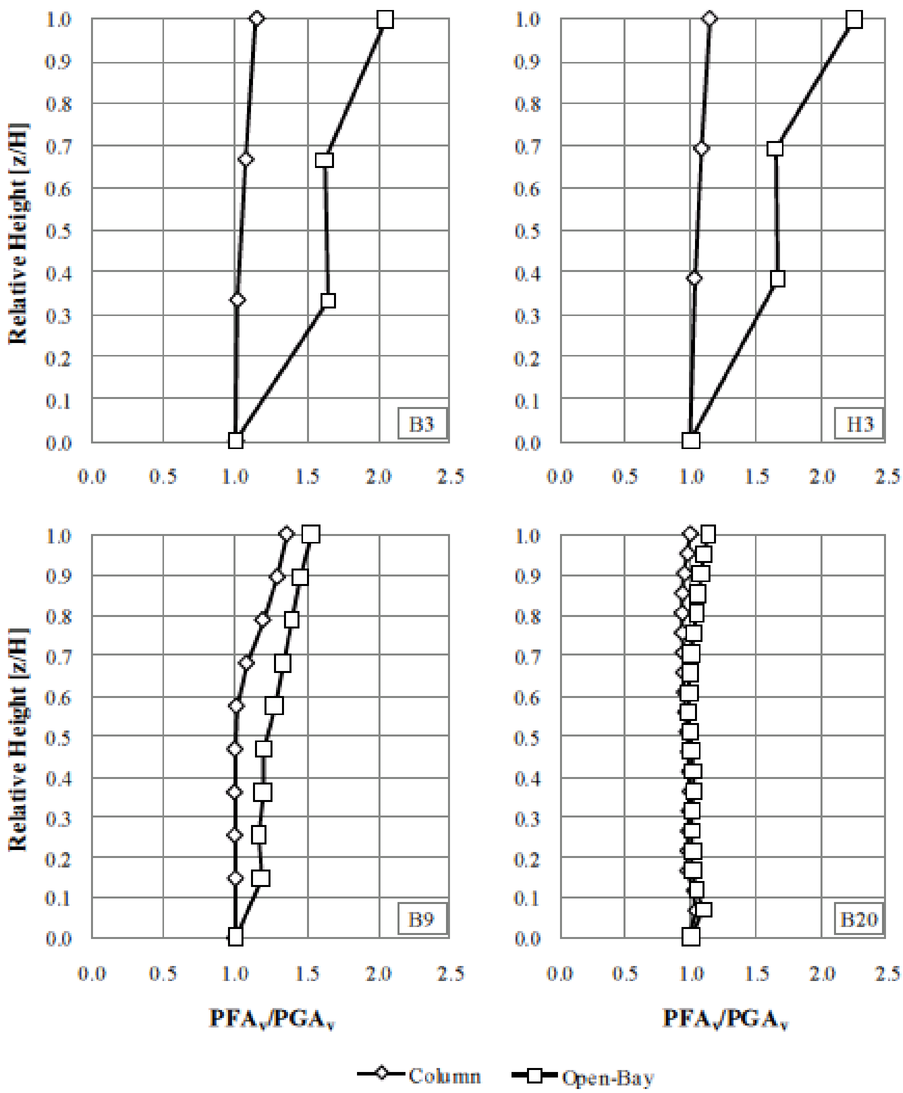


Figure 41: Median PFA/PGA values for all the building which Pekcan et al. investigated.

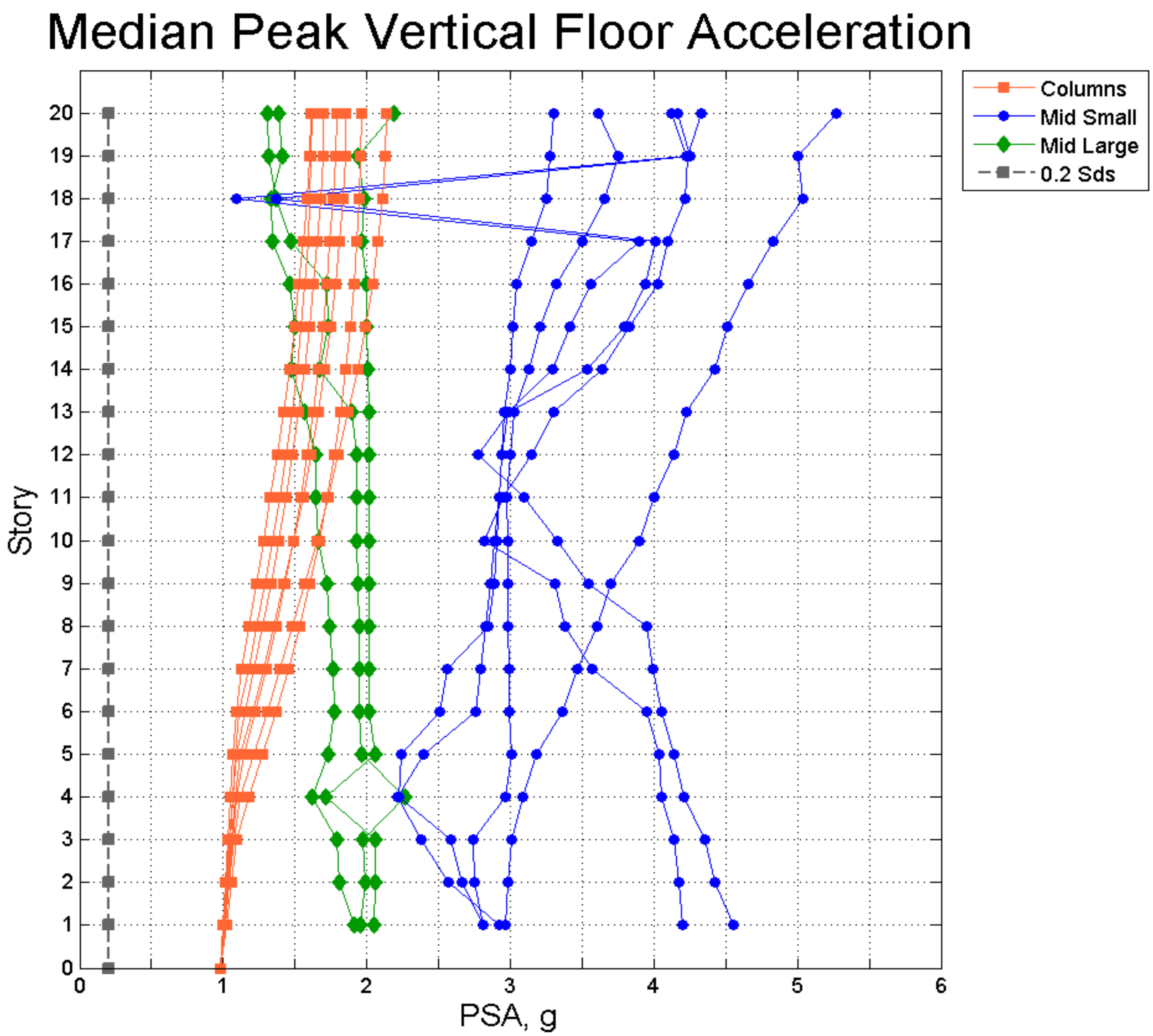


Figure 42: Median PVFA values. 20-story building with infinitely rigid columns.

A model with infinitely rigid columns was also developed in this study to evaluate the effect that column rigidity has on the results. PVFA results corresponding to this case demonstrate that when columns are infinitely rigid, column and slab vertical accelerations are different and do not overlap as depicted in Figure 42, which shows results for a set of 18 randomly selected ground motions.

Vertical acceleration values become more uniform for example all of the interior and exterior columns exhibit nearly identical behavior. The large slab section accelerations are almost entirely constant until about the 16th floor. They also overlap with the column accelerations in the upper stories and not at the bottom stories as it is the case for the SAC building (see Figure 42). The "C" shape acceleration profile evident in the small slab sections of the model with finite column flexibilities is replaced by a much more uniform pattern. The discontinuity found in the 18th story of the small slab section is most likely explained by the small sample size of ground motions. The infinitely rigid column model is broadly consistent with the flexible column model in that the largest accelerations are found at the small slab sections. The infinitely rigid column model also suggests that column and large slab section accelerations increase towards the higher floors.

## 4.3 Evaluation of ASCE 7-10 Design Vertical Acceleration

As can be seen from the following figures, the design vertical floor acceleration of $0.2S_{ds}$ is exceeded at least 50% of the time for the majority of the cases investigated in this study. When 84th percentile responses are evaluated (mean + one standard deviation), it is evident that the prescribed value of $0.2S_{ds}$ significantly underestimates the expected PVFA demands. Furthermore there is a high degree of variability in the acceleration values. For example, the 84th percentile column values range from being 0.13 to 0.42 g larger than the median values. Similarly, the slab 84th percentile acceleration values range from 0.19 to 0.88 g larger than the median values. This variation is due to the record-to-record variability (i.e., aleatory variability) present in the analyses. Based on this case study, the $0.2S_{ds}$ code provision tends to significantly underestimate the peak vertical floor acceleration in this structure, which highlights the need for additional studies on floor acceleration demands in buildings.

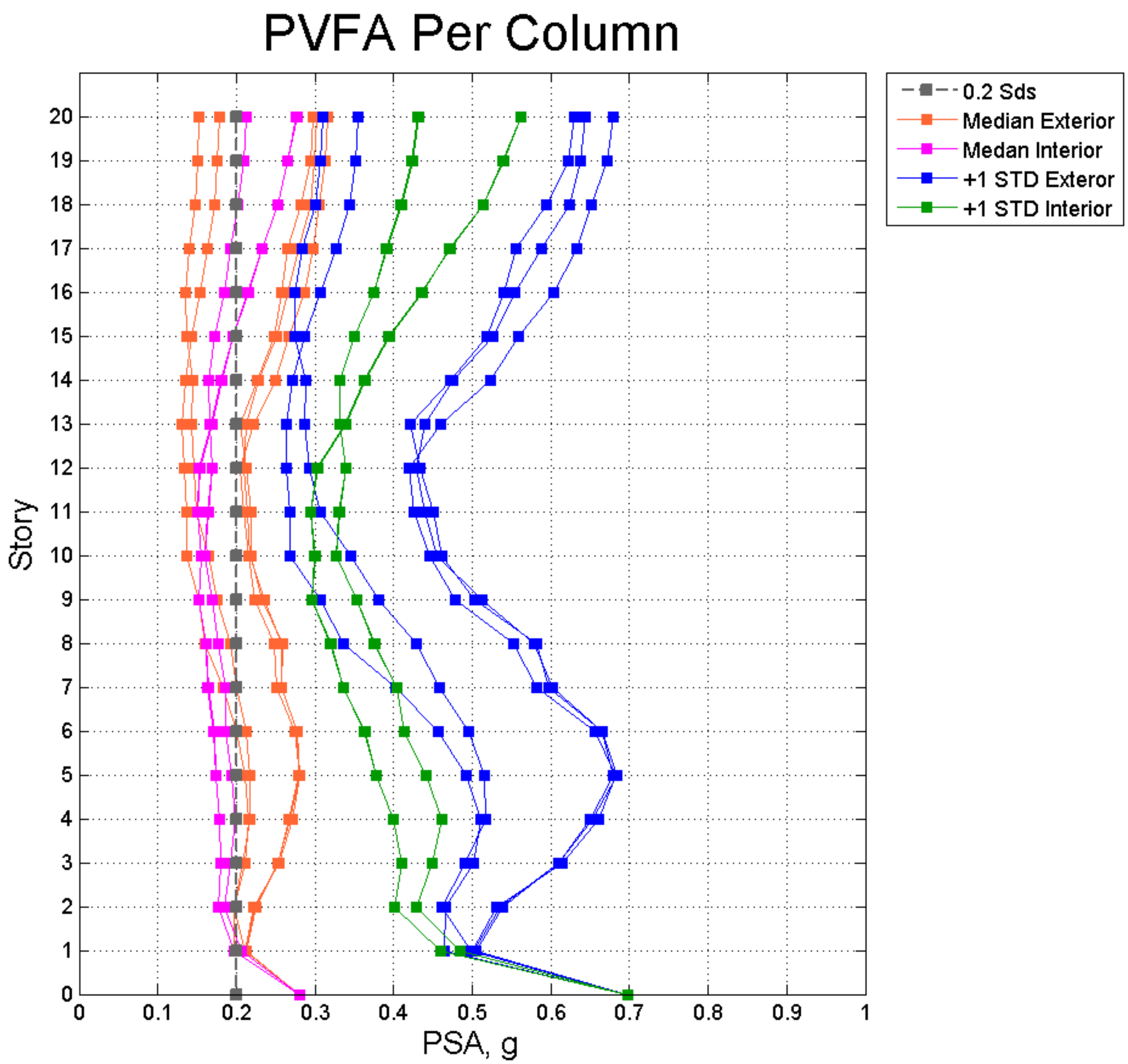

Figure 43: Mean and 84th percentile PVFA values for columns.

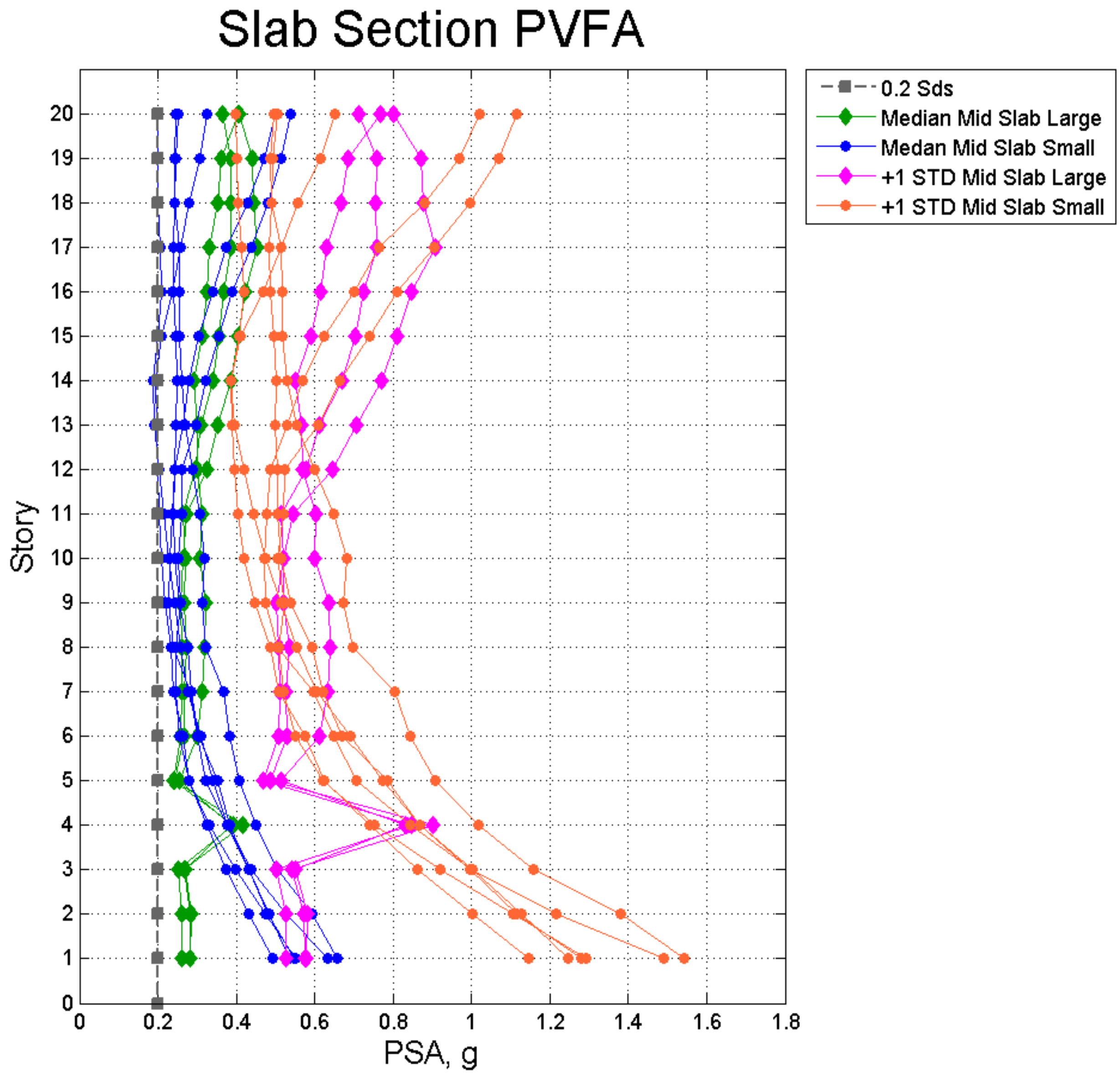


Figure 44: Mean and 84th percentile PVFA for the slab sections.

# CHAPTER 5

# CONCLUSION

## 5.1 Summary & Final Remarks

With the emergence of Performance-Based Design methods in the last two decades, society and building owners demand higher building performance standards to minimize casualties, injuries, direct losses, indirect losses due to business interruption, and loss of functionality of essential facilities. These increasing demands relate to normal operating conditions, as well as during and post extreme events including earthquakes. In order to meet these expectations, structural engineers must properly design and analyze not only the primary structural elements but also architectural, mechanical, electrical components and contents. Apart from clean up and replacement cost, inadequate performance of nonstructural elements, their supports and attachments to the primary structure, may hinder egress, result in the loss of life, and or disrupt normal building operations and services for a significant period of time. Engineers rely on buildings codes and load standards such as ASCE 7-10 for the design of NSCs. However, historically, minimal attention has been placed on understanding and quantifying floor vertical acceleration demands on NSCs. Past earthquakes have shown that the vertical component of ground motion is important to prevent failure of components such as suspended ceilings, staircases among others.

In an effort to better understand vertical acceleration demands on rigid NSCs in multistory buildings and evaluate the adequacy of building code provisions, a 20-story office building located in Los Angeles, California is designed. Vertical acceleration demands are characterized through the use of floor acceleration spectra that are obtained for various points on the plan floor of the elastic primary structure exposed to a set of 106 recorded vertical ground motions. The main observations and results of this study are as follows:

1.) Peak vertical floor acceleration demands vary in plan and are strongly dependent on the out-of-plane flexibility of the floor system.
2.) The highest vertical acceleration demands occur at smaller floor slab sections, followed by locations at larger floor slab sections, and then, smaller demands are obtained at column locations.
3.) The smaller slab sections have a "C" shape acceleration profile over the height of the building with median PVFA/PGA values ranging from 0.19 to 0.66 g.
4.) The median vertical acceleration profile for larger floor slab sections tend to increase in the upper floors of the building with PVFA.PGA values ranging from 0.24 to 0.45 g.
5.) Generally, exterior columns experience higher vertical accelerations than interior columns with median PVFA/PGA values ranging from 0.13 to 0.32 g. Interior column acceleration range from 0.15 to 0.28 g.
6.) Shorter story buildings tend to have increasing vertical floor acceleration profiles.
7.) The ASCE 7-10 vertical seismic force design provision that estimates seismic forces based on $0.2S_{ds}$ underestimates the peak vertical floor acceleration by 68% for the majority of the points found in the floor plan at least 50% of the time. This code equation significantly underestimates the 84$^{th}$ percentile peak vertical floor acceleration demands.

Thus, the ASCE 7-10 equation for estimation of component vertical floor accelerations should be further evaluated analytically and experimentally with additional structures and ground motions.

## 5.2 Future Work Considerations

The work presented here only focuses on one building. In order to further characterize vertical acceleration demands research efforts should concentrate on a parametric study with varying building designs including various concrete deck thicknesses, floor and slab aspect ratios, number of columns and their locations, column stiffness, nonlinear effects, story height and most importantly varying the primary structure beyond the steel moment frame type to include other types of lateral load resisting systems, materials, and configurations. Furthermore, practicing structural engineering designers who are designing acceleration sensitive equipment should understand ASCE 7-10 may be unconservative and they should use engineering judgment to quantify their design demands.

APPENDIX A

CONTROLLING LATERAL LOAD CASE

## A.1 ELF Summary

Table A.1.1: ELF Seismic Criteria.

| Seismic Criteria | Symbol | Value | Units |
|---|---|---|---|
| Importance Factor | $I$ | 1 | -- |
| Short Period Design Acceleration | $S_{DS}$ | 1 | g |
| One Second Period Design Acceleration | $S_{D1}$ | 0.6 | g |
| Distribution Exponent | $k$ | 1.95 | -- |
| Seismic Response Coefficient | $C_S$ | 0.044 | -- |
| Effective Seismic Weight | $W$ | 28,254 | kip |
| Base Shear | $V$ | 1,243 | kip |

Table A.1.2: Equivalent Lateral Forces and Moments.

| Story x | Elevation $h_x$ | Story Weight $w_x$ | $w_x h_x^k$ | $w_x h_x^k / \sum w_x h_x^k$ | $F_x$ | $M_x$ |
|---|---|---|---|---|---|---|
| -- | ft | kip | kip-ft | -- | kips | kip-ft |
| 20 | 262 | 1,338 | 71,248,037 | 0.130 | 161 | 42,308 |
| 19 | 249 | 1,416 | 68,262,801 | 0.124 | 155 | 38,524 |
| 18 | 236 | 1,416 | 61,471,163 | 0.112 | 139 | 32,880 |
| 17 | 223 | 1,416 | 55,027,445 | 0.100 | 125 | 27,812 |
| 16 | 210 | 1,416 | 48,932,549 | 0.089 | 111 | 23,290 |
| 15 | 197 | 1,416 | 43,187,431 | 0.079 | 98 | 19,283 |
| 14 | 184 | 1,416 | 37,793,113 | 0.069 | 86 | 15,761 |
| 13 | 171 | 1,416 | 32,750,690 | 0.060 | 74 | 12,693 |
| 12 | 158 | 1,416 | 28,061,342 | 0.051 | 64 | 10,049 |
| 11 | 145 | 1,416 | 23,726,344 | 0.043 | 54 | 7,797 |
| 10 | 132 | 1,416 | 19,747,089 | 0.036 | 45 | 5,908 |
| 9 | 119 | 1,416 | 16,125,106 | 0.029 | 37 | 4,349 |
| 8 | 106 | 1,416 | 12,862,092 | 0.023 | 29 | 3,090 |
| 7 | 93 | 1,416 | 9,959,950 | 0.018 | 23 | 2,099 |
| 6 | 80 | 1,416 | 7,420,847 | 0.014 | 17 | 1,346 |
| 5 | 67 | 1,416 | 5,247,293 | 0.010 | 12 | 797 |
| 4 | 54 | 1,416 | 3,442,275 | 0.006 | 8 | 421 |

| | | | | | | |
|---|---|---|---|---|---|---|
| 3 | 41 | 1,416 | 2,009,465 | 0.004 | 5 | 187 |
| 2 | 28 | 1,416 | 953,635 | 0.002 | 2 | 61 |
| 1 | 15 | 1,428 | 283,972 | 0.001 | 1 | 10 |
| Total | | 28,254 | 548,512,639 | 1 | **1,243** | **248,662** |

## A.2 Wind Loading Summary

Table A.2.1: Wind Loading Directional Procedure Criteria.

| Seismic Criteria | Symbol | Value | Units |
|---|---|---|---|
| Wind Loading Direction | -- | North - South | -- |
| Risk Category | -- | II | -- |
| Basic Wind Speed* | $V$ | 110 | mph |
| Exposure Category | -- | B | -- |
| Enclosure Classification | -- | Enclosed | -- |
| Wind Directionality Factor | $k_d$ | 0.85 | -- |
| Topographic Factor | $K_{zt}$ | 1 | -- |
| Gust Effect Factor | $G$ | 0.937 | -- |
| Fundamental Natural Frequency | $n_1$ | 0.218 | Hz |
| Damping Ratio | $\delta$ | 0.05 | -- |

* Note: according to the wind provisions in ASCE 7-10 Los Angeles is located in a “Special Wind Region”. The basic wind speed used herein is assumed to be the wind speed predominantly found throughout the rest of California.

Table A.2.2: Wind Forces and Moments in the North – South Direction.

| Story x | Elevation $h_x$ | Tributary Wind Area per Story $A_x$ | Total Net Wind Pressure* | Story Force $F_x$ | Overturning Moment $M_x$ |
|---|---|---|---|---|---|
| -- | ft | kip | psf | kip | kip-ft |
| 20 | 262 | 910 | 39.1 | 35.5 | 9,314 |
| 19 | 249 | 1,820 | 38.8 | 70.6 | 17,576 |
| 18 | 236 | 1,820 | 38.4 | 69.9 | 16,494 |
| 17 | 223 | 1,820 | 38.0 | 69.2 | 15,423 |
| 16 | 210 | 1,820 | 37.6 | 68.4 | 14,364 |
| 15 | 197 | 1,820 | 37.1 | 67.6 | 13,319 |
| 14 | 184 | 1,820 | 36.7 | 66.8 | 12,287 |
| 13 | 171 | 1,820 | 36.2 | 65.9 | 11,269 |
| 12 | 158 | 1,820 | 35.7 | 65.0 | 10,267 |
| 11 | 145 | 1,820 | 35.2 | 64.0 | 9,280 |
| 10 | 132 | 1,820 | 34.6 | 63.0 | 8,310 |

| | | | | | |
|---|---|---|---|---|---|
| 9 | 119 | 1,820 | 34.0 | 61.8 | 7,359 |
| 8 | 106 | 1,820 | 33.3 | 60.6 | 6,426 |
| 7 | 93 | 1,820 | 32.6 | 59.3 | 5,515 |
| 6 | 80 | 1,820 | 31.8 | 57.8 | 4,627 |
| 5 | 67 | 1,820 | 30.9 | 56.2 | 3,765 |
| 4 | 54 | 1,820 | 29.8 | 54.3 | 2,933 |
| 3 | 41 | 1,820 | 28.6 | 52.1 | 2,134 |
| 2 | 28 | 1,820 | 27.0 | 49.2 | 1,378 |
| 1 | 15 | 1,960 | 25.1 | 49.3 | 739 |
| 0 | 0 | 1,050 | 24.8 | 26.1 | 0 |
| Total | | | | **1,233** | **172,779** |

* Note: the total net wind pressure is the summation of the average leeward and windward pressure over the tributary area of each story.

APPENDIX B

GROUND MOTIONS

## B.1 Ground Motion Summary

The ground motions used in this study are selected based on the following criteria:

Table B.1.1: Ground motion selection criteria.

| Ground Motion Characteristics | Value | Units |
|---|---|---|
| Moment Magnitude | 6.5 - 8 | |
| Source Distance | 0 - 30 | km |
| Site Class | D | |
| Average Soil Shear Wave Velocity | 183-365 | m/s |

Table B.1.2: Ground motion table heading description.

| Title | Description |
|---|---|
| Number | Ground motion number in set. There are 106 ground motions. |
| NGA # | Unique number assigned to each ground record by PEER. |
| Event | Name of the earthquake event |
| Station | The name of the station where the ground motion was recorded |
| Year | The year the earthquake event took place |
| Mag. | The moment magnitude of the earthquake event |
| Mech. | Type of Fault Mechanism. Available mechanisms are:<br>1: Strike-Slip,<br>2: Normal,<br>3: Normal-Oblique,<br>4: Reverse,<br>5: Reverse-Oblique. |
| Pulse | Binary code to indicate if the unscaled ground motions have a velocity pulse.<br>0: No pulse like record<br>1: Pulse like record |
| Tp (sec) | Period of the velocity pulse. |
| D5-95 (sec) | Significant duration, the time needed to build up between 5 and 95 percent of the Arias intensity |
| Rjb (km) | Joyner-Boore distance to rupture plane |
| Rrup (km) | Closest distance to rupture plane |
| $V_{s30}$ (m/s) | Average shear velocity in the upper 30 meters of sediments |
| Lowest Usable Frequency (Hz) | The recommended lowest usable frequency for analysis due to record filtering. |
| Highest Usable Frequency (Hz) | The recommended highest usable frequency for analysis due to record filtering. |

Table B.1.3: Ground motions and their characteristics.
Note: The * indicates that there are 3 total acceleration records from the same monitoring station.

| Number | NGA # | Event | Station | Year | Mag. | Lowest Usable Frequency (Hz) | Highest Usable Frequency (Hz) |
|---|---|---|---|---|---|---|---|
| 1 | 68 | San Fernando | LA - Hollywood Stor FF | 1971 | 6.61 | 0.25 | 35 |
| 2 | 158 | Imperial Valley | Aeropuerto Mexicali | 1979 | 6.53 | 0.06 | |
| 3 | 159 | Imperial Valley | Agrarias | 1979 | 6.53 | 0.06 | |
| 4 | 160 | Imperial Valley | Bonds Corner | 1979 | 6.53 | 0.12 | 40 |
| 5 | 161 | Imperial Valley | Brawley Airport | 1979 | 6.53 | 0.12 | 40 |
| 6 | 162 | Imperial Valley | Calexico Fire Station | 1979 | 6.53 | 0.25 | 40 |
| 7 | 163 | Imperial Valley | Calipatria Fire Station | 1979 | 6.53 | 0.12 | 40 |
| 8 | 165 | Imperial Valley | Chihuahua | 1979 | 6.53 | 0.06 | |
| 9 | 167 | Imperial Valley | Compuertas | 1979 | 6.53 | 0.25 | |
| 10 | 169 | Imperial Valley | Delta | 1979 | 6.53 | 0.06 | |
| 11 | 170 | Imperial Valley | EC County Center FF | 1979 | 6.53 | 0.12 | 40 |
| 12 | 171 | Imperial Valley | EC Meloland Overpass FF | 1979 | 6.53 | 0.12 | 40 |
| 13 | 172 | Imperial Valley | El Centro Array #1 | 1979 | 6.53 | 0.12 | 40 |
| 14 | 173 | Imperial Valley | El Centro Array #10 | 1979 | 6.53 | 0.12 | 40 |
| 15 | 174 | Imperial Valley | El Centro Array #11 | 1979 | 6.53 | 0.25 | 40 |
| 16 | 175 | Imperial Valley | El Centro Array #12 | 1979 | 6.53 | 0.12 | 40 |
| 17 | 176 | Imperial Valley | El Centro Array #13 | 1979 | 6.53 | 0.25 | 40 |
| 18 | 179 | Imperial Valley | El Centro Array #4 | 1979 | 6.53 | 0.12 | 40 |
| 19 | 180 | Imperial Valley | El Centro Array #5 | 1979 | 6.53 | 0.12 | 40 |
| 20 | 181 | Imperial Valley | El Centro Array #6 | 1979 | 6.53 | 0.12 | 40 |
| 21 | 182 | Imperial Valley | El Centro Array #7 | 1979 | 6.53 | 0.12 | 40 |
| 22 | 183 | Imperial Valley | El Centro Array #8 | 1979 | 6.53 | 0.12 | 40 |
| 23 | 184 | Imperial Valley | El Centro Differential Array | 1979 | 6.53 | 0.12 | 40 |
| 24 | 185 | Imperial Valley | Holtville Post Office | 1979 | 6.53 | 0.12 | 40 |
| 25 | 187 | Imperial Valley | Parachute Test Site | 1979 | 6.53 | 0.12 | 40 |
| 26 | 189 | Imperial Valley | SAHOP Casa Flores | 1979 | 6.53 | 0.25 | |
| 27 | 190 | Imperial Valley | Superstition Mtn Camera | 1979 | 6.53 | 0.12 | 40 |
| 28 | 192 | Imperial Valley | Westmorland Fire Sta | 1979 | 6.53 | 0.12 | 40 |
| 29 | 290 | Irpinia, Italy | Mercato San Severino | 1980 | 6.9 | 0.38 | 30 |
| 30 | 721 | Superstition Hills | El Centro Imp. Co. Cent | 1987 | 6.54 | 0.12 | 40 |
| 31 | 728 | Superstition Hills | Westmorland Fire Sta | 1987 | 6.54 | 0.12 | 35 |
| 32 | 729 | Superstition Hills | Wildlife Liquef. Array | 1987 | 6.54 | 0.12 | 50 |
| 33 | 730 | Spitak, Armenia | Gukasian | 1988 | 6.77 | 0.62 | 25 |
| 34 | 737 | Loma Prieta | Agnews State Hospital | 1989 | 6.93 | 0.25 | 30 |
| 35 | 752 | Loma Prieta | Capitola | 1989 | 6.93 | 0.25 | 48 |

Table B.1.3 (continued): Ground motions and their characteristics.

| Number | NGA # | Event | Station | Year | Mag. | Lowest Usable Frequency (Hz) | Highest Usable Frequency (Hz) |
|---|---|---|---|---|---|---|---|
| 36 | 754 | Loma Prieta | Coyote Lake Dam (Downst) | 1989 | 6.93 | 0.12 | 30 |
| 37 | 764 | Loma Prieta | Gilroy - Historic Bldg. | 1989 | 6.93 | 0.25 | 38 |
| 38 | 766 | Loma Prieta | Gilroy Array #2 | 1989 | 6.93 | 0.25 | 40 |
| 39 | 767 | Loma Prieta | Gilroy Array #3 | 1989 | 6.93 | 0.12 | 33 |
| 40 | 768 | Loma Prieta | Gilroy Array #4 | 1989 | 6.93 | 0.25 | 28 |
| 41 | 770 | Loma Prieta | Gilroy Array #7 | 1989 | 6.93 | 0.25 | 40 |
| 42* | 778 | Loma Prieta | Hollister Diff. Array | 1989 | 6.93 | 0.12 | 40 |
| 43 | 806 | Loma Prieta | Sunnyvale - Colton Ave. | 1989 | 6.93 | 0.12 | 40 |
| 44 | 821 | Erzican, Turkey | Erzincan | 1992 | 6.69 | 0.12 | |
| 45 | 829 | Cape Mendocino | Rio Dell Overpass - FF | 1992 | 7.01 | 0.07 | 23 |
| 46 | 850 | Landers | Desert Hot Springs | 1992 | 7.28 | 0.07 | 23 |
| 47 | 880 | Landers | Mission Creek Fault | 1992 | 7.28 | 0.11 | |
| 48 | 881 | Landers | Morongo Valley | 1992 | 7.28 | 0.28 | |
| 49 | 882 | Landers | North Palm Springs | 1992 | 7.28 | 0.28 | |
| 50 | 900 | Landers | Yermo Fire Station | 1992 | 7.28 | 0.07 | 23 |
| 51 | 949 | Northridge | Arleta - Nordhoff Fire Sta | 1994 | 6.69 | 0.12 | 23 |
| 52 | 953 | Northridge | Beverly Hills - 14145 Mulhol | 1994 | 6.69 | 0.25 | 30 |
| 53 | 959 | Northridge | Canoga Park - Topanga Can | 1994 | 6.69 | 0.06 | 30 |
| 54 | 960 | Northridge | Canyon Country - W Lost Cany | 1994 | 6.69 | 0.12 | 30 |
| 55 | 978 | Northridge | Hollywood - Willoughby Ave | 1994 | 6.69 | 0.16 | 30 |
| 56 | 985 | Northridge | LA - Baldwin Hills | 1994 | 6.69 | 0.16 | 23 |
| 57 | 987 | Northridge | LA - Centinela St | 1994 | 6.69 | 0.25 | 30 |
| 58 | 988 | Northridge | LA - Century City CC North | 1994 | 6.69 | 0.14 | 23 |
| 59 | 995 | Northridge | LA - Hollywood Stor FF | 1994 | 6.69 | 0.2 | 23 |
| 60 | 998 | Northridge | LA - N Westmoreland | 1994 | 6.69 | 0.25 | 30 |
| 61 | 1003 | Northridge | LA - Saturn St | 1994 | 6.69 | 0.12 | 30 |
| 62 | 1044 | Northridge | Newhall - Fire Sta | 1994 | 6.69 | 0.12 | 23 |
| 63 | 1045 | Northridge | Newhall - W Pico Canyon Rd. | 1994 | 6.69 | 0.12 | 30 |
| 64 | 1063 | Northridge | Rinaldi Receiving Sta | 1994 | 6.69 | 0.11 | 30 |
| 65 | 1077 | Northridge | Santa Monica City Hall | 1994 | 6.69 | 0.14 | 23 |
| 66 | 1082 | Northridge | Sun Valley - Roscoe Blvd | 1994 | 6.69 | 0.12 | 30 |
| 67 | 1084 | Northridge | Sylmar - Converter Sta | 1994 | 6.69 | 0.41 | |
| 68 | 1087 | Northridge | Tarzana - Cedar Hill A | 1994 | 6.69 | 0.1 | 23 |
| 69 | 1106 | Kobe, Japan | KJMA | 1995 | 6.9 | 0.06 | |
| 70 | 1107 | Kobe, Japan | Kakogawa | 1995 | 6.9 | 0.12 | |

Table B.1.3 (continued): Ground motions and their characteristics.

| Number | NGA # | Event | Station | Year | Mag. | Lowest Usable Frequency (Hz) | Highest Usable Frequency (Hz) |
|---|---|---|---|---|---|---|---|
| 71 | 1113 | Kobe, Japan | OSAJ | 1995 | 6.9 | 0.06 | |
| 72 | 1116 | Kobe, Japan | Shin-Osaka | 1995 | 6.9 | 0.12 | 23 |
| 73 | 1119 | Kobe, Japan | Takarazuka | 1995 | 6.9 | 0.36 | 40 |
| 74 | 1120 | Kobe, Japan | Takatori | 1995 | 6.9 | 0.36 | |
| 75 | 1158 | Kocaeli, Turkey | Duzce | 1999 | 7.51 | 0.24 | 20 |
| 76 | 1176 | Kocaeli, Turkey | Yarimca | 1999 | 7.51 | 0.09 | 50 |
| 77 | 1180 | Chi-Chi, Taiwan | CHY002 | 1999 | 7.62 | 0.04 | 50 |
| 78 | 1194 | Chi-Chi, Taiwan | CHY025 | 1999 | 7.62 | 0.06 | 50 |
| 79 | 1195 | Chi-Chi, Taiwan | CHY026 | 1999 | 7.62 | 0.05 | 33 |
| 80 | 1203 | Chi-Chi, Taiwan | CHY036 | 1999 | 7.62 | 0.06 | 50 |
| 81 | 1209 | Chi-Chi, Taiwan | CHY047 | 1999 | 7.62 | 0.04 | 50 |
| 82 | 1238 | Chi-Chi, Taiwan | CHY092 | 1999 | 7.62 | 0.06 | 24 |
| 83 | 1244 | Chi-Chi, Taiwan | CHY101 | 1999 | 7.62 | 0.05 | 50 |
| 84 | 1246 | Chi-Chi, Taiwan | CHY104 | 1999 | 7.62 | 0.06 | 50 |
| 85 | 1481 | Chi-Chi, Taiwan | TCU038 | 1999 | 7.62 | 0.06 | 50 |
| 86 | 1483 | Chi-Chi, Taiwan | TCU040 | 1999 | 7.62 | 0.04 | 50 |
| 87 | 1498 | Chi-Chi, Taiwan | TCU059 | 1999 | 7.62 | 0.04 | 30 |
| 88 | 1500 | Chi-Chi, Taiwan | TCU061 | 1999 | 7.62 | 0.05 | 50 |
| 89 | 1502 | Chi-Chi, Taiwan | TCU064 | 1999 | 7.62 | 0.04 | 50 |
| 90 | 1503 | Chi-Chi, Taiwan | TCU065 | 1999 | 7.62 | 0.07 | 50 |
| 91 | 1513 | Chi-Chi, Taiwan | TCU079 | 1999 | 7.62 | 0.25 | 50 |
| 92 | 1536 | Chi-Chi, Taiwan | TCU110 | 1999 | 7.62 | 0.05 | 50 |
| 93 | 1537 | Chi-Chi, Taiwan | TCU111 | 1999 | 7.62 | 0.05 | 50 |
| 94 | 1538 | Chi-Chi, Taiwan | TCU112 | 1999 | 7.62 | 0.06 | 40 |
| 95 | 1540 | Chi-Chi, Taiwan | TCU115 | 1999 | 7.62 | 0.06 | 50 |
| 96 | 1542 | Chi-Chi, Taiwan | TCU117 | 1999 | 7.62 | 0.04 | 50 |
| 97 | 1543 | Chi-Chi, Taiwan | TCU118 | 1999 | 7.62 | 0.06 | 50 |
| 98 | 1547 | Chi-Chi, Taiwan | TCU123 | 1999 | 7.62 | 0.05 | 50 |
| 99 | 1553 | Chi-Chi, Taiwan | TCU141 | 1999 | 7.62 | 0.06 | 50 |
| 100 | 1602 | Duzce, Turkey | Bolu | 1999 | 7.14 | 0.06 | |
| 101 | 1605 | Duzce, Turkey | Duzce | 1999 | 7.14 | 0.1 | 50 |
| 102* | 1615 | Duzce, Turkey | Lamont 1062 | 1999 | 7.14 | 0.06 | 50 |

Table B.1.4: Reno ground motions and their characteristics.

| Number | NGA # | Event | Station | Year | Mag. | Lowest Usable Frequency (Hz) | Highest Usable Frequency (Hz) |
|---|---|---|---|---|---|---|---|
| 1 | 68 | San Fernando | LA - Hollywood Stor FF | 1971 | 6.61 | 0.25 | 35 |
| 2 | 125 | Friuli- Italy | Tolmezzo | 1976 | 6.5 | 0.125 | 30 |
| 3 | 169 | Imperial Valley | Delta | 1979 | 6.53 | 0.0625 | |
| 4 | 174 | Imperial Valley | El Centro Array #11 | 1979 | 6.53 | 0.25 | 40 |
| 5 | 721 | Superstition Hills | El Centro Imp. Co. Cent | 1987 | 6.54 | 0.125 | 40 |
| 6 | 752 | Loma Prieta | Capitola | 1989 | 6.93 | 0.25 | 48 |
| 7 | 767 | Loma Prieta | Gilroy Array #3 | 1989 | 6.93 | 0.125 | 33 |
| 8 | 829 | Cape Mendocino | Rio Dell Overpass - FF | 1992 | 7.01 | 0.07 | 23 |
| 9 | 848 | Landers | Coolwater | 1992 | | 0.125 | 30 |
| 10 | 900 | Landers | Yermo Fire Station | 1992 | 7.28 | 0.07 | 23 |
| 11 | 953 | Northridge | Beverly Hills - 14145 Mulhol | 1994 | 6.69 | 0.1625 | 30 |
| 12 | 960 | Northridge | Canyon Country - W Lost Cany | 1994 | 6.69 | 0.0625 | 30 |
| 13 | 1111 | Kobe- Japan | Nishi-Akashi | 1995 | 6.9 | 0.125 | 23 |
| 14 | 1116 | Kobe- Japan | Shin-Osaka | 1995 | 6.9 | 0.125 | 23 |
| 15 | 1148 | Kocaeli- Turkey | Arcelik | 1999 | 7.51 | 0.0875 | 50 |
| 16 | 1158 | Kocaeli- Turkey | Duzce | 1999 | 7.51 | 0.237 | 20 |
| 17 | 1244 | Chi-Chi- Taiwan | CHY101 | 1999 | 7.62 | 0.0375 | 50 |
| 18 | 1485 | Chi-Chi- Taiwan | TCU045 | 1999 | | 0.025 | 50 |
| 19 | 1602 | Duzce- Turkey | Bolu | 1999 | 7.14 | 0.0625 | |
| 20 | 1633 | Manjil, Iran | Abbar | 1990 | | 0.13 | 20 |
| 21 | 1787 | Hector Mine | Hector | 1999 | 7.13 | 0.025 | 53 |

APPENDIX C

N-S SEISMC FRAME, GRAVITY BEAMS & COLUMN DESIGN

## C.1 Perimeter Frame Design Summary

Table C.1.1: Interior Left Girders of N-S Frame Final Design and Checks.

| Floor | Section | $M_{u,max}$ (kip-in) | $V_{u,max}$ (kip) | Flexure | Shear | Flexure ≤ 1 Shear ≤ 1 |
|---|---|---|---|---|---|---|
| 20 | W27X146 | 1,495 | 10.4 | 0.072 | 0.023 | OK |
| 19 | W27X94 | 1,791 | 14.5 | 0.143 | 0.039 | OK |
| 18 | W27X94 | 2,350 | 19.5 | 0.188 | 0.052 | OK |
| 17 | W27X94 | 2,372 | 20.5 | 0.190 | 0.055 | OK |
| 16 | W33X221 | 4,176 | 35.0 | 0.108 | 0.048 | OK |
| 15 | W33X221 | 4,303 | 34.8 | 0.112 | 0.048 | OK |
| 14 | W33X221 | 4,568 | 36.7 | 0.118 | 0.050 | OK |
| 13 | W33X221 | 4,873 | 40.7 | 0.126 | 0.056 | OK |
| 12 | W33X221 | 5,393 | 45.7 | 0.140 | 0.063 | OK |
| 11 | W27X194 | 4,756 | 41.5 | 0.167 | 0.073 | OK |
| 10 | W27X194 | 5,259 | 46.2 | 0.185 | 0.081 | OK |
| 9 | W27X194 | 5,809 | 50.7 | 0.205 | 0.089 | OK |
| 8 | W27X194 | 6,097 | 53.1 | 0.215 | 0.093 | OK |
| 7 | W27X194 | 6,181 | 54.0 | 0.218 | 0.094 | OK |
| 6 | W27X194 | 5,849 | 51.0 | 0.206 | 0.089 | OK |
| 5 | W33X291 | 8,398 | 71.1 | 0.161 | 0.079 | OK |
| 4 | W33X291 | 8,059 | 69.0 | 0.154 | 0.076 | OK |
| 3 | W33X291 | 8,029 | 69.8 | 0.154 | 0.077 | OK |
| 2 | W33X291 | 7,715 | 67.8 | 0.148 | 0.075 | OK |
| 1 | W33X291 | 6,358 | 55.7 | 0.122 | 0.062 | OK |

Table C.1.2: Interior Right Girders of N-S Frame Final Design and Checks.

| Floor | Section | $M_{u,max}$ (kip-in) | $V_{u,max}$ (kip) | Flexure | Shear | Flexure ≤ 1 Shear ≤ 1 |
|---|---|---|---|---|---|---|
| 20 | W27X146 | 788 | 42 | 0.038 | 0.090 | OK |
| 19 | W27X94 | 1,592 | 51 | 0.127 | 0.138 | OK |
| 18 | W27X94 | 2,649 | 75 | 0.212 | 0.202 | OK |
| 17 | W27X94 | 3,064 | 80 | 0.245 | 0.214 | OK |
| 16 | W33X221 | 3,650 | 85 | 0.095 | 0.116 | OK |
| 15 | W33X221 | 3,833 | 86 | 0.099 | 0.118 | OK |
| 14 | W33X221 | 4,591 | 102 | 0.119 | 0.140 | OK |
| 13 | W33X221 | 4,768 | 100 | 0.124 | 0.137 | OK |
| 12 | W33X221 | 5,295 | 102 | 0.137 | 0.140 | OK |
| 11 | W27X194 | 5,740 | 102 | 0.202 | 0.179 | OK |
| 10 | W27X194 | 6,464 | 107 | 0.228 | 0.188 | OK |
| 9 | W27X194 | 6,533 | 106 | 0.230 | 0.185 | OK |
| 8 | W27X194 | 7,568 | 115 | 0.267 | 0.201 | OK |
| 7 | W27X194 | 7,908 | 113 | 0.278 | 0.197 | OK |
| 6 | W27X194 | 8,554 | 115 | 0.301 | 0.201 | OK |
| 5 | W33X291 | 9,070 | 117 | 0.174 | 0.129 | OK |
| 4 | W33X291 | 9,955 | 124 | 0.191 | 0.137 | OK |
| 3 | W33X291 | 10,272 | 128 | 0.197 | 0.142 | OK |
| 2 | W33X291 | 10,446 | 130 | 0.200 | 0.144 | OK |
| 1 | W33X291 | 8,508 | 111 | 0.163 | 0.123 | OK |

Table C.1.3: Exterior Left Girders of N-S Frame Final Design and Checks.

| Floor | Section | $M_{u,max}$ (kip-in) | $V_{u,max}$ (kip) | Flexure | Shear | Flexure ≤ 1 Shear ≤ 1 |
|---|---|---|---|---|---|---|
| 20 | W27X146 | 1,541 | 14 | 0.074 | 0.031 | OK |
| 19 | W27X94 | 1,842 | 17 | 0.147 | 0.045 | OK |
| 18 | W27X94 | 2,273 | 21 | 0.182 | 0.056 | OK |
| 17 | W27X94 | 2,575 | 24 | 0.206 | 0.065 | OK |
| 16 | W33X221 | 5,132 | 50 | 0.133 | 0.068 | OK |
| 15 | W33X221 | 4,874 | 47 | 0.126 | 0.065 | OK |
| 14 | W33X221 | 4,990 | 48 | 0.129 | 0.066 | OK |
| 13 | W33X221 | 5,628 | 55 | 0.146 | 0.075 | OK |
| 12 | W33X221 | 6,185 | 60 | 0.160 | 0.082 | OK |
| 11 | W27X194 | 5,246 | 51 | 0.185 | 0.088 | OK |
| 10 | W27X194 | 5,692 | 55 | 0.200 | 0.096 | OK |
| 9 | W27X194 | 5,904 | 57 | 0.208 | 0.099 | OK |
| 8 | W27X194 | 6,039 | 58 | 0.213 | 0.102 | OK |
| 7 | W27X194 | 6,049 | 58 | 0.213 | 0.102 | OK |
| 6 | W27X194 | 5,696 | 55 | 0.201 | 0.096 | OK |
| 5 | W33X291 | 8,007 | 78 | 0.153 | 0.086 | OK |
| 4 | W33X291 | 7,464 | 73 | 0.143 | 0.081 | OK |
| 3 | W33X291 | 7,478 | 73 | 0.143 | 0.081 | OK |
| 2 | W33X291 | 6,960 | 68 | 0.133 | 0.075 | OK |
| 1 | W33X291 | 5,410 | 53 | 0.104 | 0.058 | OK |

Table C.1.4: Exterior Right Girders of N-S Frame Final Design and Checks.

| Floor | Section | $M_{u,max}$ (kip-in) | $V_{u,max}$ (kip) | Flexure | Shear | Flexure ≤ 1 Shear ≤ 1 |
|---|---|---|---|---|---|---|
| 20 | W27X146 | 18,500 | 235 | 0.886 | 0.509 | OK |
| 19 | W27X94 | 7,082 | 129 | 0.566 | 0.344 | OK |
| 18 | W27X94 | 6,464 | 107 | 0.517 | 0.287 | OK |
| 17 | W27X94 | -1,872 | 29 | -0.150 | 0.077 | OK |
| 16 | W33X221 | -1,337 | 21 | -0.035 | 0.028 | OK |
| 15 | W33X221 | -1,328 | 21 | -0.034 | 0.028 | OK |
| 14 | W33X221 | 3,196 | 56 | 0.083 | 0.077 | OK |
| 13 | W33X221 | 23,775 | 279 | 0.616 | 0.383 | OK |
| 12 | W33X221 | 10,734 | 131 | 0.278 | 0.180 | OK |
| 11 | W27X194 | 24,626 | 280 | 0.867 | 0.489 | OK |
| 10 | W27X194 | 3,189 | 74 | 0.112 | 0.129 | OK |
| 9 | W27X194 | 26,362 | 294 | 0.928 | 0.514 | OK |
| 8 | W27X194 | 11,347 | 150 | 0.400 | 0.262 | OK |
| 7 | W27X194 | 9,070 | 117 | 0.319 | 0.204 | OK |
| 6 | W27X194 | -832 | 20 | -0.029 | 0.034 | OK |
| 5 | W33X291 | -594 | 14 | -0.011 | 0.016 | OK |
| 4 | W33X291 | -375 | 12 | -0.007 | 0.013 | OK |
| 3 | W33X291 | 5,340 | 67 | 0.102 | 0.074 | OK |
| 2 | W33X291 | 31,221 | 344 | 0.598 | 0.381 | OK |
| 1 | W33X291 | 14,236 | 160 | 0.273 | 0.177 | OK |

Table C.1.5: Girders of N-S Frame Seismic Compactness Checks.

| Floor | Section | $\frac{1}{2}\frac{b_f}{t_f}$ | Flange Thickness Ratio Flexure $\leq 7.22$ | $\frac{h}{t_w}$ | Web Thickness Ratio $\leq 59$ | $\frac{h}{t_w}$ | Web Thickness Ratio Shear $\leq 53.95$ |
|---|---|---|---|---|---|---|---|
| 20 | W27X146 | 7.16 | OK | 19.70 | OK | 19.70 | OK |
| 19 | W27X94 | 6.70 | OK | 24.75 | OK | 24.75 | OK |
| 18 | W27X94 | 6.70 | OK | 24.75 | OK | 24.75 | OK |
| 17 | W27X94 | 6.70 | OK | 24.75 | OK | 24.75 | OK |
| 16 | W33X221 | 6.20 | OK | 19.25 | OK | 19.25 | OK |
| 15 | W33X221 | 6.20 | OK | 19.25 | OK | 19.25 | OK |
| 14 | W33X221 | 6.20 | OK | 19.25 | OK | 19.25 | OK |
| 13 | W33X221 | 6.20 | OK | 19.25 | OK | 19.25 | OK |
| 12 | W33X221 | 6.20 | OK | 19.25 | OK | 19.25 | OK |
| 11 | W27X194 | 5.24 | OK | 15.90 | OK | 15.90 | OK |
| 10 | W27X194 | 5.24 | OK | 15.90 | OK | 15.90 | OK |
| 9 | W27X194 | 5.24 | OK | 15.90 | OK | 15.90 | OK |
| 8 | W27X194 | 5.24 | OK | 15.90 | OK | 15.90 | OK |
| 7 | W27X194 | 5.24 | OK | 15.90 | OK | 15.90 | OK |
| 6 | W27X194 | 5.24 | OK | 15.90 | OK | 15.90 | OK |
| 5 | W33X291 | 4.60 | OK | 15.50 | OK | 15.50 | OK |
| 4 | W33X291 | 4.60 | OK | 15.50 | OK | 15.50 | OK |
| 3 | W33X291 | 4.60 | OK | 15.50 | OK | 15.50 | OK |
| 2 | W33X291 | 4.60 | OK | 15.50 | OK | 15.50 | OK |
| 1 | W33X291 | 4.60 | OK | 15.50 | OK | 15.50 | OK |

Table C.1.6: N-S Frame Drift Limit Check.

| Floor | Floor Drift | Drift Limit | Drift Check $\leq 0.02$ |
|---|---|---|---|
| 20 | 0.0108 | 0.02 | OK |
| 19 | 0.0140 | 0.02 | OK |
| 18 | 0.0155 | 0.02 | OK |
| 17 | 0.0140 | 0.02 | OK |
| 16 | 0.0129 | 0.02 | OK |
| 15 | 0.0129 | 0.02 | OK |
| 14 | 0.0132 | 0.02 | OK |
| 13 | 0.0136 | 0.02 | OK |
| 12 | 0.0149 | 0.02 | OK |
| 11 | 0.0162 | 0.02 | OK |
| 10 | 0.0168 | 0.02 | OK |
| 9 | 0.0170 | 0.02 | OK |
| 8 | 0.0170 | 0.02 | OK |
| 7 | 0.0164 | 0.02 | OK |
| 6 | 0.0145 | 0.02 | OK |
| 5 | 0.0121 | 0.02 | OK |
| 4 | 0.0114 | 0.02 | OK |
| 3 | 0.0107 | 0.02 | OK |
| 2 | 0.0094 | 0.02 | OK |
| 1 | 0.0055 | 0.02 | OK |

Table C.1.7: RBS Design Coefficients and Factored Moments and Shear.

| Floor | Section | a (in) | b (in) | c (in) | $M_{u,RBS}$ (kip-in) | $V_{u,RBS}$ (kip) | $M_{u,f}$ (kip-in) |
|---|---|---|---|---|---|---|---|
| 20 | W27X146 | 8.75 | 20.55 | 3.50 | 1,806 | 218 | 22,097 |
| 19 | W27X94 | 6.25 | 20.18 | 2.50 | 2,101 | 136 | 13,635 |
| 18 | W27X94 | 6.25 | 20.18 | 2.50 | 2,539 | 136 | 13,643 |
| 17 | W27X94 | 6.25 | 20.18 | 2.50 | 2,859 | 174 | 14,259 |
| 16 | W33X221 | 9.88 | 25.43 | 3.95 | 5,243 | 649 | 47,991 |
| 15 | W33X221 | 9.88 | 25.43 | 3.95 | 4,947 | 525 | 45,208 |
| 14 | W33X221 | 9.88 | 25.43 | 3.95 | 5,064 | 675 | 48,584 |
| 13 | W33X221 | 9.88 | 25.43 | 3.95 | 5,685 | 466 | 43,864 |
| 12 | W33X221 | 9.88 | 25.43 | 3.95 | 6,169 | 677 | 48,631 |
| 11 | W27X194 | 8.75 | 21.08 | 3.50 | 5,408 | 403 | 31,814 |
| 10 | W27X194 | 8.75 | 21.08 | 3.50 | 5,825 | 373 | 31,236 |
| 9 | W27X194 | 8.75 | 21.08 | 3.50 | 6,005 | 305 | 29,916 |
| 8 | W27X194 | 8.75 | 21.08 | 3.50 | 6,143 | 302 | 29,855 |
| 7 | W27X194 | 8.75 | 21.08 | 3.50 | 6,155 | 303 | 29,886 |
| 6 | W27X194 | 8.75 | 21.08 | 3.50 | 5,809 | 339 | 30,578 |
| 5 | W33X291 | 9.94 | 26.10 | 3.98 | 7,731 | 878 | 64,776 |
| 4 | W33X291 | 9.94 | 26.10 | 3.98 | 7,212 | 711 | 60,944 |
| 3 | W33X291 | 9.94 | 26.10 | 3.98 | 7,392 | 892 | 65,097 |
| 2 | W33X291 | 9.94 | 26.10 | 3.98 | 6,927 | 619 | 58,826 |
| 1 | W33X291 | 9.94 | 26.10 | 3.98 | 5,474 | 896 | 65,201 |

Table C.1.8: Demand to Capacity Ratios for the Column Face Moment, Shear and Moment at Center of RBS.

| Floor | $\frac{M_{u,f}}{M_p}$ | $\frac{M_{u,f}}{M_p} \leq 1$ | $\frac{V_{u,RBS}}{V_{n,RBS}}$ | $\frac{V_{u,RBS}}{V_{n,RBS}} \leq 1$ | $\frac{M_{u,RBS}}{M_{p,RBS}}$ | $\frac{M_{u,RBS}}{M_{p,RBS}} \leq 1$ |
|---|---|---|---|---|---|---|
| 20 | 0.87 | OK | 0.47 | OK | 0.29 | OK |
| 19 | 0.89 | OK | 0.36 | OK | 0.33 | OK |
| 18 | 0.89 | OK | 0.36 | OK | 0.33 | OK |
| 17 | 0.93 | OK | 0.47 | OK | 0.32 | OK |
| 16 | 1.02 | OK* | 0.89 | OK | 0.81 | OK |
| 15 | 0.96 | OK | 0.72 | OK | 0.36 | OK |
| 14 | 1.03 | OK* | 0.93 | OK | 0.89 | OK |
| 13 | 0.93 | OK | 0.64 | OK | 0.22 | OK |
| 12 | 1.03 | OK* | 0.93 | OK | 0.90 | OK |
| 11 | 0.92 | OK | 0.71 | OK | 0.47 | OK |
| 10 | 0.90 | OK | 0.65 | OK | 0.44 | OK |
| 9 | 0.86 | OK | 0.53 | OK | 0.32 | OK |
| 8 | 0.86 | OK | 0.53 | OK | 0.32 | OK |
| 7 | 0.86 | OK | 0.53 | OK | 0.32 | OK |
| 6 | 0.88 | OK | 0.59 | OK | 0.31 | OK |
| 5 | 1.02 | OK* | 0.97 | OK | 0.90 | OK |
| 4 | 0.96 | OK | 0.79 | OK | 0.40 | OK |
| 3 | 1.02 | OK* | 0.99 | OK | 0.94 | OK |
| 2 | 0.92 | OK | 0.69 | OK | 0.20 | OK |
| 1 | 1.02 | OK* | 0.99 | OK | 0.94 | OK |

* Note: The demand to capacity ratio is slightly exceeded however it is acceptable by common engineering practice.

Table C.1.9: Exterior Column Factored Axial Force, Moment and Governing Axial & Moment Interaction Equation from the AISC Steel Construction Manual.

| Floor | Section | $P_u$ | $M_u$ | EQ H1-1a/b | H1-1a/b ≤1 |
|---|---|---|---|---|---|
| 20 | W36X160 | 77 | 690 | 0.044 | OK |
| 19 | W36X160 | 155 | 1,368 | 0.089 | OK |
| 18 | W36X160 | 236 | 2,475 | 0.136 | OK |
| 17 | W36X160 | 316 | 3,003 | 0.182 | OK |
| 16 | W36X160 | 408 | 2,555 | 0.230 | OK |
| 15 | W36X210 | 499 | 2,746 | 0.211 | OK |
| 14 | W36X210 | 590 | 2,965 | 0.250 | OK |
| 13 | W36X210 | 684 | 2,804 | 0.290 | OK |
| 12 | W36X210 | 782 | 2,560 | 0.331 | OK |
| 11 | W36X210 | 878 | 3,249 | 0.378 | OK |
| 10 | W36X210 | 978 | 3,654 | 0.421 | OK |
| 9 | W36X256 | 1,084 | 4,222 | 0.379 | OK |
| 8 | W36X256 | 1,191 | 4,606 | 0.416 | OK |
| 7 | W36X256 | 1,299 | 5,277 | 0.454 | OK |
| 6 | W36X256 | 1,405 | 6,849 | 0.491 | OK |
| 5 | W36X361 | 1,529 | 6,029 | 0.345 | OK |
| 4 | W36X361 | 1,645 | 5,866 | 0.371 | OK |
| 3 | W36X361 | 1,763 | 6,118 | 0.397 | OK |
| 2 | W36X361 | 1,880 | 7,451 | 0.424 | OK |
| 1 | W36X361 | 1,987 | 13,599 | 0.462 | OK |

Table C.1.10: Exterior Column Final Factored Axial Force with Overstrength Consideration.

| Floor | Section | $P_u$ | $\frac{P_u}{P_c}$ | $\frac{P_u}{P_c} \leq 1$ |
|---|---|---|---|---|
| 20 | W36X160 | 92 | 0.053 | OK |
| 19 | W36X160 | 192 | 0.110 | OK |
| 18 | W36X160 | 303 | 0.174 | OK |
| 17 | W36X160 | 413 | 0.237 | OK |
| 16 | W36X160 | 561 | 0.316 | OK |
| 15 | W36X210 | 704 | 0.298 | OK |
| 14 | W36X210 | 850 | 0.360 | OK |
| 13 | W36X210 | 1,002 | 0.424 | OK |
| 12 | W36X210 | 1,168 | 0.495 | OK |
| 11 | W36X210 | 1,324 | 0.570 | OK |
| 10 | W36X210 | 1,493 | 0.643 | OK |
| 9 | W36X256 | 1,675 | 0.585 | OK |
| 8 | W36X256 | 1,864 | 0.651 | OK |
| 7 | W36X256 | 2,055 | 0.718 | OK |
| 6 | W36X256 | 2,239 | 0.782 | OK |
| 5 | W36X361 | 2,476 | 0.558 | OK |
| 4 | W36X361 | 2,703 | 0.609 | OK |
| 3 | W36X361 | 2,929 | 0.660 | OK |
| 2 | W36X361 | 3,151 | 0.710 | OK |
| 1 | W36X361 | 3,344 | 0.778 | OK |

Table C.1.11: Exterior Column Seismic Compactness Checks

| Floor | Section | $\frac{1}{2}\frac{b_f}{t_f}$ | Flange Thickness Ratio Flexure $\leq 7.22$ | $\frac{h}{t_w}$ | $\frac{h}{t_w}$ Limit | Web Thickness Ratio $\leq$ Limit |
|---|---|---|---|---|---|---|
| 20 | W36X160 | 5.88 | OK | 49.9 | 57.0 | OK |
| 19 | W36X160 | 5.88 | OK | 49.9 | 55.0 | OK |
| 18 | W36X160 | 5.88 | OK | 49.9 | 52.9 | OK |
| 17 | W36X160 | 5.88 | OK | 49.9 | 51.6 | OK |
| 16 | W36X160 | 5.88 | OK | 49.9 | 50.8 | OK |
| 15 | W36X210 | 4.49 | OK | 39.1 | 51.0 | OK |
| 14 | W36X210 | 4.49 | OK | 39.1 | 50.4 | OK |
| 13 | W36X210 | 4.49 | OK | 39.1 | 49.8 | OK |
| 12 | W36X210 | 4.49 | OK | 39.1 | 49.1 | OK |
| 11 | W36X210 | 4.49 | OK | 39.1 | 48.5 | OK |
| 10 | W36X210 | 4.49 | OK | 39.1 | 47.8 | OK |
| 9 | W36X256 | 3.53 | OK | 33.8 | 48.4 | OK |
| 8 | W36X256 | 3.53 | OK | 33.8 | 47.8 | OK |
| 7 | W36X256 | 3.53 | OK | 33.8 | 47.2 | OK |
| 6 | W36X256 | 3.53 | OK | 33.8 | 46.7 | OK |
| 5 | W36X361 | 4.15 | OK | 28.6 | 48.4 | OK |
| 4 | W36X361 | 4.15 | OK | 28.6 | 47.9 | OK |
| 3 | W36X361 | 4.15 | OK | 28.6 | 47.5 | OK |
| 2 | W36X361 | 4.15 | OK | 28.6 | 47.0 | OK |
| 1 | W36X361 | 4.15 | OK | 28.6 | 46.6 | OK |

Table C.1.12: Strong Column Weak Beam Check for Exterior Columns.

| Floor | Section | $\sum M_{pc}^{*}$ | $\sum M_{pb}^{*}$ | SCWB Ratio | Check > 1 |
|---|---|---|---|---|---|
| 19 | W36X160 | 69,252 | 16,170 | 4.28 | OK |
| 18 | W36X160 | 65,683 | 16,019 | 4.10 | OK |
| 17 | W36X160 | 62,149 | 16,033 | 3.88 | OK |
| 16 | W36X160 | 60,702 | 50,413 | 1.20 | OK |
| 15 | W36X210 | 82,164 | 50,672 | 1.62 | OK |
| 14 | W36X210 | 77,168 | 50,790 | 1.52 | OK |
| 13 | W36X210 | 71,913 | 50,740 | 1.42 | OK |
| 12 | W36X210 | 66,203 | 50,699 | 1.31 | OK |
| 11 | W36X210 | 58,064 | 35,100 | 1.65 | OK |
| 10 | W36X210 | 52,502 | 35,121 | 1.49 | OK |
| 9 | W36X256 | 70,481 | 35,300 | 2.00 | OK |
| 8 | W36X256 | 64,138 | 35,296 | 1.82 | OK |
| 7 | W36X256 | 57,715 | 35,374 | 1.63 | OK |
| 6 | W36X256 | 51,529 | 35,469 | 1.45 | OK |
| 5 | W36X361 | 106,306 | 69,001 | 1.54 | OK |
| 4 | W36X361 | 97,765 | 69,087 | 1.42 | OK |
| 3 | W36X361 | 89,232 | 69,077 | 1.29 | OK |
| 2 | W36X361 | 80,894 | 69,073 | 1.17 | OK |
| 1 | W36X361 | 70,932 | 69,062 | 1.03 | OK |

Table C.1.13: Interior Column Factored Axial Force, Moment and Governing Axial & Moment Interaction Equation from the AISC Steel Construction Manual.

| Floor | Section | $P_u$ | $M_u$ | EQ H1-1a/b | H1-1a/b ≤1 |
|---|---|---|---|---|---|
| 20 | W36X150 | 86 | 733 | 0.052 | OK |
| 19 | W36X150 | 171 | 2,080 | 0.105 | OK |
| 18 | W36X150 | 256 | 3,349 | 0.157 | OK |
| 17 | W36X282 | 343 | 6,166 | 0.100 | OK |
| 16 | W36X282 | 442 | 5,090 | 0.128 | OK |
| 15 | W36X282 | 537 | 4,733 | 0.155 | OK |
| 14 | W36X282 | 632 | 5,114 | 0.183 | OK |
| 13 | W36X330 | 729 | 5,356 | 0.180 | OK |
| 12 | W36X330 | 824 | 4,715 | 0.203 | OK |
| 11 | W36X330 | 913 | 5,854 | 0.227 | OK |
| 10 | W36X330 | 1,001 | 6,676 | 0.249 | OK |
| 9 | W36X330 | 1,084 | 6,898 | 0.269 | OK |
| 8 | W36X330 | 1,167 | 7,522 | 0.290 | OK |
| 7 | W36X330 | 1,249 | 8,355 | 0.310 | OK |
| 6 | W36X330 | 1,330 | 10,652 | 0.331 | OK |
| 5 | W36X395 | 1,411 | 9,148 | 0.290 | OK |
| 4 | W36X395 | 1,487 | 8,934 | 0.306 | OK |
| 3 | W36X441 | 1,570 | 9,780 | 0.288 | OK |
| 2 | W36X441 | 1,652 | 10,931 | 0.303 | OK |
| 1 | W36X441 | 1,731 | 17,334 | 0.327 | OK |

Table C.1.14: Interior Column Final Factored Axial Force with Overstrength Consideration.

| Floor | Section | $P_u$ | $\frac{P_u}{P_c}$ | $\frac{P_u}{P_c} \leq 1$ |
|---|---|---|---|---|
| 20 | W36X150 | 90 | 0.055 | OK |
| 19 | W36X150 | 175 | 0.107 | OK |
| 18 | W36X150 | 258 | 0.158 | OK |
| 17 | W36X282 | 346 | 0.101 | OK |
| 16 | W36X282 | 469 | 0.136 | OK |
| 15 | W36X282 | 583 | 0.168 | OK |
| 14 | W36X282 | 693 | 0.200 | OK |
| 13 | W36X330 | 811 | 0.200 | OK |
| 12 | W36X330 | 927 | 0.229 | OK |
| 11 | W36X330 | 1,025 | 0.255 | OK |
| 10 | W36X330 | 1,121 | 0.279 | OK |
| 9 | W36X330 | 1,207 | 0.300 | OK |
| 8 | W36X330 | 1,290 | 0.321 | OK |
| 7 | W36X330 | 1,371 | 0.341 | OK |
| 6 | W36X330 | 1,450 | 0.360 | OK |
| 5 | W36X395 | 1,533 | 0.315 | OK |
| 4 | W36X395 | 1,613 | 0.332 | OK |
| 3 | W36X441 | 1,696 | 0.311 | OK |
| 2 | W36X441 | 1,772 | 0.325 | OK |
| 1 | W36X441 | 1,839 | 0.348 | OK |

Table C.1.15: Interior Column Seismic Compactness Checks

| Floor | Section | $\frac{1}{2}\frac{b_f}{t_f}$ | Flange Thickness Ratio Flexure ≤ 7.22 | $\frac{h}{t_w}$ | $\frac{h}{t_w}$ Limit | Web Thickness Ratio ≤ Limit |
|---|---|---|---|---|---|---|
| 20 | W36X150 | 6.38 | 51.9 | 56.6 | 46.6 | OK |
| 19 | W36X150 | 6.38 | 51.9 | 54.3 | 47.0 | OK |
| 18 | W36X150 | 6.38 | 51.9 | 52.0 | 47.5 | OK |
| 17 | W36X282 | 5.29 | 36.2 | 54.0 | 47.9 | OK |
| 16 | W36X282 | 5.29 | 36.2 | 52.5 | 48.4 | OK |
| 15 | W36X282 | 5.29 | 36.2 | 51.7 | 46.7 | OK |
| 14 | W36X282 | 5.29 | 36.2 | 51.2 | 47.2 | OK |
| 13 | W36X330 | 4.49 | 31.4 | 51.2 | 47.8 | OK |
| 12 | W36X330 | 4.49 | 31.4 | 50.8 | 48.4 | OK |
| 11 | W36X330 | 4.49 | 31.4 | 50.5 | 47.8 | OK |
| 10 | W36X330 | 4.49 | 31.4 | 50.1 | 48.5 | OK |
| 9 | W36X330 | 4.49 | 31.4 | 49.7 | 49.1 | OK |
| 8 | W36X330 | 4.49 | 31.4 | 49.4 | 49.8 | OK |
| 7 | W36X330 | 4.49 | 31.4 | 49.0 | 50.4 | OK |
| 6 | W36X330 | 4.49 | 31.4 | 48.7 | 51.0 | OK |
| 5 | W36X395 | 3.82 | 26.3 | 49.3 | 50.8 | OK |
| 4 | W36X395 | 3.82 | 26.3 | 49.1 | 51.6 | OK |
| 3 | W36X441 | 3.48 | 23.6 | 49.4 | 52.9 | OK |
| 2 | W36X441 | 3.48 | 23.6 | 49.1 | 55.0 | OK |
| 1 | W36X441 | 3.48 | 23.6 | 48.8 | 57.0 | OK |

Table C.1.16: Strong Column Weak Beam Check for Interior Columns.

| Floor | Section | $\sum M_{pc}^{*}$ | $\sum M_{pb}^{*}$ | SCWB Ratio | Check > 1 |
|---|---|---|---|---|---|
| 19 | W36X150 | 64,646 | 32,231 | 2.01 | OK |
| 18 | W36X150 | 62,017 | 32,097 | 1.93 | OK |
| 17 | W36X282 | 131,794 | 33,485 | 3.94 | OK |
| 16 | W36X282 | 134,829 | 110,665 | 1.22 | OK |
| 15 | W36X282 | 130,672 | 105,709 | 1.24 | OK |
| 14 | W36X282 | 126,606 | 111,976 | 1.13 | OK |
| 13 | W36X330 | 150,032 | 103,458 | 1.45 | OK |
| 12 | W36X330 | 145,721 | 112,301 | 1.30 | OK |
| 11 | W36X330 | 135,617 | 74,665 | 1.82 | OK |
| 10 | W36X330 | 132,237 | 73,542 | 1.80 | OK |
| 9 | W36X330 | 129,186 | 71,007 | 1.82 | OK |
| 8 | W36X330 | 126,248 | 70,883 | 1.78 | OK |
| 7 | W36X330 | 123,380 | 71,023 | 1.74 | OK |
| 6 | W36X330 | 120,574 | 72,486 | 1.66 | OK |
| 5 | W36X395 | 161,940 | 150,436 | 1.08 | OK |
| 4 | W36X395 | 158,882 | 143,797 | 1.10 | OK |
| 3 | W36X441 | 181,710 | 151,555 | 1.20 | OK |
| 2 | W36X441 | 178,840 | 140,197 | 1.28 | OK |
| 1 | W36X441 | 169,777 | 151,955 | 1.12 | OK |

Table C.1.17: Panel Zone and Doubler Platting of Exterior Columns.

| Floor | Beam Section | Column Section | $R_u$ (kip) | $R_n$ (kip) | Doubler Plate? | Side Plate Thickness (in) | Total Plate Thickness (in) |
|---|---|---|---|---|---|---|---|
| 20 | W27X146 | W36X160 | 689 | 743 | No | 0 | 0 |
| 19 | W27X94 | W36X160 | 431 | 744 | No | 0 | 0 |
| 18 | W27X94 | W36X160 | 432 | 744 | No | 0 | 0 |
| 17 | W27X94 | W36X160 | 451 | 744 | No | 0 | 0 |
| 16 | W33X221 | W36X160 | 1,151 | 735 | Yes | 4/16 | 0.500 |
| 15 | W33X221 | W36X210 | 1,085 | 974 | Yes | 1/16 | 0.125 |
| 14 | W33X221 | W36X210 | 1,166 | 974 | Yes | 2/16 | 0.250 |
| 13 | W33X221 | W36X210 | 1,052 | 974 | Yes | 1/16 | 0.125 |
| 12 | W33X221 | W36X210 | 1,167 | 974 | Yes | 2/16 | 0.250 |
| 11 | W27X194 | W36X210 | 975 | 986 | No | 0 | 0 |
| 10 | W27X194 | W36X210 | 957 | 986 | No | 0 | 0 |
| 9 | W27X194 | W36X256 | 917 | 1,194 | No | 0 | 0 |
| 8 | W27X194 | W36X256 | 915 | 1,194 | No | 0 | 0 |
| 7 | W27X194 | W36X256 | 916 | 1,194 | No | 0 | 0 |
| 6 | W27X194 | W36X256 | 937 | 1,194 | No | 0 | 0 |
| 5 | W33X291 | W36X361 | 1,522 | 1,451 | Yes | 1/16 | 0.125 |
| 4 | W33X291 | W36X361 | 1,432 | 1,451 | No | 0 | 0 |
| 3 | W33X291 | W36X361 | 1,529 | 1,451 | Yes | 1/16 | 0.125 |
| 2 | W33X291 | W36X361 | 1,382 | 1,451 | No | 0 | 0 |
| 1 | W33X291 | W36X361 | 1,590 | 1,451 | Yes | 1/16 | 0.125 |

Table C.1.18: Panel Zone and Doubler Platting of Interior Columns.

| Floor | Beam Section | Column Section | $R_u$ (kip) | $R_n$ (kip) | Doubler Plate? | Side Plate Thickness (in) | Total Plate Thickness (in) |
|---|---|---|---|---|---|---|---|
| 20 | W27X146 | W36X150 | 1,379 | 708 | Yes | 5/16 | 0.625 |
| 19 | W27X94 | W36X150 | 863 | 709 | Yes | 2/16 | 0.250 |
| 18 | W27X94 | W36X150 | 863 | 709 | Yes | 2/16 | 0.250 |
| 17 | W27X94 | W36X282 | 902 | 1,122 | No | 0 | 0 |
| 16 | W33X221 | W36X282 | 2,303 | 1,094 | Yes | 9/16 | 1.125 |
| 15 | W33X221 | W36X282 | 2,169 | 1,094 | Yes | 8/16 | 1.000 |
| 14 | W33X221 | W36X282 | 2,331 | 1,094 | Yes | 9/16 | 1.125 |
| 13 | W33X221 | W36X330 | 2,105 | 1,304 | Yes | 6/16 | 0.750 |
| 12 | W33X221 | W36X330 | 2,334 | 1,304 | Yes | 8/16 | 1.000 |
| 11 | W27X194 | W36X330 | 1,949 | 1,336 | Yes | 5/16 | 0.625 |
| 10 | W27X194 | W36X330 | 1,914 | 1,336 | Yes | 5/16 | 0.625 |
| 9 | W27X194 | W36X330 | 1,833 | 1,336 | Yes | 4/16 | 0.500 |
| 8 | W27X194 | W36X330 | 1,829 | 1,336 | Yes | 4/16 | 0.500 |
| 7 | W27X194 | W36X330 | 1,831 | 1,336 | Yes | 4/16 | 0.500 |
| 6 | W27X194 | W36X330 | 1,874 | 1,336 | Yes | 4/16 | 0.500 |
| 5 | W33X291 | W36X395 | 3,044 | 1,616 | Yes | 10/16 | 1.250 |
| 4 | W33X291 | W36X395 | 2,864 | 1,616 | Yes | 9/16 | 1.125 |
| 3 | W33X291 | W36X441 | 3,059 | 1,849 | Yes | 9/16 | 1.125 |
| 2 | W33X291 | W36X441 | 2,764 | 1,849 | Yes | 7/16 | 0.875 |
| 1 | W33X291 | W36X441 | 3,181 | 1,849 | Yes | 10/16 | 1.250 |

Table C.1.19: Stability Coefficient Check.

| Story | **θ** | **$\theta_{max}$** | **$\theta \leq 0.10 \leq \theta_{max}$** |
|---|---|---|---|
| 20 | 0.03 | 0.25 | OK |
| 19 | 0.02 | 0.25 | OK |
| 18 | 0.02 | 0.25 | OK |
| 17 | 0.02 | 0.25 | OK |
| 16 | 0.01 | 0.25 | OK |
| 15 | 0.01 | 0.25 | OK |
| 14 | 0.01 | 0.25 | OK |
| 13 | 0.01 | 0.25 | OK |
| 12 | 0.01 | 0.25 | OK |
| 11 | 0.01 | 0.25 | OK |
| 10 | 0.01 | 0.25 | OK |
| 9 | 0.01 | 0.25 | OK |
| 8 | 0.01 | 0.25 | OK |
| 7 | 0.01 | 0.25 | OK |
| 6 | 0.01 | 0.25 | OK |
| 5 | 0.01 | 0.25 | OK |
| 4 | 0.01 | 0.25 | OK |
| 3 | 0.01 | 0.25 | OK |
| 2 | 0.01 | 0.25 | OK |
| 1 | 0.00 | 0.25 | OK |

<u>**C.2 Gravity System Design Summary**</u>

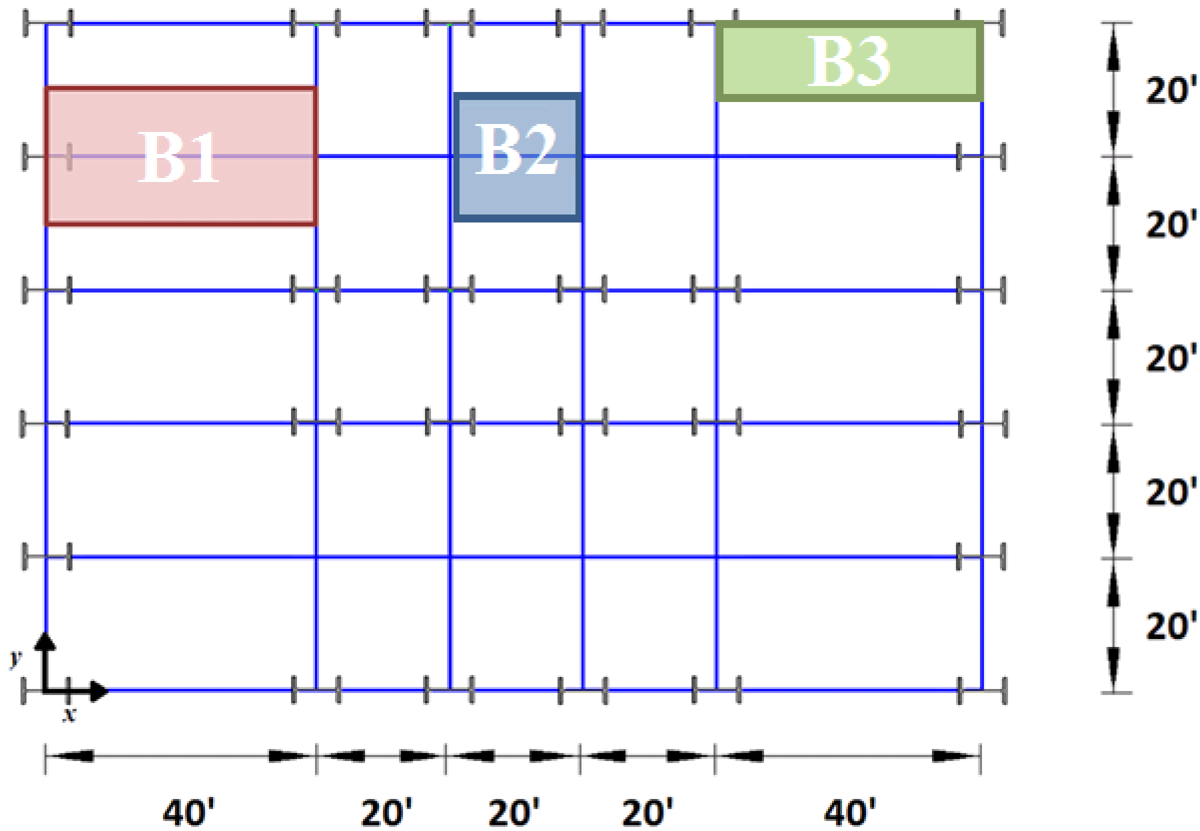


Figure C.2.1: Typical gravity beams.

Table C.2.1: Typical Composite Floor Beam Flexural, Shear and Deflection Checks.

| Gravity Beam | Section | $M_u$ (kip-ft) | $\varphi M_N$ (kip-ft) | $V_u$ (kip) | $\varphi V_N$ (kip) | Deflection (inches) | L/360 (inches) | Check Limit |
|---|---|---|---|---|---|---|---|---|
| B1 | W21X68 | 756 | 820 | 76 | 272 | 1.324 | 1.333 | OK |
| B2 | W21X68 | 200 | 820 | 40 | 272 | 0.110 | 1.333 | OK |
| B3 | W21X68 | 478 | 820 | 48 | 272 | 1.191 | 1.333 | OK |

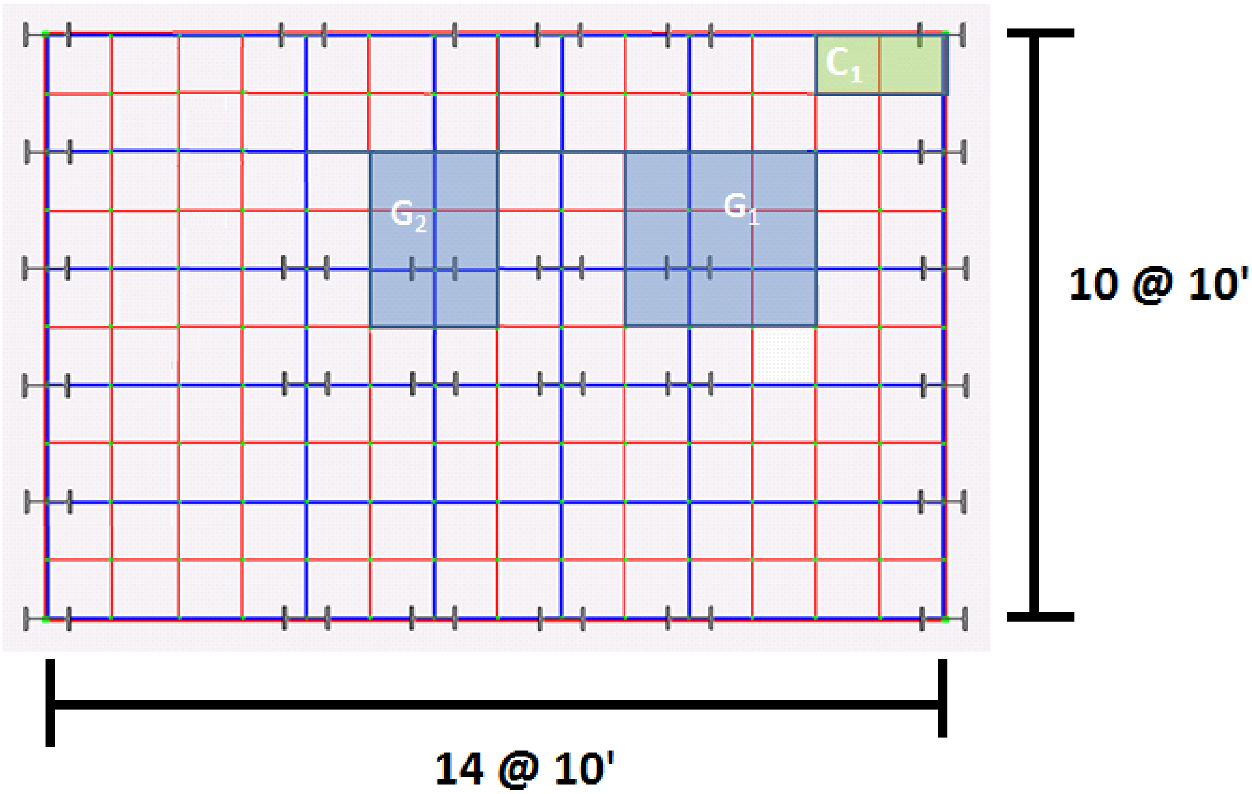


Figure C.2.2: Tributary area and location of gravity columns.

Table C.2.2: Interior Column G2 Strength Checks.

| Floor | Design $P_u$ (kips) | Section | $\frac{P_u}{\phi P_n}$ | $\frac{P_u}{\phi P_n} \leq 1$ |
|---|---|---|---|---|
| 20 | 80 | W14X48 | 0.205 | OK |
| 19 | 160 | W14X48 | 0.411 | OK |
| 18 | 240 | W14X48 | 0.616 | OK |
| 17 | 320 | W14X53 | 0.739 | OK |
| 16 | 400 | W14X53 | 0.923 | OK |
| 15 | 480 | W14X74 | 0.653 | OK |
| 14 | 560 | W14X74 | 0.762 | OK |
| 13 | 640 | W14X90 | 0.611 | OK |
| 12 | 720 | W14X90 | 0.688 | OK |
| 11 | 800 | W14X99 | 0.695 | OK |
| 10 | 880 | W14X99 | 0.765 | OK |
| 9 | 960 | W14X120 | 0.686 | OK |
| 8 | 1040 | W14X120 | 0.744 | OK |
| 7 | 1120 | W14X145 | 0.652 | OK |
| 6 | 1200 | W14X145 | 0.699 | OK |
| 5 | 1280 | W14X176 | 0.613 | OK |
| 4 | 1360 | W14X176 | 0.651 | OK |
| 3 | 1440 | W14X193 | 0.628 | OK |
| 2 | 1520 | W14X193 | 0.663 | OK |
| 1 | 1600 | W14X193 | 0.723 | OK |

Table C.2.3: Interior Column G2 Limit Checks.

| Floor | Section | $\frac{1}{2}\frac{b_f}{t_f}$ | Flange Thickness Ratio Flexure $\leq 13.49$ | $\frac{h}{t_w}$ | Web Thickness Ratio $\leq 35.9$ |
|---|---|---|---|---|---|
| 20 | W14X48 | 6.75 | OK | 33.6 | OK |
| 19 | W14X48 | 6.75 | OK | 33.6 | OK |
| 18 | W14X48 | 6.75 | OK | 33.6 | OK |
| 17 | W14X53 | 6.11 | OK | 30.9 | OK |
| 16 | W14X53 | 6.11 | OK | 30.9 | OK |
| 15 | W14X74 | 6.43 | OK | 25.4 | OK |
| 14 | W14X74 | 6.43 | OK | 25.4 | OK |
| 13 | W14X90 | 10.21 | OK | 25.9 | OK |
| 12 | W14X90 | 10.21 | OK | 25.9 | OK |
| 11 | W14X99 | 9.36 | OK | 23.5 | OK |
| 10 | W14X99 | 9.36 | OK | 23.5 | OK |
| 9 | W14X120 | 7.82 | OK | 19.3 | OK |
| 8 | W14X120 | 7.82 | OK | 19.3 | OK |
| 7 | W14X145 | 7.11 | OK | 16.8 | OK |
| 6 | W14X145 | 7.11 | OK | 16.8 | OK |
| 5 | W14X176 | 5.99 | OK | 13.7 | OK |
| 4 | W14X176 | 5.99 | OK | 13.7 | OK |
| 3 | W14X193 | 5.45 | OK | 12.8 | OK |
| 2 | W14X193 | 5.45 | OK | 12.8 | OK |
| 1 | W14X193 | 5.45 | OK | 12.8 | OK |

Table C.2.4: Corner Column C1 Strength Checks.

| Floor | Design $P_u$ (kips) | Section | $\frac{P_u}{\phi P_n}$ | $\frac{P_u}{\phi P_n} \leq 1$ |
|---|---|---|---|---|
| 20 | 51 | W14X48 | 0.13 | OK |
| 19 | 105 | W14X48 | 0.27 | OK |
| 18 | 159 | W14X48 | 0.41 | OK |
| 17 | 212 | W14X48 | 0.55 | OK |
| 16 | 266 | W14X48 | 0.68 | OK |
| 15 | 320 | W14X48 | 0.82 | OK |
| 14 | 374 | W14X48 | 0.96 | OK |
| 13 | 428 | W14X61 | 0.71 | OK |
| 12 | 482 | W14X61 | 0.80 | OK |
| 11 | 536 | W14X61 | 0.89 | OK |
| 10 | 590 | W14X61 | 0.98 | OK |
| 9 | 644 | W14X74 | 0.88 | OK |
| 8 | 698 | W14X74 | 0.95 | OK |
| 7 | 753 | W14X82 | 0.93 | OK |
| 6 | 808 | W14X82 | 1.00 | OK |
| 5 | 862 | W14X90 | 0.82 | OK |
| 4 | 912 | W14X90 | 0.87 | OK |
| 3 | 967 | W14X109 | 0.76 | OK |
| 2 | 1,022 | W14X109 | 0.81 | OK |
| 1 | 1,078 | W14X109 | 0.89 | OK |

Table C.2.5: Corner Column C1 Limit Checks.

| Floor | Section | $\frac{1}{2}\frac{b_f}{t_f}$ | Flange Thickness Ratio Flexure $\leq 13.49$ | $\frac{h}{t_w}$ | Web Thickness Ratio $\leq 35.9$ |
|---|---|---|---|---|---|
| 20 | W14X48 | 6.75 | OK | 33.6 | OK |
| 19 | W14X48 | 6.75 | OK | 33.6 | OK |
| 18 | W14X48 | 6.75 | OK | 33.6 | OK |
| 17 | W14X48 | 6.75 | OK | 33.6 | OK |
| 16 | W14X48 | 6.75 | OK | 33.6 | OK |
| 15 | W14X48 | 6.75 | OK | 33.6 | OK |
| 14 | W14X48 | 6.75 | OK | 33.6 | OK |
| 13 | W14X61 | 7.75 | OK | 30.4 | OK |
| 12 | W14X61 | 7.75 | OK | 30.4 | OK |
| 11 | W14X61 | 7.75 | OK | 30.4 | OK |
| 10 | W14X61 | 7.75 | OK | 30.4 | OK |
| 9 | W14X74 | 6.43 | OK | 25.4 | OK |
| 8 | W14X74 | 6.43 | OK | 25.4 | OK |
| 7 | W14X82 | 5.91 | OK | 22.4 | OK |
| 6 | W14X82 | 5.91 | OK | 22.4 | OK |
| 5 | W14X90 | 10.21 | OK | 25.9 | OK |
| 4 | W14X90 | 10.21 | OK | 25.9 | OK |
| 3 | W14X109 | 8.49 | OK | 21.7 | OK |
| 2 | W14X109 | 8.49 | OK | 21.7 | OK |
| 1 | W14X109 | 8.49 | OK | 21.7 | OK |

APPENDIX D

FRS CONTINUED

## D.1 FRS Figure Summary

In order of appearance:

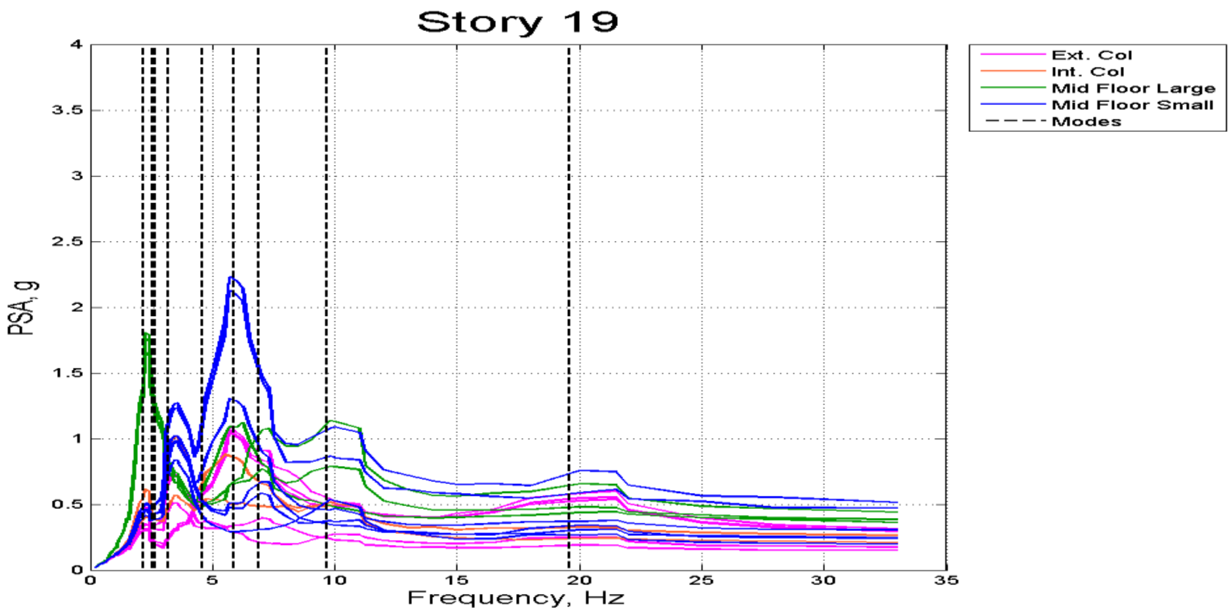
Story 19
PSA, g
Frequency, Hz
Ext. Col
Int. Col
Mid Floor Large
Mid Floor Small
Modes

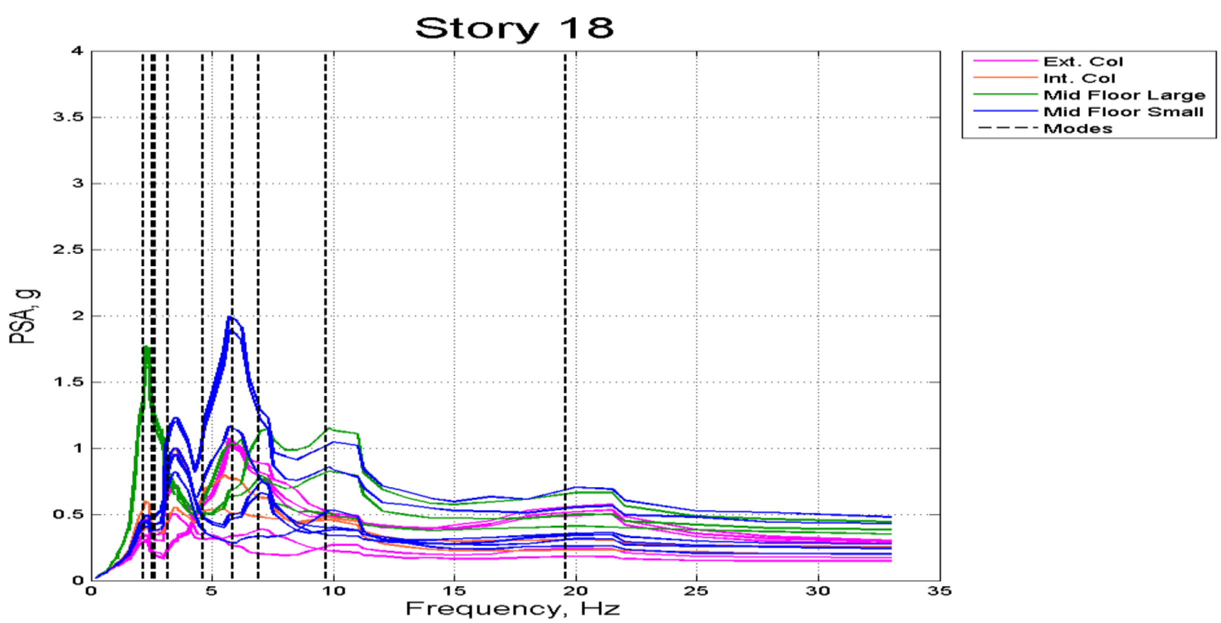
Story 18
PSA, g
Frequency, Hz
Ext. Col
Int. Col
Mid Floor Large
Mid Floor Small
Modes

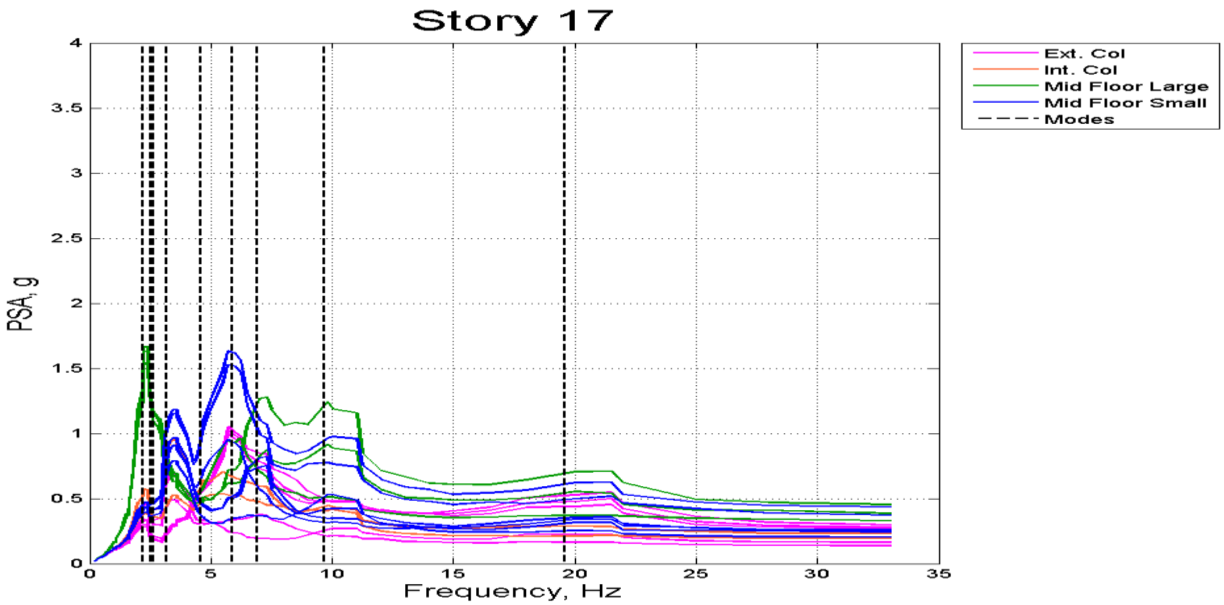
Story 17
PSA, g
Frequency, Hz
Ext. Col
Int. Col
Mid Floor Large
Mid Floor Small
Modes

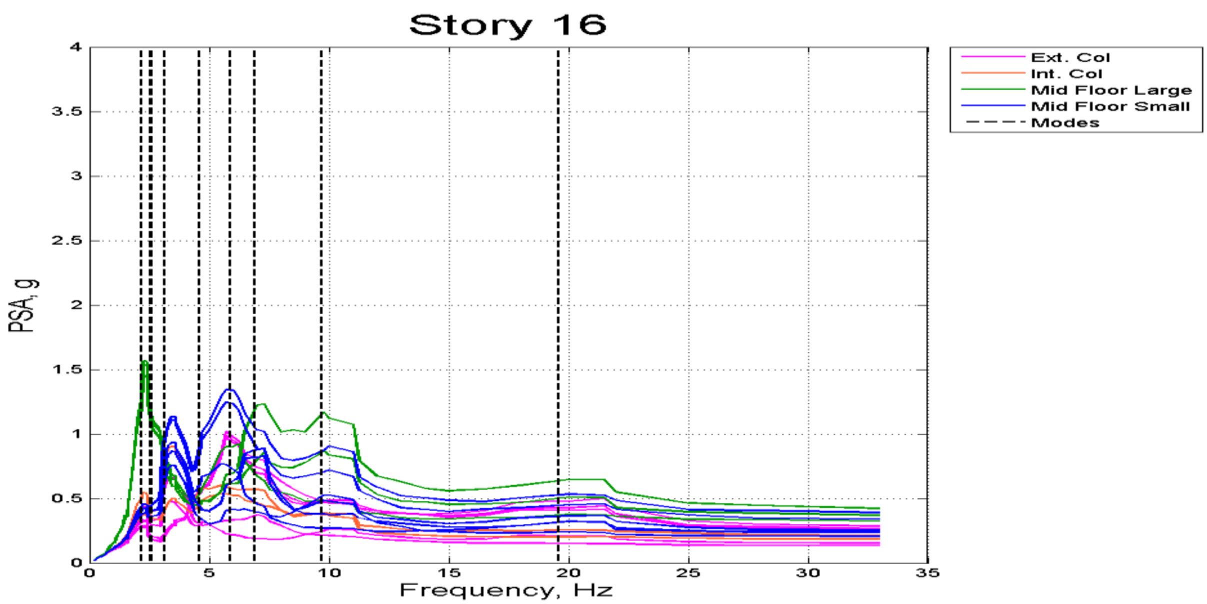
Story 16
PSA, g
Frequency, Hz
Ext. Col
Int. Col
Mid Floor Large
Mid Floor Small
Modes

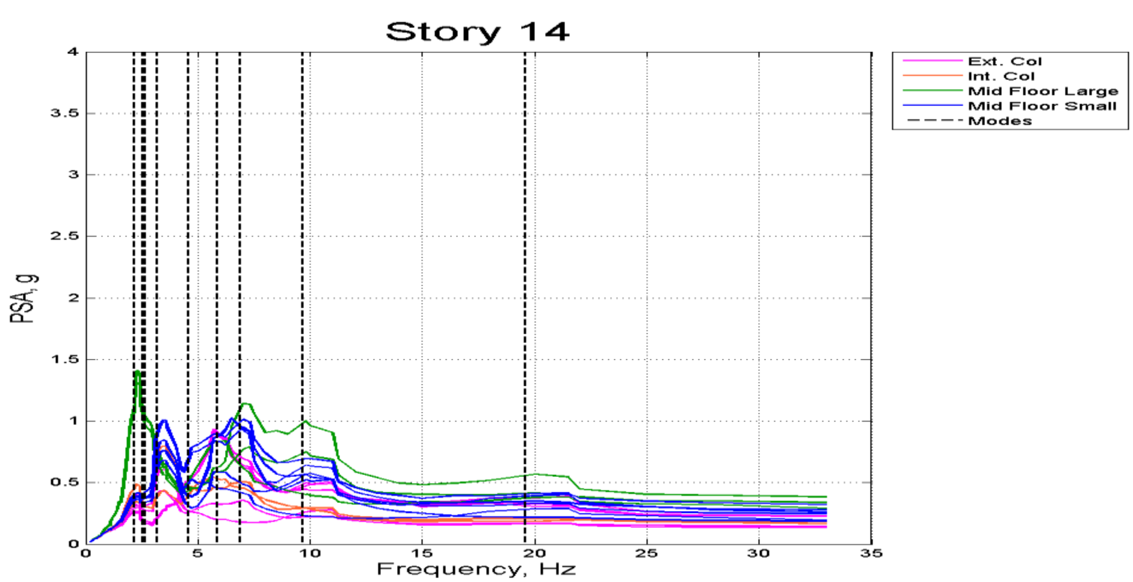
Story 14
PSA, g
Frequency, Hz
Ext. Col
Int. Col
Mid Floor Large
Mid Floor Small
Modes

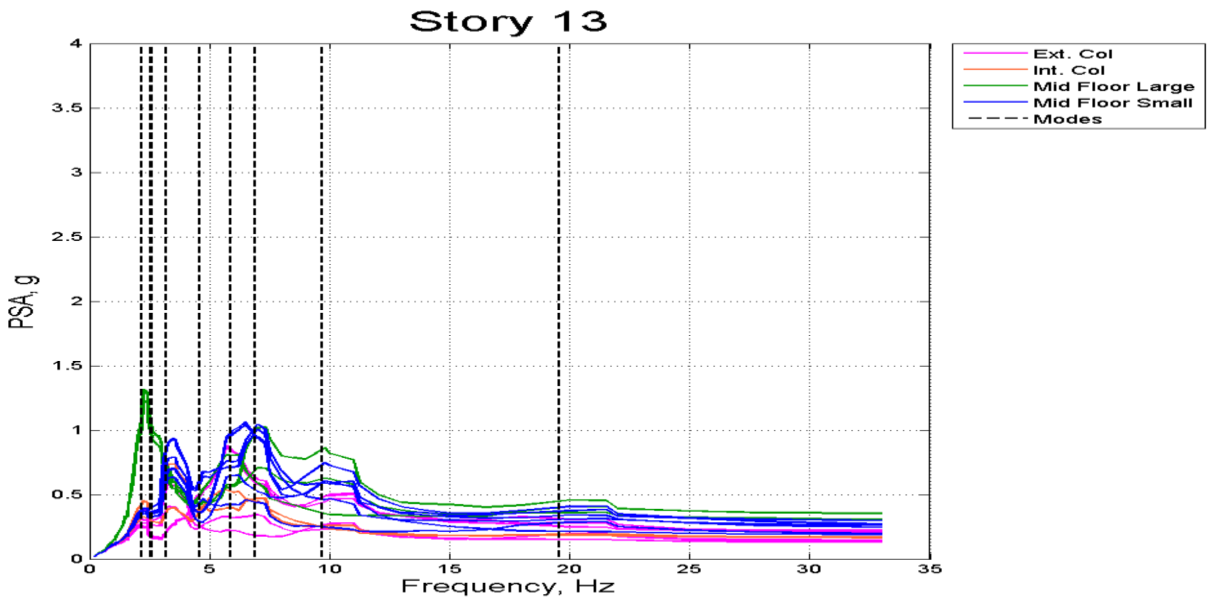

Story 13
PSA, g
Frequency, Hz
Ext. Col
Int. Col
Mid Floor Large
Mid Floor Small
Modes
0
0.5
1
1.5
2
2.5
3
3.5
4
5
10
15
20
25
30
35


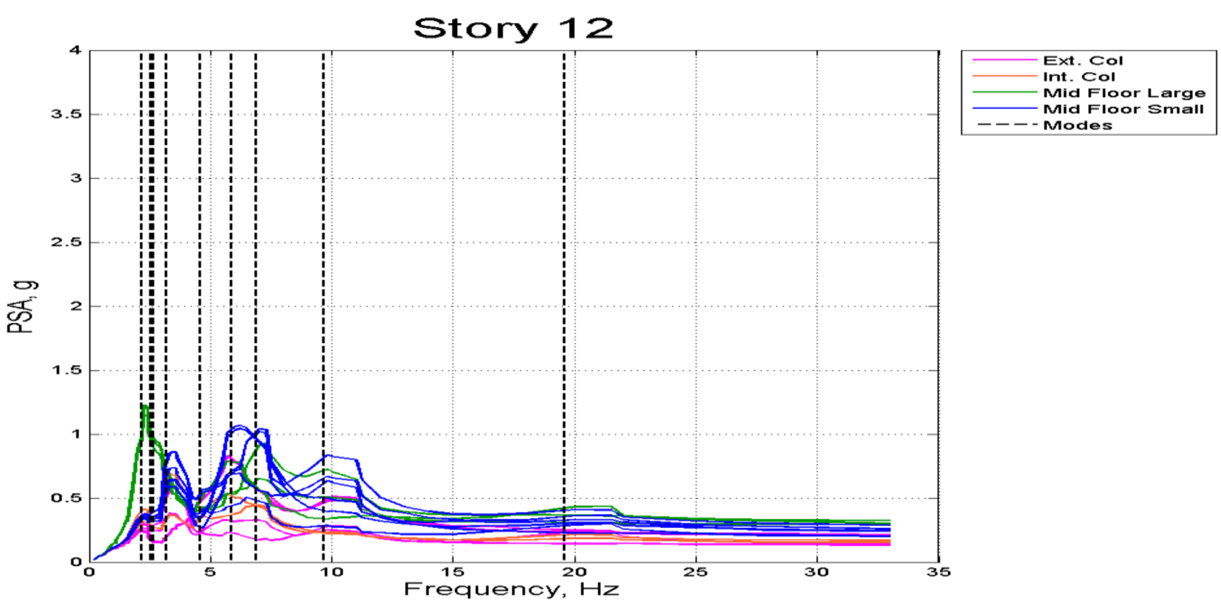

Story 12
PSA, g
Frequency, Hz
Ext. Col
Int. Col
Mid Floor Large
Mid Floor Small
Modes
0
0.5
1
1.5
2
2.5
3
3.5
4
5
10
15
20
25
30
35


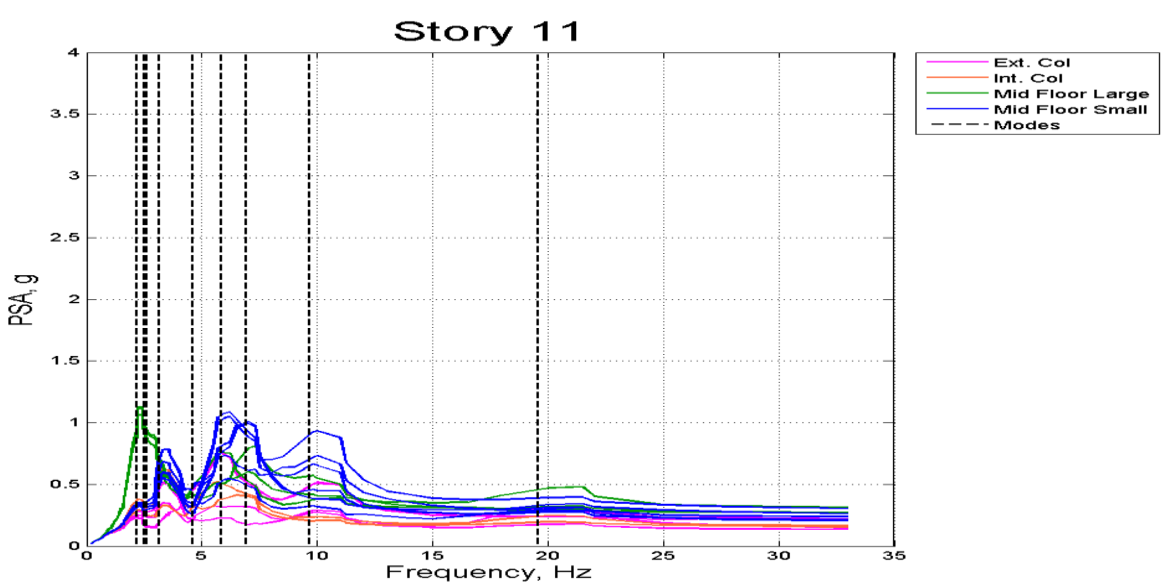

Story 11
PSA, g
Frequency, Hz
Ext. Col
Int. Col
Mid Floor Large
Mid Floor Small
Modes
0
0.5
1
1.5
2
2.5
3
3.5
4
5
10
15
20
25
30
35

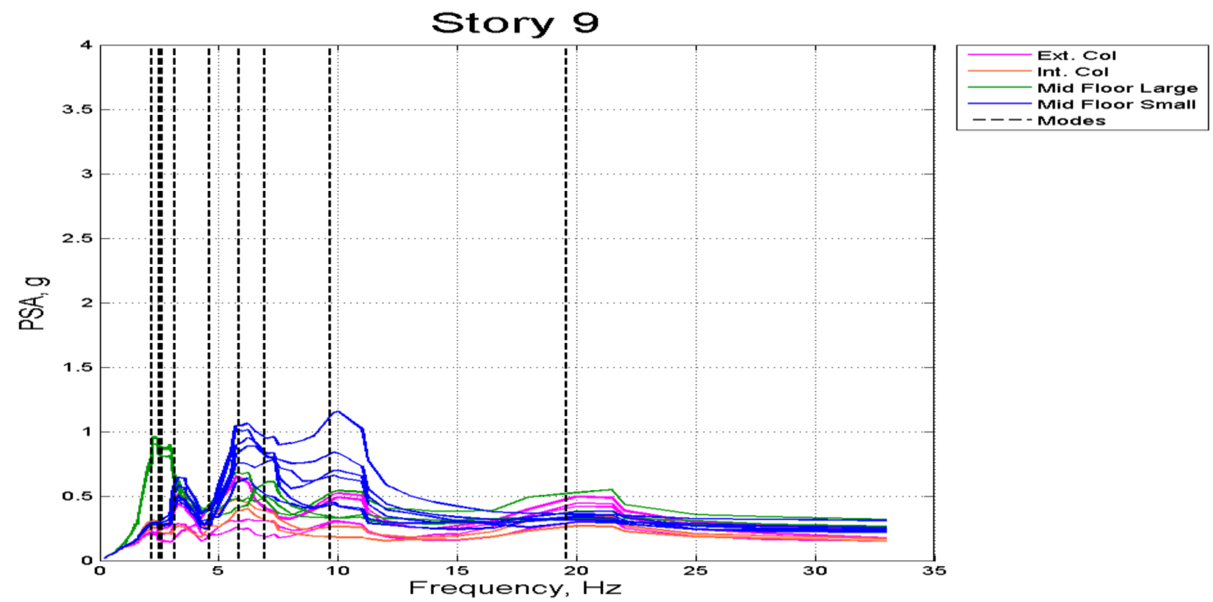

Story 9
PSA, g
Frequency, Hz
Ext. Col
Int. Col
Mid Floor Large
Mid Floor Small
Modes


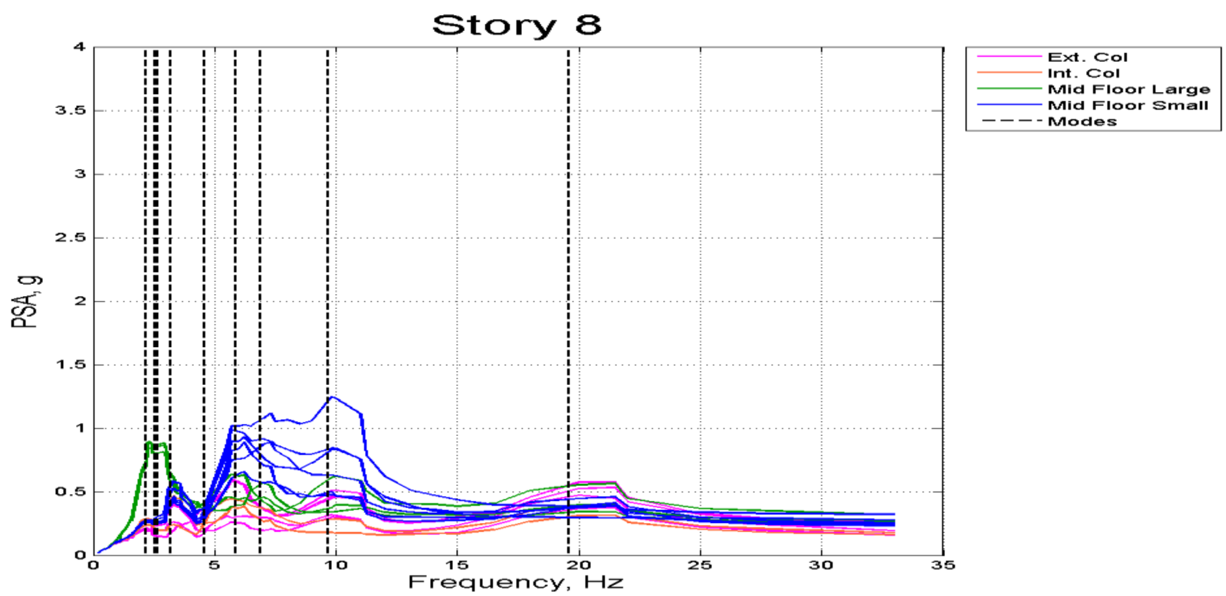

Story 8
PSA, g
Frequency, Hz
Ext. Col
Int. Col
Mid Floor Large
Mid Floor Small
Modes


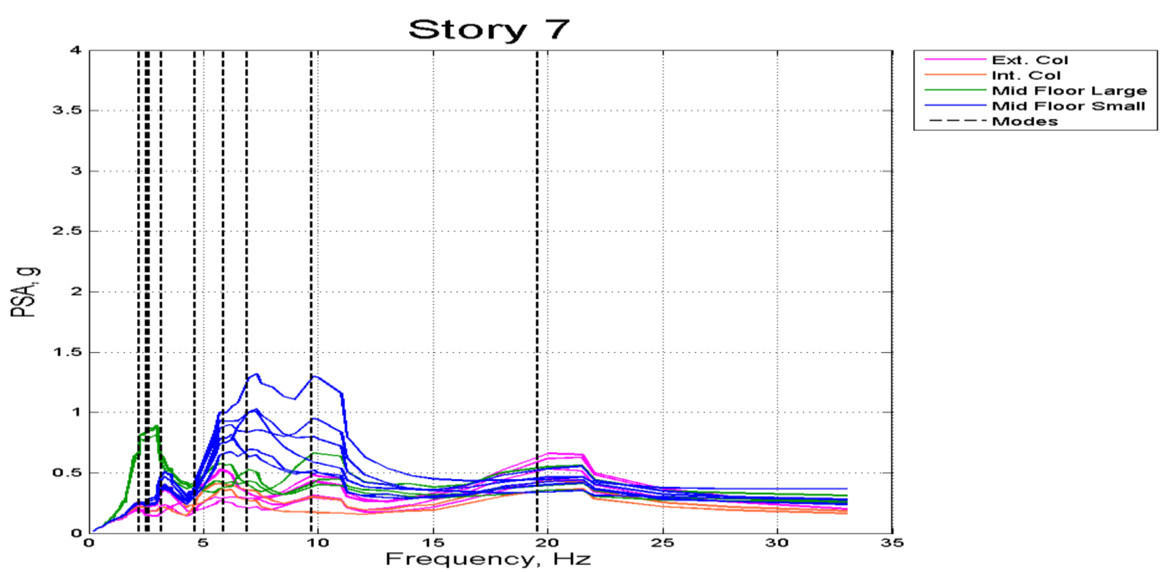

Story 7
PSA, g
Frequency, Hz
Ext. Col
Int. Col
Mid Floor Large
Mid Floor Small
Modes

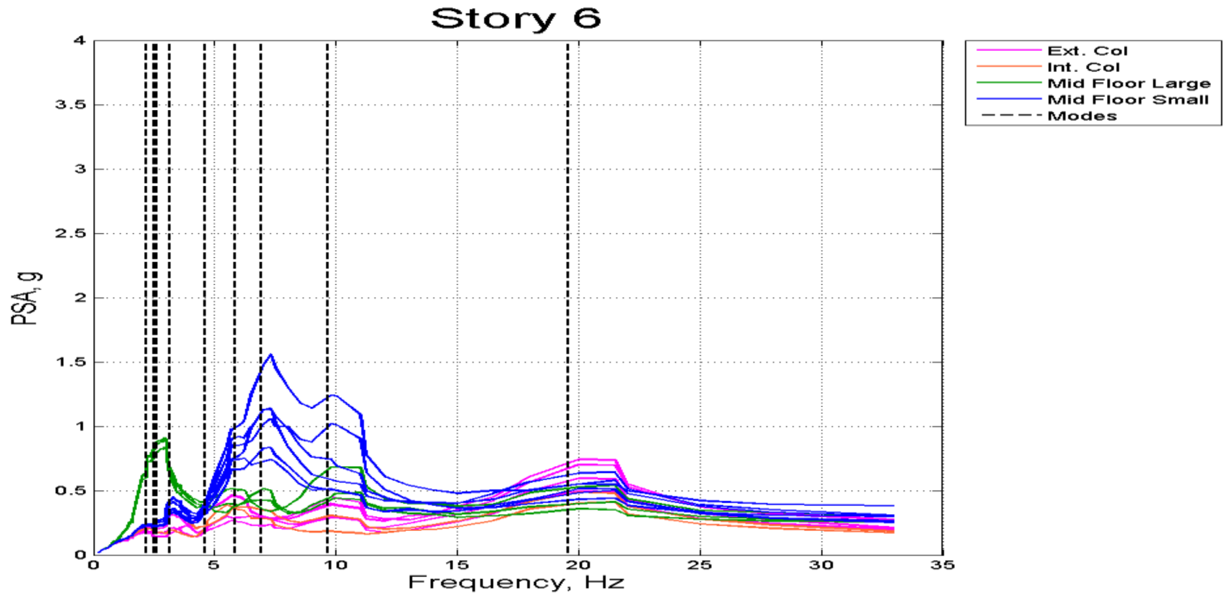
Story 6
PSA, g
Frequency, Hz
Ext. Col
Int. Col
Mid Floor Large
Mid Floor Small
Modes

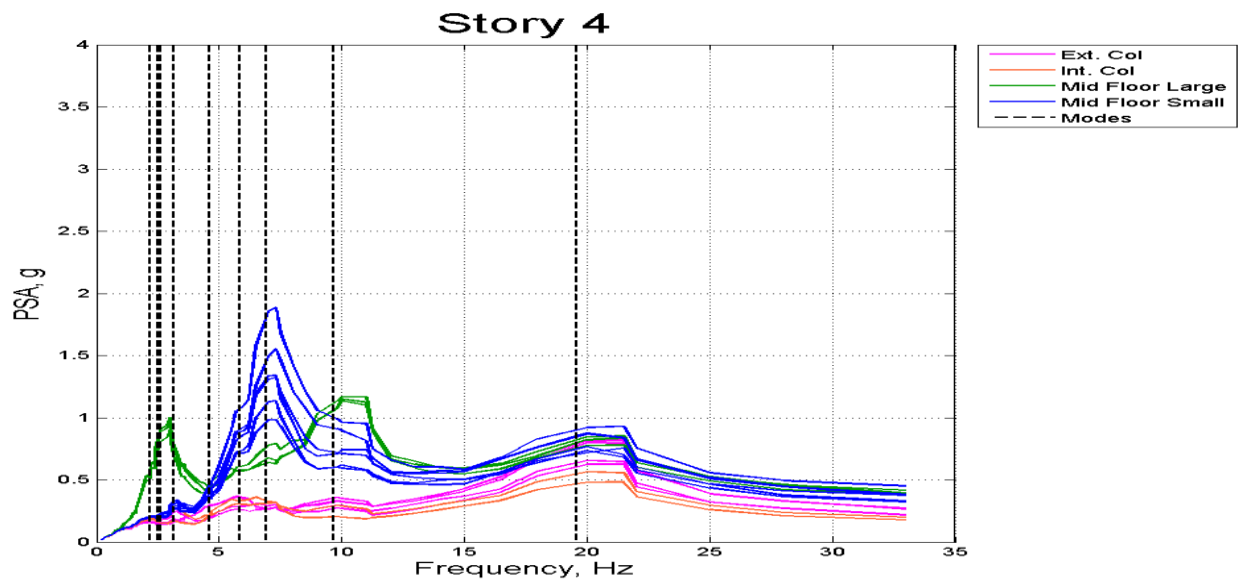
Story 4
PSA, g
Frequency, Hz
Ext. Col
Int. Col
Mid Floor Large
Mid Floor Small
Modes

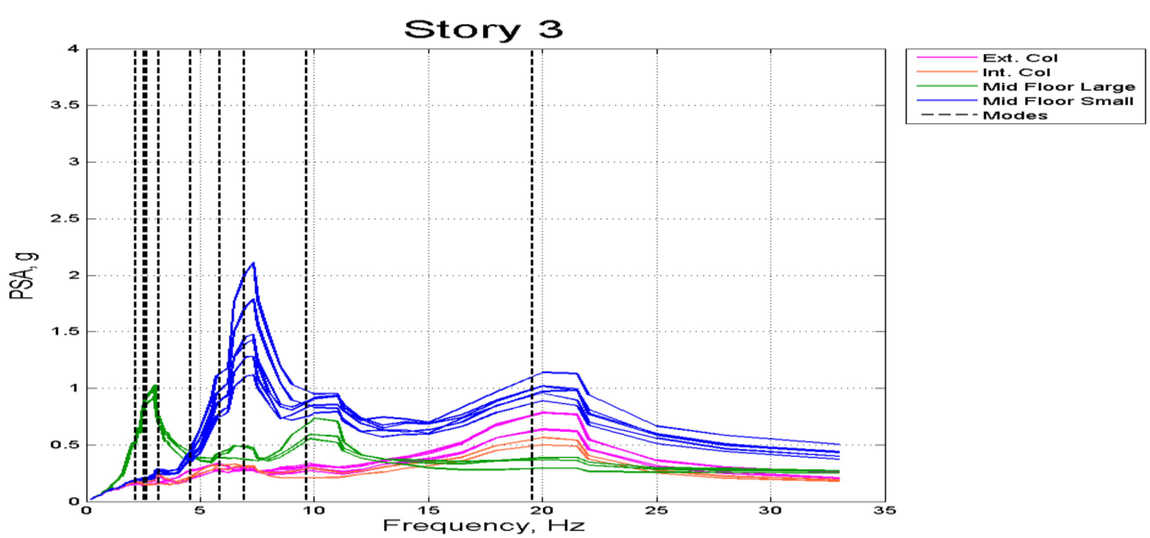
Story 3
PSA, g
Frequency, Hz
Ext. Col
Int. Col
Mid Floor Large
Mid Floor Small
Modes

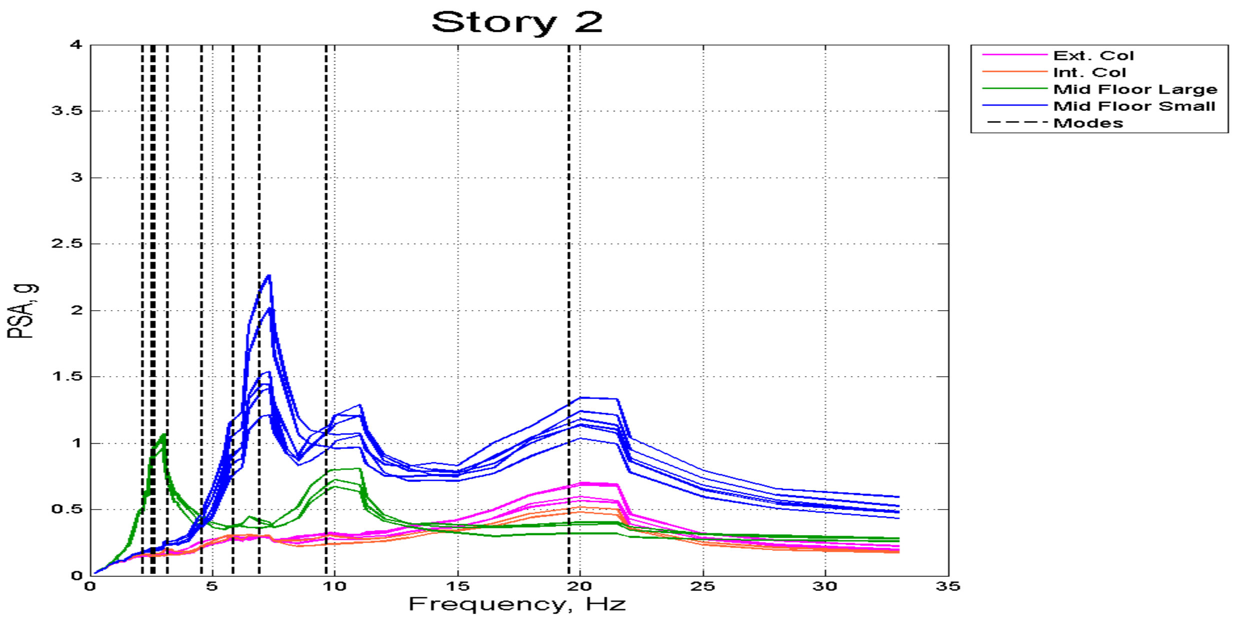
Story 2
PSA, g
Frequency, Hz
Ext. Col
Int. Col
Mid Floor Large
Mid Floor Small
Modes

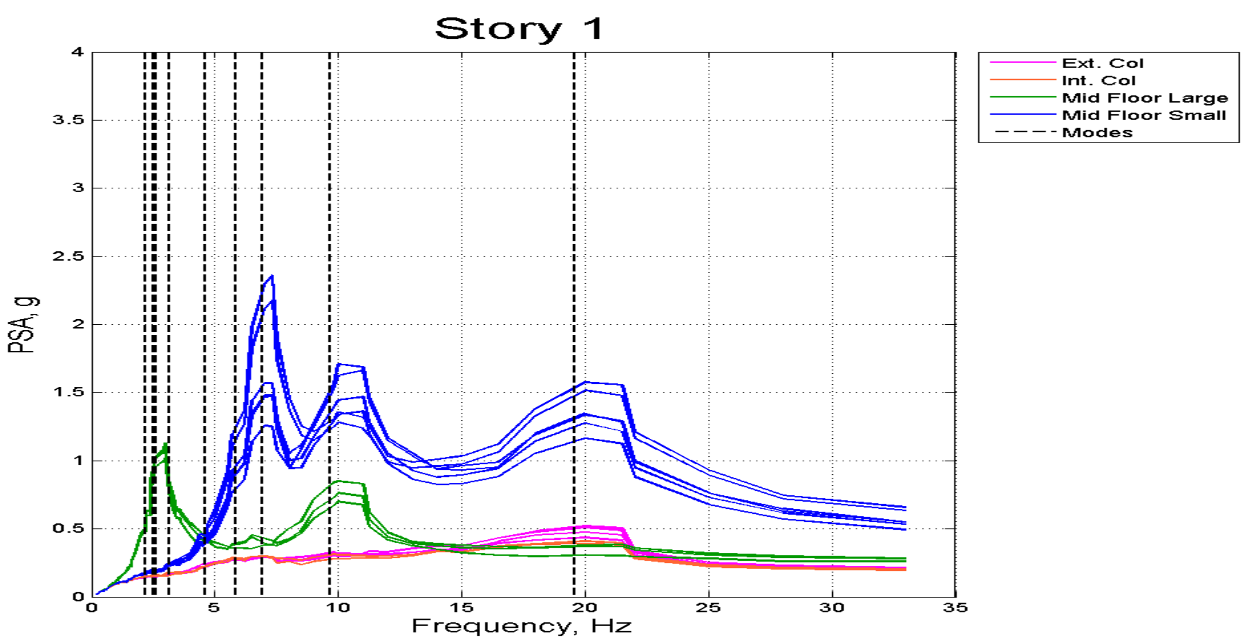
Story 1
PSA, g
Frequency, Hz
Ext. Col
Int. Col
Mid Floor Large
Mid Floor Small
Modes

LIST OF REFERENCES


[1] R. Villaverde, "Seismic Design of Secondary Structures: State of the Art," *Structural Engineering*, vol. 123, no. 8, pp. 1011-1019, August 1997.

[2] A. T. Council, "Reducing The Risks of Nonstructural Earthquake Damage-A Practical Guide," Washington, D.C., 2011.

[3] A. S. o. C. Engineers, "Seismic Rehabilitation of Existing buildings," Reston, Virginia, 2007.

[4] G. P. A. E. Z. A. M. I. E. M. Joseph D. Wieser, "Assessment of Floor Accelerations in Yielding Buildings," Reno, Nevada, October 5, 2012.

[5] R. P. Dhakal, "Damage To Nonstructural Components And Contents In 2010 Darfield Earthquake," *Bulletin of the New Zealand Society for Earthquake Engineering*, vol. 43, no. 4, pp. 404-411, December 2010.

[6] S. P. Weng Yuen Kam, "General Building Performance in Christchurch Central Business District," Christchurch, New Zealand, November 2011.

[7] T. S. Andrew Whittaker, "An Overview of Nonstructural Components Research at Three U.S. Earthquake Engineering Research Centers," in *Proceedings of Seminar on Seismic Design Performance, and Retrofit of Nonstructural Components in Critical Facilities, Applied Technology Council, ATC-29-2*, Redwood City, California, 2003.

[8] A. T. Council, "Reducing the Risks of Nonstructural Earthquake Damage," Washington, D.C., February 29, 2008.

[9] A. T. Council, "Proceedings of Seminar on Seismic Design, Performance, and Retrofit of Nonstructural Components in Critical Facilities," in *ATC 29-2 Seminar on Seismic Design, Performance, and Retrofit of Nonstructural Components in Critical Facilities*, Redwood City, California, 2003.

[10] P. Chapman, February 2 2012. [Online]. Available: http://www.telegraph.co.uk/news/worldnews/australiaandthepacific/newzealand/9056031/Briton-died-in-crushed-bus-in-New-Zealands-Christchurch-earthquake.html.

[11] C. a. S. Inc., *SAP2000 Version 15.0.0,* 2011.

[12] S. T. Eduardo Miranda, "Approximate floor acceleration demands in multistory buildings. I: Formulation," *Structural Engineering,* vol. 131, no. 2, pp. 203-211, February 2005.

[13] E. M. Eduardo Reinoso, "Estimation of Floor Acceleration Demands in High-Rise Buildings During Earthquakes," *The Structural Design of Tall and Special Buildings,* vol. 14, no. 2, pp. 107-130, April 2005.

[14] E. M. Shahram Taghavi, "Effect of Interaction Between Primary and Secondary Systems on Floor Response Spectra," *The 14th World Conference on Earthquake Engineering,* October 2008.

[15] R. M. Joshua Clayton, "Proposed Method for Probabilistic Estimation of Peak Component Acceleration Demands," *Earthquake Spectra,* vol. 28, no. 1, pp. 55-72, February 2012.

[16] R. S. K. K. Ricardo Medina, "Floor Response Specra for Light Components Mounted on Regular Moment Resisting Frame Structures," *Engineering Structures,* vol. 28, pp. 1927-1940, May 2006.

[17] R. V. Samit Ray Chaudhuri, "Effect of Building Nonlinearity on Seismic Response of Nonstructural Compoenents: A Parametric Study," *Structural Engineering,* vol. 134, no. 4, pp. 661-670, April 2008.

[18] K. C. Yousef Bozorgnia, "The Vertical-to-Horizontal Response Spectral Ratio and Tentative Procedures for Developing Simplified V/H and Vertical Design Spectra," *Earthquake Engineering,* vol. 8, no. 2, pp. 175-207, 2004.

[19] B. S. S. Council, "NEHRP Recommendd Seismic Provisions for New Buildings and Other Structures," Washington, D.C., 2009.

[20] A. I. W. S. G. Pekcan, "Nonstructural System Response to Vertical Excitation and Implications for Seismic Design and Qualification," in *ATC-29-2 Seminar on Seismic Design, Performance, and Retrofit of Nonstructural Compoenents in Critical Facilities*, Los Angeles, California, 2003.

[21] G. P. A. Z. A. I. M. M. Joseph Wieser, "Floor Accelerations in Yielding Special Moment Resisting Frame Structures," *Earthquake Spectra*, vol. 29, no. 3, pp. 987-1002, August 2013.

[22] H. K. Akshay Gupta, "Seismc Demands for Performance Evaluation of Steel Moment Resisting Frame Structures," Stanford, CA, June 1999.

[23] C. Adam, "Dynamics of Elastic-Plastic Shear Frames with Secondary Structures: Shake Table and Numberical Studies," *Earthquake Engineering and Structural Dynamics,* vol. 30, pp. 257-277, 2001.

[24] K.-P. R. G. M. Andrei Reinhorn, "Modeling and Seismic Evaluation of Nonstructural Components: Testing Frame for Experimental Evaluation of Suspended Ceiling Systems," Reno, Nevada, 2010.

[25] M. P. J. R. J. S. L. F. U. B. H. G. Matthew Hoehler, "PErformance of Suspended Pipes and Their Anchorages During Shake Table Testing of a Seven Story Building," *EArthquake Spectra,* vol. 25, no. 1, pp. 71-91, February 2009.

[26] K. R. M. M. E. S. T. S. T. O. L. T. A. Z. G. M. D. A. Siavash Soroushian, "Seismic Response of Ceiling/Sprinkler Piping Nonstrucural Systems in NEES TIPS/NEES Nonstructural/NIED Collaborative Tests on a Full Scale 5 Story Building," *Structures Congress* , pp. 1315-1326, March 2012.

[27] K. S. S. Y. Y. S. M. A. Y. Matsuoka, "Non-Structrual Component Performance in 4 Story Frame Tested to Collapse," *14th World Conference on Earthquake Engineering,* October 2008.

[28] D. N. F. K. K. D. Tara Hutchinson, "Vibration Studies of Nonstructural Components and Systems Within a Full Scale Building," *Earthquake Spectra,* vol. 26, no. 2, pp. 327-347, May 2010.

[29] R. D. G. M. A. F. Rodrigo Retamales, "NEESR Nonstructural Grand Challenege Project Simulation of the Seismic Performance of Nonstructural Systems Experimental Phase 1: Seismic Perofmance of Partition Wall Subbsystems," Buffalo, New York, 2006.

[30] G. M. A. R. M. P. S. W. R. R. Andre Filiatrault, "Preliminary Report Seismic Performance Assessment of a Full Scale Hospital Emergency Room," Buffalo, New York, 2008.

[31] J. I. R. A. J. C. M. E. Rodriguez, "Earthquake Induced Floor Horizontal Accelerations in Buildings," *Earthquake Engineering and Structural Dynamics,* vol. 31, pp. 693-718, 2002.

[32] T. H. Samit Ray Chaudhuri, "Distribution of Peak Horizontal Floor Acceleration For Estimating Nonstructural Element Vulnerability," in *13th World Conference on Earthquake Engineering*, Vancouver, B.C., Canada, 2004.

[33] R. Villaverde, "Simple Method to Estimate the Seismic Nonlinear REsponse of Compoenets in Buildings," *Engineering Structures,* vol. 28, no. 8, pp. 1209-1221, July 2006.

[34] L. M. L. E. S. E. E. M. M. P. Singh, "Seismic Design Forces. I: Rigid Nonstrcutural Components," *Structural Engineering,* vol. 132, no. 10, pp. 1524-1532, October 2006.

[35] A. S. M. H. Akhlaghi, "Height-Wise Distribution of Peak Horizontal Floor Acceleration (PHFA)," in *14th World Conference on Earthquake Engineering*, Beijing, China, 2008.

[36] M. S. N. N. S. F. M. Shooshtari, "Floor Response Spectra for Seismic Design of Operational and Functional Components of Concrete Buildings in Canada," *Canadian Journal of Civil Engineering,* vol. 37, pp. 1590-1599, October 2010.

[37] E. L. Wilson, Static & Dynamic Analysis of Structures: A Physical Approach with Emphasis on Earthquake Engineering, 4th ed., Berkely, California: Computers and Structures, 2010.

[38] M. Abell, June 2012. [Online]. Available: https://wiki.csiamerica.com/display/kb/Ritz+vs.+Eigen+vectors.

[39] A. T. C. (ATC), "Quantification of Building Seismic Performance Factors," Redwood City, California, June 2009.

[40] A. 7-10, "Minimum Design Loads for Buildings and other Structures," Reston, Virginia, 2010.

[41] A. 341-1, "Seismic Provisions for Structural Steel Buildings," Chicago, Illinois , 2010.

[42] A. I. o. S. Construction, Specifications for Structural Steel Buildings, 2nd ed., Chicago, Illinois: AISC, 2010.

[43] AISC, "American Steel Construction Manual," Chicago, Illinois, 2005.

[44] A. International, August 2013. [Online]. Available: http://www.unitedmetalproducts.info/downloads/ASTM_A_653_REDLINE.pdf.

[45] A. S. Deck, August 2013. [Online]. Available: http://www.ascsd.com/files/FloorDeck.pdf.

[46] E. L. W.F. Chen, Earthquake Engineering for Structural Design, Boca Raton, Florida: Taylor & Francis Group, LLC, 2006.

[47] B. S. S. Council, "NEHRP Recommended Seismic Provisions for New Buildings and Other Structures," Washington D.C., 2009.

[48] I. Computers & Structures, "ETABS Nonlinear version 9.7.3," 2011.

[49] D. R. Medina, *CiE 887: Lecture 21 Modal Response Spectral Analysis,* 2012.

[50] A. K. Chopra, Dynamics of Structures, 4th ed., Upper Saddle River, New Jersey: Prentice Hall, 2012.

[51] J. M. a. M. E. Kevin Moore, "Design of RBS Moment Frame Connections," Moraga, California, August 1999.

[52] R. Sudisman, September 2013. [Online]. Available: http://ranggasudisman.files.wordpress.com/2009/02/untitled21.jpg.

[53] a. M. D. E. Kee Dong Kim, "Monotonic and cyclic loading models for panel zones in steel moment frames," *Journal of Constructional Steel Research,* Vols. Volume 58, Issues 5–8, 2002, no. 5–8, p. 605–635, 2002.

[54] S. P. S. a. A. Amidi, "Seismic Behavior of Steel Frames with Deformable Panel Zones," *Journal of Structural Engineering,* vol. 121 , no. No. 1, pp. 35-36, January 1998.

[55] H. K. J. O. M. a. S. M. A. Ronald O. Hamburger, "Seismic Design of Steel Special Moment Frames," National Institute of Standards and Technology, Gaithersburg, Maryland, June 2009.

[56] R. Vogel, "LRFD-Composite Beam Design With Metal Deck," Lafayette, California, March 1991.

[57] T. B. Products, September 2013. [Online]. Available: http://www.tegral.com/index.php?page=Comflor.

[58] C. a. S. Inc., *ETABS Version 9.7.3,* 2011.

[59] A. S. Deck, October 2013. [Online]. Available: http://www.ascsd.com/floor.html.

[60] I. Tsukrov, *ME 986 Advanced Finite Element Analysis Notes*, October 25, 2012.

[61] P. NGA, "Pacific Earthquake Engineering Research Next Generation Attenuation," 2013.

[62] A. K. Chopra, Dynamics of Structures, 4th ed., H. Stark, Ed., Upper Saddle River, New Jersey: Pearson, 2012.

[63] T. M. Inc., *MATLAB Version 2011b*, 2011.

[64] N. I. o. S. a. T. (NEHRP), "Evaluation of the FEMA P695 Methodology for Quantification of Building Seismic Performance Factors," Redwood City, California, November 2010.